

We are IntechOpen, the world's leading publisher of Open Access books Built by scientists, for scientists

6,300

Open access books available

171,000

International authors and editors

190M

Downloads

Our authors are among the

154

Countries delivered to

TOP 1%

most cited scientists

12.2%

Contributors from top 500 universities



WEB OF SCIENCE™

Selection of our books indexed in the Book Citation Index
in Web of Science™ Core Collection (BKCI)

Interested in publishing with us?
Contact book.department@intechopen.com

Numbers displayed above are based on latest data collected.
For more information visit www.intechopen.com



Application of Ferrate for Advanced Water and Wastewater Treatment

Ansaf V. Karim, Sukanya Krishnan, Lakshmi Pisharody and Milan Malhotra

Abstract

Treatment of recalcitrant organics and inorganics present in wastewater is a major challenge. Conventional biological treatments alone are not capable of removing these toxic compounds from wastewater. To overcome these problems, advanced oxidation processes (AOPs) have been used to completely mineralize or transform the organics into simpler compounds, which can then be treated through biological processes. However, conventional AOPs result in the generation of byproducts, which are known to have higher toxicity. Among various AOPs, ferrate has been gaining popularity because of its advantages such as high oxidation potential, no byproduct formation and also non-toxic end products. The end product generated also acts as a coagulant, which thereby enhances the removal efficiency. In the present chapter, the chemical properties, preparation methods and the factors affecting the stability of ferrate were evaluated based on literature. Further, ferrate oxidation as a potential method for the treatment of both organic and inorganic pollutants in drinking and real wastewater is discussed.

Keywords: ferrate, oxidation process, disinfection, iron chemistry, synthesis

1. Introduction

Scientific discoveries and development in pharmaceuticals, pesticides, personal care products (PCP) and basic sanitation have improved the lifestyle and living standards of humans across the globe. However, these developments come with an environmental cost. In recent past, environmental and human health risks associated with traces of pharmaceutical, pesticides and microplastics (from PCP) have been studied by various researchers. Due to the transformation and interaction of these compounds with the environment, they can enhance the resistance of microbes, thus making them resistant to antibiotics. Furthermore, some of the pesticides have been proven to have a carcinogenic effect. The microplastics generated from PCP have now been reported to be the part of the food chain mostly from sea salts and fish. With these environmental challenges, there has been a sharp increase in the research for the treatment and removal of these emerging contaminants.

Various research groups have used different physicochemical techniques such as adsorption, Fenton treatment, zero-valent iron, ultraviolet (UV)-catalytic,

electro-oxidation and wet oxidation [1–3] for the sustainable treatment of these contaminants. The techniques mentioned above have their advantages regarding their nonselective behaviour, high removal efficacy, and simpler byproducts. The higher cost associated with AOPs is a major limitation for field applicability.

From the past two decades, advanced oxidation processes (AOPs) have been gaining popularity for the treatment of water and wastewater contaminants. AOPs use hydrogen peroxide and ozone, among other chemicals that have high oxidation potential. These chemicals can oxidize organic molecules to simpler molecules and themselves get reduced. During AOPs, in situ hydroxyl radicals are formed, which

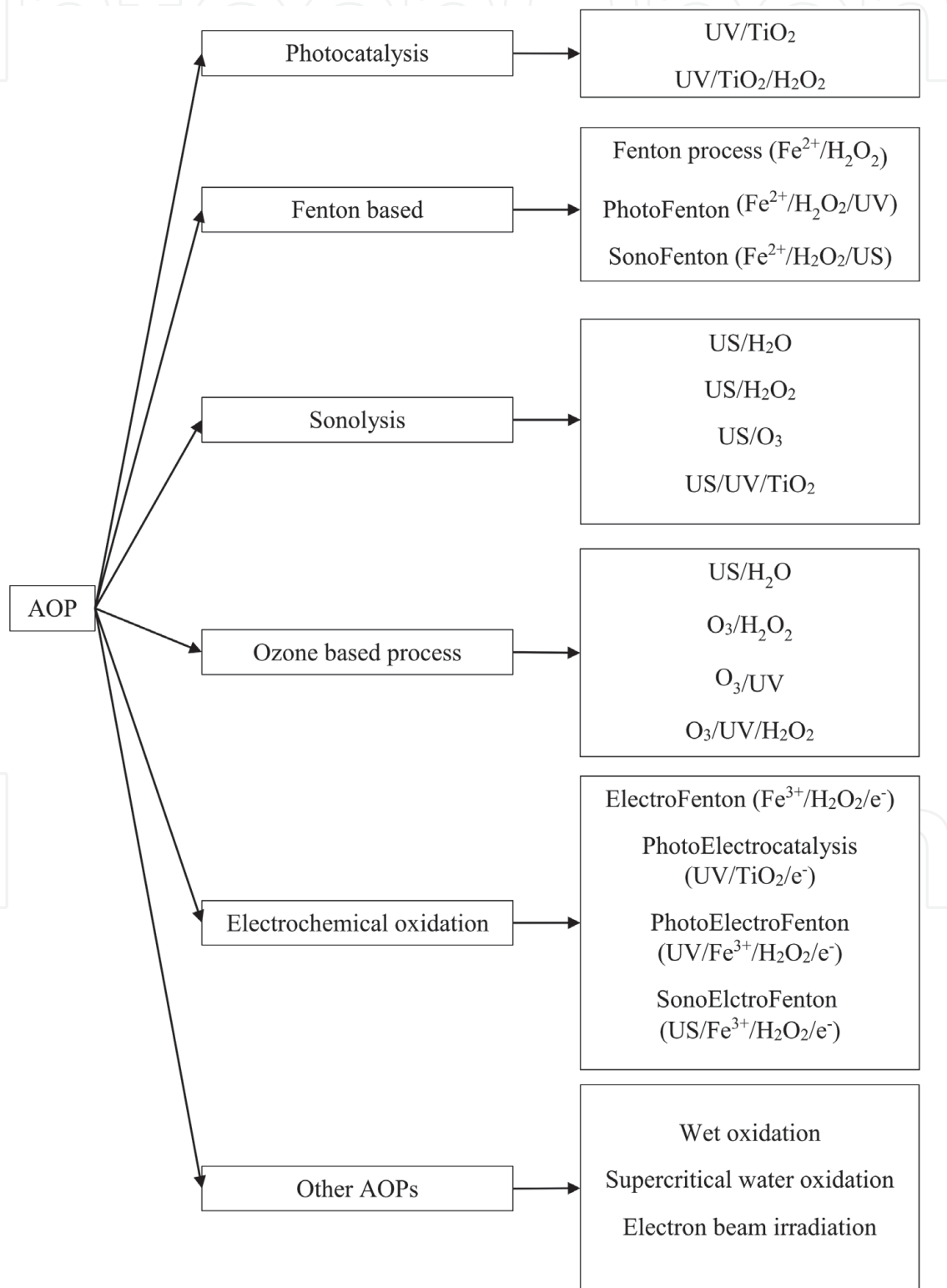


Figure 1.
Broad category of AOPs [4].

further reacts with organic molecules. The organic molecule may undergo various reactions such as partial cleavage, dechlorination, fragmentation or complete mineralization, depending on the chemical structure of molecule and reaction condition. The broad category of AOPs is shown in **Figure 1**.

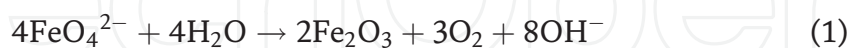
Innovative technologies using alternative sources such as peroxides, ferrates, ozone, etc. can significantly improve the wastewater treatment due to their higher selectivity and efficiency. Among them, ferrate [Fe(VI)] is a promising choice for environmental remediation. It does not produce any harmful byproducts during treatment and provides efficient degradation of organic, inorganics and microorganisms over a wide range of pH. This chapter provides a detailed review of chemical properties, preparation methods and factors affecting the stability of ferrates. Further, the chapter also reviews the oxidation potential of ferrates for the environmental remediation and disinfection.

2. Chemical structure and stability of ferrate

Typically iron (Fe) exists in two oxidation states either as ferrous (Fe(II)) or ferric (Fe(III)). However, under strong oxidizing conditions, a higher oxidation state (i.e. +IV, +V and +VI) of iron can be achieved, which is referred to as a ferrate. Based on the pE-pH diagram, which is also known as Pourbaix diagram of iron (**Figure 2**), we can visualize the presence of various forms of iron at different pH and under oxidative/reductive environment. A reducing environment is represented by low pE values; high pE values represent an oxidizing environment. Ferrates are predominating in the top region of the pE-pH diagram, whereas iron exists as Fe (0) at the bottom.

Among the various higher oxidation state, the +VI state of iron is comparatively stable and easier to produce. The literatures, based on XRD of solid ferrate, proposed a tetrahedral structure of ferrate (**Figure 3**). In ferrate, centrally placed Fe⁺⁶ is covalently bonded to four equivalent oxygen atoms at the corner of the tetrahedron.

In the aqueous phase, there are many factors (such as pH, temperature and ferrate concentration) on which the stability of ferrate depends. Ferrate ions and water molecules reacts to form ferric oxide (Fe₂O₃), oxygen gas, and hydroxyl ions (Eq. (1)). Due to the release of hydroxyl ions, the resulting pH of the solution is highly alkaline. The ferric oxide generated as an end product acts as a coagulant:



Under the acidic environment, ferrate is quite unstable and rapidly undergoes exothermic degradation. In aqueous solution of pH ~5, the ferrate (1 mM) was reported to be completely degraded within 7 min [5]. The stability of ferrate tends to improve with an increase in pH, as can be seen in **Figure 4**. For pH ~10, the ferrate concentration remained almost constant. At pH of above 10, the stability of ferrate also tends to deteriorate. For a ferrate concentration of 0.25 mM and a pH of 12, reductions of ~ 60% were reported within 10 min [6].

A diluted ferrate solution is reported to be more stable than a concentrated solution. The critical ferrate concentration is 0.025 M; a ferrate concentration higher than this (0.025 M) in solution tends to degrade rapidly. When comparing the stability of ferrate at different concentrations, it was reported that ~89% of ferrate concentration remained as ferrate for 0.02 and 0.025 M strength for 1 h. However, complete degradation was reported for solution with a 0.03 M concentration in that specific duration [7].

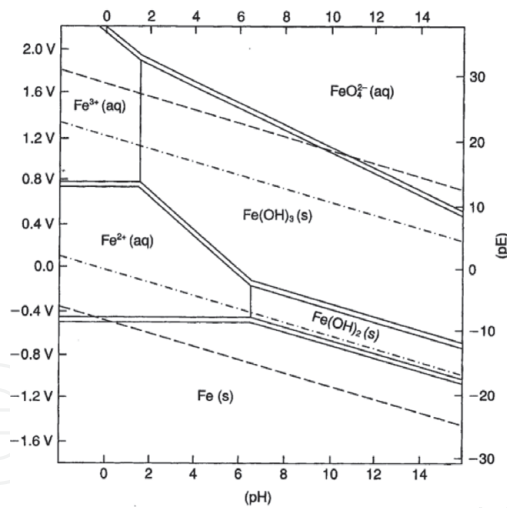


Figure 2.
Pourbaix diagram for iron (1 M) solution.

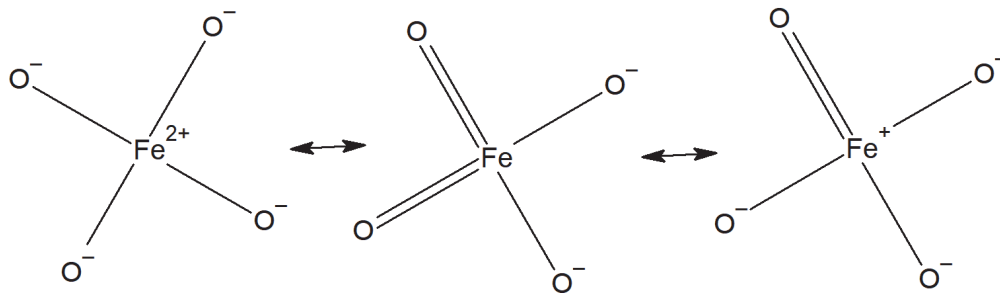


Figure 3.
Resonance hybrid structure of ferrate.

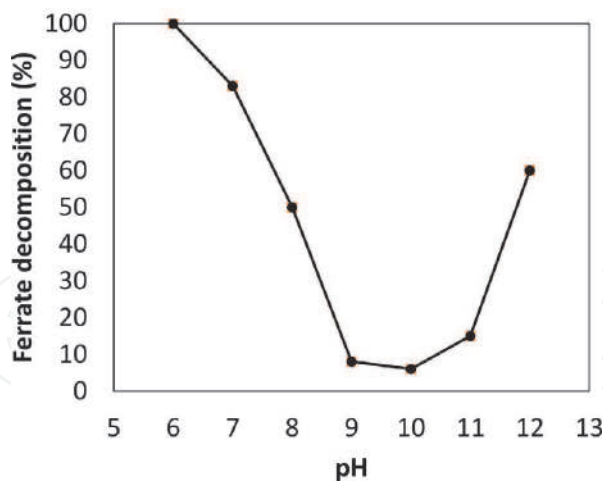


Figure 4.
Stability of ferrate in the aqueous phase at different pH [6].

Co-ions such as Ni(II) and Co(II) in 100 μ M concentration were reported to increase the decomposition rate of ferrate (2 mM). However, at lower concentration, the influence of co-ion (0.1 μ M) on ferrate decomposition was reported to diminish. No significant influence of other ions (Ba(II), Ca(II), Fe(III), Mg(II), Zn(II), Pb(II), Cu(II), Sr.(II)) and salts (KIO₄, K₂O₉B₄, K₃PO₄, Na₂WO₄, Na₂MoO₄, Na₂SiF₆) on ferrate degradation was reported [8].

The temperature of the aqueous phase can also influence the stability of ferrate. Ferrate solution (0.01 M) kept at 0.5°C was reported to remain stable

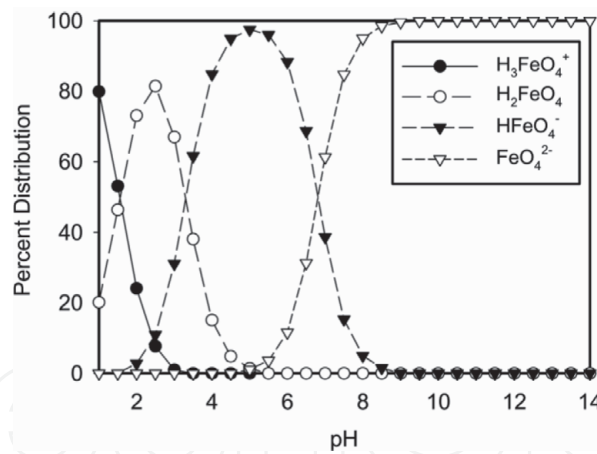
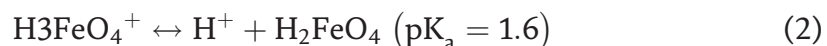


Figure 5.
 Different species of ferrate in the aqueous phase [10].

(~2% reduction) even after 2 h. On the other hand, the ferrate concentration was found to be reduced by ~10% at a temperature of 25°C [9]. External factors such as light are not known to have any significant influence on the stability of ferrate (0.01 M) [9].

Depending on the pH of the solution, four different species of ferrate can exist, as shown in **Figure 5**. Initially, two unstable species of Fe(VI) (i.e. H₂FeO₄ and HFeO₄⁻) were reported in phosphate buffer (0.2 M solution). Three protonated species of Fe(VI) were reported in phosphate/acetate buffer (0.025). Based on pK_a values, it can be seen that in the alkaline environment, most of the ferrate exist as FeO₄²⁻. In neutral conditions, HFeO₄⁻ is the dominating species:

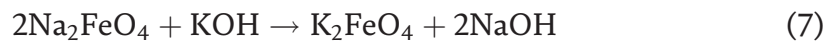
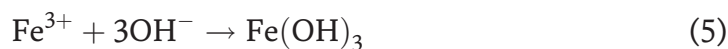


3. Synthesis of ferrate

3.1 Wet synthesis

The wet oxidation synthesis of ferrate involves oxidation of ferric to ferrate under high pH conditions. The solution containing ferrate obtained by this procedure is highly unstable, which thereby demands subsequent procedures of precipitation, washing and drying to obtain a stable solid product. Numerous methods have been tried to prepare a stable solid product containing ferrate(VI). However, the subsequent recovery of ferrate is difficult because of the increased solubility of Na₂FeO₄ in solution saturated with NaOH. The procedure involving the flow of chlorine gas through the ferric salt resulted in a solid product with 41.38% of Na₂FeO₄ [11, 12].

The method of production of ferrate by wet oxidation is known since the 1950s. The method involves a reaction between ferric chloride and sodium hypochlorite in the presence of an alkali such as sodium hydroxide. Further recovery of potassium ferrate is obtained by precipitation with potassium hydroxide. Even though a percentage recovery of potassium ferrate as high as 96% could be obtained, the maximum yield percentage obtained by continuous efforts was 75%. Earlier the recovery was poor as 10–15%. The basic reactions involved in the process are shown below [13, 14]:



3.2 Dry synthesis

The dry oxidation method for ferrate synthesis is a very old method. However, the method involves high risks as it can lead to an explosion at elevated temperature. Recent developments include synthesis of ferrate salt by calcination of a mixture of potassium peroxide and ferric oxide at a temperature ranging from 350 to 370°C. Another method involves oxidation of iron oxide with sodium peroxide at a temperature of 370°C, with a continuous flow of dry oxygen in a ratio of 4:1, yielding sodium ferrate. The product by this reaction results in a red-violet colored solution containing tetrahedral ion FeO_4^{2-} [11, 15, 16]. The % recovery of ferrate was not higher than 55% in this method [17]. The equation for the reaction is given below:

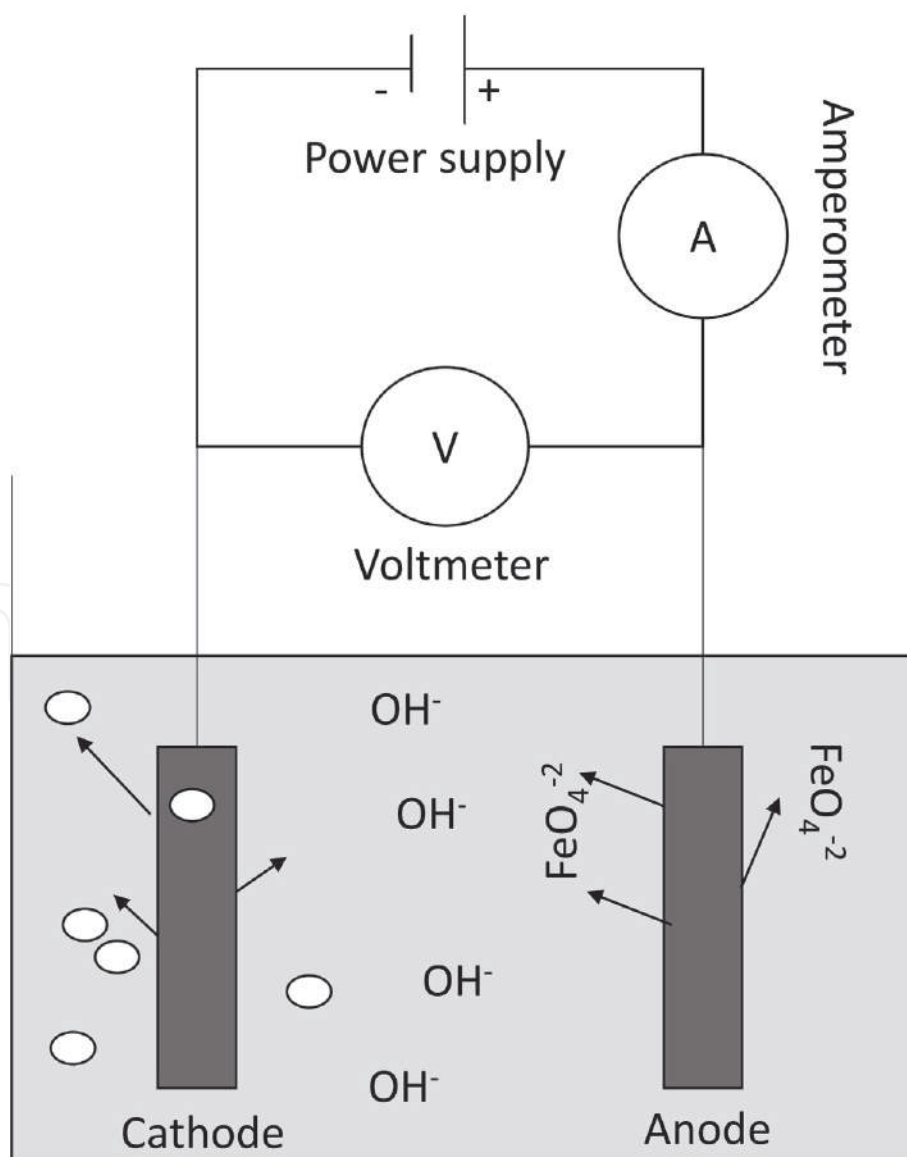
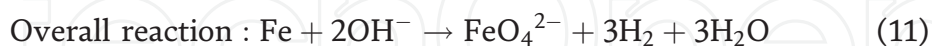
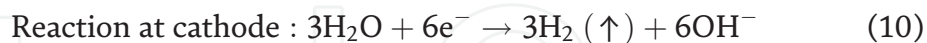
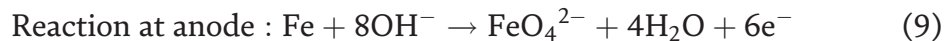


Figure 6.
Electrochemical cell for ferrate production [18].

3.3 Electrochemical synthesis

During the electrochemical synthesis of ferrate, anodic dissolution of iron takes place in a strongly alkaline solution. The current applied during the synthesis process oxidizes the iron to ferrate in the alkaline solution (KOH or NaOH) (**Figure 6**). The reactions at the anode and cathode are as follow:



Factors such as anode composition, current density and strength of electrolyte govern the production of ferrate. The major advantage of electrochemical synthesis is its simplicity and no costly chemical requirement.

4. Application of ferrate in environmental remediation

The increasing occurrence of emerging pollutants such as pharmaceuticals, dyes, heavy metals and endocrine disrupting compounds, among others, in wastewater has generated a growing concern. Due to the recalcitrant nature of these compounds, they remain in the environmental matrices for longer duration and are not degraded naturally or by biological reactions. Ferrate as an oxidizing agent is a promising choice for the remediation of water and wastewater containing recalcitrant pollutants. They are able to oxidize compounds in a shorter time period when compared to permanganate and chromate [19]. The degradation potential of ferrate for water and wastewater treatment mainly depends upon the pH, initial ferrate concentration, presence of coexisting ions and temperature [20]. They can be easily reduced to insoluble and non-toxic Fe(III) species and can adsorb organic compounds, resulting in its removal [21]. In addition to the higher oxidizing ability of Fe(VI), other intermediate oxidation states of iron Fe(V) and Fe(IV) are claimed to help oxidation of organic and inorganic compounds [19]. The following section describes the application of ferrate as an oxidant for remediation of various pollutants.

4.1 Phenolic compounds

The removal of phenolic compounds from environmental matrices has attained considerable attention in recent years due to its recalcitrant and hazardous properties. The oxidative removal of these types of compounds from water and wastewater using ferrates Fe(VI) has been extensively studied by the researchers these days. Chen et al. [22] have examined the removal of four different types of phenolic compounds, such as 2-benzylphenol, phenol, chlorophene and 4-chlorophenol by Fe(VI) at pH 8. It was observed that the presence of chlorine and benzyl groups helps in the increased reactivity of Fe(VI) with phenolic compounds, and the degradation was observed to be in the order of chlorophene > 4-chlorophenol > 2-benzylphenol > phenol. They established the complete degradation pathway and various intermediates formed by mainly four pathways, such as hydroxylation of the benzene ring, C—C bond cleavage, chlorine atom substitution by a hydroxyl group and single-electron coupling.

A similar study of Chen et al. [23] demonstrated almost complete degradation of polychlorinated diphenyl sulphides (PCDPSs) within a short period of time

(~240 s) at pH 8. Also, they established the pathway of degradation and toxicity potential of products, which suggests that PCDEPs' oxidations occur at the S(II) moiety by ferrates and form oxidation products that are non-toxic to aquatic organisms. pH is one of the critical factors for oxidation reactions which also affects the stability and oxidation potential of ferrate ion [6]. However, high alkaline pH of liquid ferrates imparts an adverse effect on disinfection treatment by the formation of harmful disinfection byproducts [24]. Hence, detailed research should be carried out for understanding the effect of pH in the treatment of various recalcitrant pollutants with different ferrate concentrations.

The study conducted by Zhang et al. [25] demonstrated the use of Fe(VI) for the removal of one of the most renowned endocrine disruptors, bisphenol-A, from water. They observed the complete degradation of BPA at Fe(VI)/BPA molar ratio of 3.0 and 1.5 mg L^{-1} BPA initial concentration within 30 minutes of oxidation under weak acidic pH. In order to enhance the degradation of various recalcitrant compounds, various homogeneous reducing agents such as sodium thiosulfate ($\text{Na}_2\text{S}_2\text{O}_3$) and sodium sulphite (Na_2SO_3) have been used in recent years. In the recent study by Sun et al. [26], the application of heterogeneous carbon nanotube along with ferrates for enhanced degradation of bromophenols. The reaction kinetics was found to follow second-order over a wide range of pH (6-10). It was found that the coupling of one-electron transfer mechanism caused the formation of some undesirable products, such as di-brominated phenoxyphenols and dihydroxylated biphenyls.

4.2 Dyes and dye wastewater

The application of Fe(VI) for removal of textile dyes is one of the promising technologies because it can act as an oxidant as well as a coagulant at the same time and it enhances the biodegradability property of dye. Li et al. [27] investigated the azo dye orange II removal by different types of Fe(VI), namely, potassium permanganate, potassium ferrate(VI) and the ferrate(VI) hypochlorite liquid mixture. It was observed that within 30 minutes, maximum discoloration of 95.6% was achieved with ferrate(VI) hypochlorite liquid mixture over a pH range of 3 to 11. Whereas, only 17.7% and 62 % of discoloration was observed respectively when only potassium permanganate and potassium ferrate(VI) were employed. However, one of the drawbacks of the above process is that residual hypochlorite in ferrate(VI) hypochlorite liquid mixture produces dangerous disinfection byproducts.

In another study, Xu et al. [28] utilized a highly stable composite ferrate(VI) solution produced by the chemical method with KOH at 65°C for the degradation of azo dye reactive brilliant red X-3B. The optimal conditions were found with dye concentration 0.08 mmol L^{-1} , pH = 8.4 and ferrate dosage 2.5 mg L^{-1} , giving discoloration of 99% after 20 min also; about 42% COD removal and 9% TOC removal were observed after 60 min. Also, the degradation pathway was theoretically established by the cleavage of by the C—N and N=N bond yielding muconic acid as the final reduced compound. In addition, the study by Turkay et al. [29] investigated the kinetics and mechanism of degradation of methylene blue by ferrate(VI). It was observed that about 96.82% methylene blue removal is achieved with initial methylene blue concentration of 50 mg L^{-1} , pH = 13.6 and ferrate dosage = 59.5 mg L^{-1} over 35 minutes of reaction time and followed second-order kinetics.

4.3 Pesticides

Fe(VI)-based oxidation processes are effective in improving the biodegradability of wastewater containing persistent organic pollutants such as pesticides.

In a study conducted by Zhu et al. [21], the ferrate-based pretreatment of wastewater containing a higher concentration of alachlor improved its biodegradability and resulted in the total removal of alachlor within 10 min under optimized conditions. A comparison of the oxidation property of peroxymonosulfate (PMS) and Fe(VI) and for the degradation of atrazine was studied by Wu et al. [30]. They have observed a significant enhancement in the degradation of atrazine in Fe(VI)/PMS system when compared to Fe(VI) or PMS alone.

In another study conducted by Chen et al. [31], the combined oxidation ability of the UV/Fe(VI) system for the removal of an organophosphorus pesticide profenofos was studied. They have observed that degradation of the compound was dependent on the pH and Fe(VI) dosage, and the degradation progressed through de-ethylation and de-propylation with subsequent C—O cleavage with the release of orthophosphate. The effect of operational parameters such as pH, Fe(VI) dosage and other water constituents (anions and cations) was studied while evaluating the potential of Fe(VI) oxidant on parathion (PTH) degradation [32]. Under the operation condition of pH 7 and Fe(VI): PTH 15:1, 99% of removal was observed, the presence of Fe^{3+} , HCO_3^- , Cu^{2+} , HA, Ca^{2+} decreased the removal rate, while no significant effect was observed for Cl^- and NO_3^- . In a similar study conducted by Liu et al. [33], they have concluded that the degradation of chlorpyrifos was mainly through C=O cleavage and hydroxyl substitution reactions.

4.4 Pharmaceuticals

The presence of pharmaceutically active compounds in the aquatic environment can cause serious health issues to the living organism. The strong oxidation potential of Fe(VI) and its ability to remove nitrogen- and sulfur-containing compounds had gained attention for the removal of pharmaceuticals from wastewater. The kinetics of removal of an antibacterial drug sulfamethoxazole (SMX) using potassium ferrate oxidant was studied by Sharma et al. [34]. They found that the rate constants are pH-dependent, and at higher concentrations of potassium ferrate (10 μM), the half-life of the compound was found to be 2 min at pH 7. In a similar kind of study, when the kinetics of removal of antiphlogistic drug ibuprofen (IBP) was studied, the degradation rates decreased with an increase in pH, which was related to protonation of Fe(VI) [35].

Another study conducted by Ma et al. [36] used sodium-potassium ferrate for the removal of tetracycline hydrochloride (TC) antibiotics at different pH and molar concentrations. Although maximum degradation was observed within a pH range of 9–10 and at a molar ratio between 1:1 and 1:10 [Fe(VI):TC], only 15% mineralization of the compound was observed due to the formation of stable intermediate products. The toxicity and kinetics of diclofenac removal by Fe(VI) under simulated disinfection conditions were studied by Wang et al. [37], and they have observed a rapid increase of the inhibition rate of the luminescent bacteria due to the formation of toxic intermediates. Also, the toxicity of Fe(VI)-treated wastewater containing pharmaceuticals was assessed on zebrafish embryo by Jiang et al. [38] and found that the level of toxicity decreased after the treatment.

The combination of Fe(VI) treatment with radiation for the removal of carbamazepine was studied by Wang et al. [39] for increasing the degradation efficiency and mineralization. They observed an increase in TOC removal during simultaneous treatment. Although the overall degradation rate of carbamazepine decreased, enhanced mineralization was observed with the sequential treatment of radiation, followed by Fe(VI), which may be due to a decrease in pH of the solution from 7.0 to 5.4, where the Fe(VI) oxidation was higher. The performance of electrogenerated ferrate(VI) and solid form of Fe(VI) were compared for the

degradation of amoxicillin and ciprofloxacin [40]. By modeling the ferrate decomposition to understand its oxidation potential, they have concluded that the increased removal efficiency of compounds was due to the presence of a deprotonated form of ferrate ion.

In a study conducted by Yang et al. [41] for the removal of a mixture of emerging contaminants spiked in secondary effluent, only selective oxidation of electron-rich compounds was observed with Fe(VI)-based treatment process. Nevertheless, higher Fe(VI) exposure involved faster destruction of these recalcitrant compounds, proving the effectiveness of these treatments as an efficient tertiary treatment for broad-spectrum micropollutants in wastewater. In another study where mixture of four pharmaceuticals were treated with Fe(VI) (3 mg/L) all the compounds except bezafibrate were degraded effectively [42]. From this observation they have suggested that Fe(VI) is a selective oxidant, and the degradation efficiency will decrease if a carboxylic group is present in the compound.

4.5 Inorganic removal by ferrates

Fe(VI) became environmentally friendly oxidants due to its high oxidizing ability and did not produce any toxic compounds on decomposition. Therefore, the application of ferrates has been widely investigated among the researches for the removal of inorganics from water. Inorganic pollutants such as heavy metals, inorganic salts, trace elements and complexes of metals, among others, can also be removed by Fe(VI). There are basically two types of mechanisms in the ferrate oxidation of inorganic compounds, namely, one-electron transfer and two-electron transfer. Also, the degradation of inorganics is observed to be finished in milliseconds to seconds [19]. For instance, the study by Johnson and Hornstein [43] reported the complete oxidation of hydroxylamine to nitrous oxide by ferrates following a two-electron transfer oxidation mechanism, where the transfer occurs from either ferrates or water.

The application of ferrates for phosphate removal in municipal wastewater treatment plants is a feasible option and needed to be explored in detail. Lee and Zu [44] reported around 80% phosphate removal with a ferrate dose of 7.5 mg Fe L^{-1} . They investigated the performance of various forms of iron such as Fe(VI), Fe(II) and Fe(III) and observed that the efficiency of Fe(VI) is 1.5 times higher than Fe(III) because of the larger aggregate formation with Fe(VI) having higher specific surface. A similar study by Lee and Um [45, 46] utilized the combined use of Fe(III) and Fe(VI) for removal of arsenic by coagulation from river water samples and observed that 90% removal was achieved with an optimum dose of 2 mg L^{-1} Fe(VI) at pH 7.8. Also, potassium ferrate was used to remediate a solution containing a mixture of arsenic and antimony, where at first the compound was oxidized by Fe(VI) and then separated from the solution by the adsorption of its decomposition product [47]. In addition, the kinetics and mechanism of As(III) oxidation by Fe(VI) were studied by Lee et al. [45, 46], and they concluded that oxygen transfer mechanism in aqueous solution resulted in oxidation of As(III) to less toxic As(V).

Ferrate-based oxidation process was used for the removal of insoluble Cr(III) compounds from high-level radioactive tank waste, which was alkaline media [48]. $\text{Fe}_3\text{O}_4^{2-}$ concentration played a significant role in the Cr(III) removal; however, increasing the Fe(VI)/Cr(III) ratio greater than 10 reduced the removal efficiency. Ferrates are also capable of oxidizing organic metal complex species with its simultaneous removal from aqueous solutions [49, 50]. They are successfully used in industrial wastewater containing metal complexes, and treatment process efficiency

depends on pH and Fe(IV) dosage. Among the different metal complexes, zinc cyanide (CN) found in the effluent wastewater of metal finishing industries had a significant environmental impact.

The effect of Zn(II) on the removal of cyanide by Fe(VI) was studied by Yngard et al. [51] at different alkaline pH conditions. Although they have observed a decrease in the oxidation rate of cyanide in the presence of Zn(II), complete removal was achieved by Fe(VI). Another ferrate-based oxidation study was conducted by Lee and Tiwari [52] for the simultaneous removal of CN, CN-Cu and CN-Ni. They have observed that in the CN-Cu and CN-Ni systems, rapid oxidation of CN was observed, while a relatively slower degradation of CN was observed in the mixed CN-Cu-Ni. In another study, Ni(II)-CN and Ni(II)-CN-ethylenediamine-tetraacetate (EDTA) solutions were removed using Fe(VI) as a function of pH ranging from 8 to 11 [53]. The presence of an organic ligand EDTA enhanced the removal of cyanide in Ni(II)-CN-EDTA, while only 60% removal was observed with Ni(II)-CN metal-cyanide complex. The stronger complexes formed due to the addition of EDTA into the Ni(II)-CN metal-cyanide complex reduced the amount of additional Fe(VI) required to oxidize cyanide in it. A similar study conducted by Pachau et al. [54] assessed the suitability of ferrate(VI) for the simultaneous oxidation of Cu(II)-IDA and Zn(II)-IDA (iminodiacetic acid). It was observed that maximum removal Cu(II) or Zn(II) occurred at higher pH values.

4.6 Organic matter and wastewater

Fe(VI) can be effectively and efficiently used for removal of the organic matter present in wastewater. The stronger oxidizing property along with its disinfection and coagulation property makes Fe(VI) an ideal chemical for sewage treatment [55]. One of the main advantages of ferrate treatment is that it produces very less volume of sludge and thus makes sludge treatment much easier [56].

The study by Jiang et al. [12] investigated the applicability of ferrates for disinfection/coagulant and compared the performance with conventional disinfectants and coagulants such as sodium hypochlorite (NaOCl) and NaOCl combined with ferric sulphate or alum for the treatment of water and observed around 20% more removal with ferrates at a pH between 6 and 8. Among the three chemicals, ferric sulphate, potassium ferrate(VI) and aluminum sulphate used by Jiang et al. [55] for sewage treatment, maximum color removal and COD reduction were observed for potassium ferrate(VI). The dual properties of Fe(VI) species capable of oxidizing micropollutants and inorganics in wastewater were assessed for municipal wastewater treatment [57]. They have observed that Fe(VI) was efficient in oxidizing micropollutants and subsequently removing phosphate from a secondary treated effluent in a single treatment step.

In another study, natural organic matter (NOM) present in river and stream water was removed using potassium ferrate [58]. They have observed more than 70% removal of humic and fulvic acids by varying the Fe(VI) dosage, pH and temperature of the solution. The efficiency of ferrate and chlorine on removing organic matters present in secondary treated effluent was compared for two different wastewater treatment plants by Gombos et al. [59]. When comparing the bacterial inactivation, both Fe(VI) and chlorine were very effective even at their lower concentration, while a higher COD and TOC removal were observed for Fe(VI) in comparison to chlorine. The results showed that the higher oxidation capacity along with its coagulation and flocculation property of the reduced Fe(III) ions enhanced the wastewater treatment.

5. Ferrate as a disinfectant

Coagulation and disinfection are the two major unit operations that are important to ensure proper water quality. Disinfection has been known to be a tertiary treatment for the removal of pathogens. While coagulation destabilized the colloids and aggregates them, after which they can be settled and thereafter removed. Over the years, there has been rapid deterioration of the water quality due to increased water pollution. Hence, efficient chemical reagents and treatment techniques are required to meet stringent water quality standards. Various disinfection processes are used these days such as chlorination, UV irradiation and advanced oxidation processes [60].

The most common disinfection method used is chlorination. However, chlorine in the presence of organic substances such as humic acid is known to produce trihalomethanes (THM), which are known carcinogens. Ozonation results in the formation of N-nitrosodimethylamine (NDMA). While, presence of bromide ion also initiates formation of a potential carcinogen bromate [12, 13]. Thus, removing these disinfection byproducts is another challenge. An ideal chemical reagent would thus be a treatment reagent capable of carrying out both disinfections and should also be capable of oxidizing organic as well as inorganic pollutants such as heavy metals. Ferrate, with a redox potential of 2.2 V, higher than ozone (2.0 V), satisfies both requirements [61]. Ferrate is also considered as a “green” chemical. This is primarily because ferrate oxidation does not lead to the production of any harmful byproducts. The product of Fe(VI) oxidation is either ferric hydroxide or Fe(III) [14, 15].

5.1 Effect of ferrate ions on bacteria

Murmann and Robinson were the first to demonstrate the disinfection property of ferrate in the year 1974. The disinfection studies were conducted on two pure strains of non-recombining *Pseudomonas*, combining *Pseudomonas* and Missouri River Water. It was observed that complete killing of bacteria occurred at ferrate concentrations of 4, 50 and 100 ppm, respectively, for all the three tested samples. It was found that ferrate(VI) could kill 99.9% of microbes, such as *E. coli*, within 7 min of contact time and at a dose of 6 mg L⁻¹ at a pH of 8. Also, the disinfection ability enhanced when the pH was below 8. For the same concentration of bacteria, a contact time of 17 min was required in order to achieve the same level of disinfection when the ferrate concentration was reduced to 2.4 mg L⁻¹ [62].

The performance of ferrate as a disinfectant for drinking water was also compared with chlorine. Ferrate was found to achieve >6log₁₀ inactivation of *E. coli* at a very low dose of 6 mg L⁻¹, while 10 mg L⁻¹ of Cl₂ was required to achieve the same level of disinfection. Also, ferrate(VI) was found to work efficiently over a wide range of pH [12]. Similarly, for sewage treatment, potassium ferrate was found to achieve >4 log₁₀ inactivation of bacteria, while alum sulphate and ferric sulphate were able to inactivate only 1 log₁₀ and 1.5 log₁₀ bacteria. Also, the dosage of ferrate required was lesser than that of alum sulphate and ferric sulphate [55]. Effectiveness of ferrate as a disinfectant was also studied on aerobic spore-bearing bacteria, which suggested that sodium ferrate is a powerful disinfectant of this group of bacteria. The study showed that sodium ferrate was a better indicator than even chlorine [63].

Ferrate was also found to inhibit the dehydrogenase activity by inactivating the —SH radical and thus inhibiting both the exogenous and endogenous respiration of bacteria *Sphaerotilus*. The study suggests that intermediates generated during the ferrate decomposition penetrate the cell wall of the bacterium and inactivate the

—SH radical which is necessary for dehydrogenase activity and thus respiration of the bacterium. *Sphaerotilus* is known to cause bulking in activated sludge [64]. Clostridia resistant to chlorination were also found to be killed by ferrate. *Bacillus cereus*, *Streptococcus bovis*, *Staphylococcus aureus*, *Shigella flexneri*, *Streptococcus faecalis* and *Salmonella typhimurium* were also found to be susceptible to ferrate disinfection [4, 9, 10]. However, the gram-positive organisms are found to be more resistant to the ferrate action compared to gram-negative organisms such as *E. coli*.

5.2 Effect of ferrate ions on viruses

Effectiveness of ferrate as a disinfectant on virus removal was checked on human surrogate viruses such as MS2, f2, Q β and P22 bacteriophages [11–13]. Studies suggested that Fe(VI) was more efficient against naked icosahedral coliphages such as MS2 than gram-negative bacteria, *E. coli*. The k_i value for *E. coli* was reported to be 6.25×10^{-1} L/(mgFe \times min) (pH 7.2, 25°C), while the k_i value for MS2 inactivation was 2.27 (± 0.05) L/(mgFe \times min). The faster kinetics for virus inactivation might be because of the denaturation of the genome or transformation of the capsid proteins [65]. Furthermore, coliphages inactivation was found to be affected by pH and dissolved oxygen, thereby supporting the hypothesis stating that slower iron oxidation enhances virus inactivation. The adsorption of intermediates formed during the oxidation on the virus capsids was also necessary to inactivate the virus.

Heffron et al. suggested that coupling iron oxidation with regulated pH, similar to enhanced coagulation, will be able to achieve higher disinfection because of slow ferrous oxidation [66]. f2 and Q β were also found to be removed at a pH range of 6–8 by ferrate oxidation [9, 13]. Also, it was found that ferrate action is not as influenced by the disinfecting matrix compared to that of chlorine [67].

5.3 Effect of ferrate ions on algae

Eutrophication of lakes and rivers has increased rapidly due to discharge of the nutrients into the water bodies, specifically phosphate. Thus, removal of these algal blooms is now a major challenge in the drinking water treatment. Conventional coagulation is presently the method of choice for algal removal in the treatment processes. Copper sulphate and potassium permanganate are chemicals that are most commonly employed to control the algal blooms in lakes and rivers. Studies suggest that pretreatment with an oxidant enhances the algal removal on coagulation. Ferrate being an excellent oxidant was thus checked for algal removal. Algal removal on the addition of alum combined with ferrate pretreatment was found to improve the coagulation of algal cells [68].

It was observed that ferrate peroxidation enhanced the coagulation of algae by hampering the stability of algal colloids. Ferrate oxidation results in the formation of Fe(OH)₃. Fe(OH)₃ precipitates on algal cell surface resulting in increased weight and thus enhanced settleability. It was also hypothesized that on ferrate oxidation, the algal cells release certain exopolymer, which aids the coagulation. In a study conducted on *Microcystis aeruginosa*, it was observed that ferrate oxidation causes complete cell damage. Here the ferrate oxidation resulted in blocking photosynthesis by hampering the PSII functioning. The accumulation of excessive ROS further results in superoxidation of lipids, thereby increasing the cell permeability which finally results in complete cell damage of *Microcystis aeruginosa* cells. The removal of algae on ferrate was also influenced by pH and temperature. The removal efficiency was higher as the temperature increased, and also acidic pH enhanced the ferrate action on green algae [1, 10, 20].

5.4 Effect of ferrate ions on microcystins

Cyanobacteria such as *Microcystis*, *Anabaena*, *Aphanizomenon*, *Oscillatoria*, *Cylindrospermopsis* and *Lyngbya* are known to produce toxins, which affect aquatic life as well as human beings adversely. Some common toxins produced by cyanobacteria include anatoxin-a, anatoxin-as, aplysiatoxin, cylindrospermopsin, microcystin-LR, nodularin R and saxitoxin. Because of its adverse effects, US Environmental Protection Agency (EPA) in the year 2015 prescribed drinking water health advisories for microcystins and cylindrospermopsin. 0.3 mg L^{-1} was the prescribed limit for microcystins for preschool children, while the limit was 1.6 mg L^{-1} for school-age children.

The microcystins are composed of cyclic peptide ring of 7 amino acids and hepatotoxins, which are liver toxins. The peptide ring is composed of 5 non-protein amino acids and 2 protein amino acids. The microcystins' name is derived from these two protein amino acids. The most potent microcystin toxin is composed of leucine and arginine, thus the name microcystin-LR. Microcystin can remain in the water bodies from days to weeks, making it more dangerous. The toxicity of the microcystins is because of its Adda group [9, 14]. Ferrate essentially degrades the toxins by oxidation of the amino groups of microcystins. Thus, ferrate-induced degradation of algal toxins is greatly influenced by pH [69].

6. Conclusions

Ferrate [Fe(VI)] is a powerful oxidizing agent and can be used to remove organic and inorganic pollutants over a wide range of pH. Electrochemical synthesis of ferrate is the greenest and easiest method for high purity ferrate. The application of Fe(VI) for the removal of various recalcitrant pollutants such as pharmaceuticals, textile dyes, phenolic compounds, pesticides and inorganics, including heavy metals, is one of the promising technologies because it can act as oxidant as well as coagulant at the same time. The ability of ferrate to be an oxidant as well as coagulant also enhances removal of algae and microcystins. Also, ferrate is a potent disinfectant capable of removing bacteria as well as viruses. The action of ferrate, however, is dependent on pH and dissolved oxygen level of the media to be disinfected. The pH of the solution is one of the important factors which determines the stability and oxidation potential of Fe(VI). At higher pH values, the stability of Fe(VI) is higher as it increases the reaction rate with protonation of compounds. However, a high alkaline pH of liquid Fe(VI) causes the formation of harmful disinfection byproducts during disinfection treatment. Hence, a detailed research should be carried out for understanding the effect of pH in the treatment of various recalcitrant pollutants with different Fe(VI) concentrations.

Conflict of interest

The authors declare no conflict of interest.

IntechOpen

IntechOpen

Author details

Ansaf V. Karim, Sukanya Krishnan, Lakshmi Pisharody and Milan Malhotra*
Indian Institute of Technology, Mumbai, India

*Address all correspondence to: milanmalhotraiitb@gmail.com

IntechOpen

© 2020 The Author(s). Licensee IntechOpen. Distributed under the terms of the Creative Commons Attribution - NonCommercial 4.0 License (<https://creativecommons.org/licenses/by-nc/4.0/>), which permits use, distribution and reproduction for non-commercial purposes, provided the original is properly cited. 

References

- [1] Malhotra M, Suresh S, Garg A. Tea waste derived activated carbon for the adsorption of sodium diclofenac from wastewater: Adsorbent characteristics, adsorption isotherms, kinetics, and thermodynamics. *Environmental Science and Pollution Research*. 2018;**25**(32):32210-32220. DOI: 10.1007/s11356-018-3148-y
- [2] Ansaf KVK, Ambika S, Nambi IM. Performance enhancement of zero valent iron based systems using depassivators: Optimization and kinetic mechanisms. *Water Research*. 2016;**102**:436-444. DOI: 10.1016/j.watres.2016.06.064
- [3] Malhotra M, Garg A. Performance of non-catalytic thermal hydrolysis and wet oxidation for sewage sludge degradation under moderate operating conditions. *Journal of Environmental Management*. 2019;**238**:72-83. DOI: 10.1016/j.jenvman.2019.02.094
- [4] Divyapriya G, Nambi IM, Senthilnathan J. Nanocatalysts in Fenton based advanced oxidation process for water and wastewater treatment. *Journal of Bionanoscience*. 2016;**10**:356-368. DOI: 10.1166/jbns.2016.1387
- [5] Tiwari D, Kim HU, Choi BJ, Lee SM, Kwon OH, Choi KM, et al. Ferrate(VI): A green chemical for the oxidation of cyanide in aqueous/waste solutions. *Journal of Environmental Science and Health, Part A: Toxic/Hazardous Substances and Environmental Engineering*. 2007;**42**:803-810. DOI: 10.1080/10934520701304674
- [6] Graham N, Jiang CC, Li XZ, Jiang JQ, Ma J. The influence of pH on the degradation of phenol and chlorophenols by potassium ferrate. *Chemosphere*. 2004;**56**:949-956. DOI: 10.1016/j.chemosphere.2004.04.060
- [7] Schreyer JM, Ockerman LT. Stability of ferrate(VI) ion in aqueous solution. *Analytical Chemistry*. 1951;**23**:1312-1314. DOI: 10.1021/ac60057a028
- [8] Licht S, Wang B, Ghosh S. Energetic iron (VI) Chemistry: The super-iron battery, *Science*. 1999;**285**:1039-1043
- [9] Wagner WF, Gump JR, Hart EN. Factors affecting the stability of aqueous potassium ferrate(VI) solutions. *Analytical Chemistry*. 1952;**24**:1497-1498. DOI: 10.1021/ac60069a037
- [10] Virender S. K, potassium ferrate (VI): An environmentally friendly oxidant. *Advances in Environmental Research*. 2002;**6**:143-156. Available from: <http://www.sciencedirect.com/science/article/pii/S1093019101001198>
- [11] Sharma VK, Kazama F, Hu J, Ray AK. Ferrates (iron(VI) and iron(V)): Environmentally friendly oxidants and disinfectants. *Journal of Water and Health*. 2005;**3**:45-58
- [12] Jiang J, Wang S, Panagouloupoulos A. The exploration of potassium ferrate (VI) as a disinfectant/coagulant in water and wastewater treatment. *Chemosphere*. 2006;**63**:212-219. DOI: 10.1016/j.chemosphere.2005.08.020
- [13] Williams DH, Riley JT. Preparation and alcohol oxidation studies of the ferrate (VI) ion, FeO_4^{2-} . *Inorganica Chimica Acta*. 1974;**8**:177-183. DOI: 10.1016/S0020-1693(00)92612-4
- [14] Thompson GW, Ockerman L, Schreyer JM. Preparation and purification of potassium ferrate. VI. *Journal of the American Chemical Society*. 1951;**73**(3):1379-1381. DOI: 10.1021/ja01147a536
- [15] Kopelev N, Perfiliev Y, Kiselev Y. Mössbauer study of sodium ferrates (IV) and (VI). *Journal of Radioanalytical and Nuclear Chemistry*.

1992;**162**(2):239-251. DOI: 10.1016/j.watres.2019.04.045

[16] Jiang J-Q, Lloyd B. Development of ferrate(VI) salt as an oxidant and coagulant for water and wastewater treatment. *Water Research*. 2002;**36**:1397-1408. DOI: 10.4028/www.scientific.net/AMM.361-363.658

[17] Perfiliev YD, Tambiev AK, Konnychev MA, Skalny AV, Lobakova ES, Kirpichnikov MP. Mössbauer spectroscopic study of transformations of iron species by the cyanobacterium *Arthrospira platensis* (formerly *Spirulina platensis*). *Journal of Trace Elements in Medicine and Biology*. 2018;**48**:105-110. DOI: 10.1016/j.jtemb.2018.02.030

[18] Alsheyab M, Jiang JQ, Stanford C. On-line production of ferrate with an electrochemical method and its potential application for wastewater treatment—A review. *Journal of Environmental Management*. 2009;**90**:1350-1356. DOI: 10.1016/j.jenvman.2008.10.001

[19] Sharma VK. Oxidation of inorganic contaminants by ferrates (VI, V, and IV)-kinetics and mechanisms: A review. *Journal of Environmental Management*. 2011;**92**:1051-1073. DOI: 10.1016/j.jenvman.2010.11.026

[20] Jiang JQ, Lloyd B. Progress in the development and use of ferrate(VI) salt as an oxidant and coagulant for water and wastewater treatment. *Water Research*. 2002;**36**:1397-1408. DOI: 10.1016/S0043-1354(01)00358-X

[21] Zhu JH, Yan XL, Liu Y, Zhang B. Improvingalachlor biodegradability by ferrate oxidation. *Journal of Hazardous Materials*. 2006;**135**:94-99. DOI: 10.1016/j.jhazmat.2005.11.028

[22] Chen J, Qi Y, Pan X, Wu N, Zuo J, Li C, et al. Mechanistic insights into the reactivity of ferrate(VI) with phenolic

compounds and the formation of coupling products. *Water Research*. 2019;**158**:338-349. DOI: 10.1016/j.watres.2019.04.045

[23] Chen J, Xu X, Zeng X, Feng M, Qu R, Wang Z, et al. Ferrate (VI) oxidation of polychlorinated diphenyl sulfides: Kinetics, degradation, and oxidized products. *Water Research*. 2018;**143**:1-9. DOI: 10.1016/j.watres.2018.06.023

[24] Yates BJ, Zboril R, Sharma VK. Engineering aspects of ferrate in water and wastewater treatment—A review. *Toxic/Hazardous Substances and Environmental Engineering*. 2014;**4529**. DOI: 10.1080/10934529.2014.950924

[25] Zhang P, Zhang G, Dong J, Fan M, Zeng G. Bisphenol A oxidative removal by ferrate (Fe(VI)) under a weak acidic condition. *Separation and Purification Technology*. 2012;**84**:46-51. DOI: 10.1016/j.seppur.2011.06.022

[26] Sun S, Jiang J, Qiu L, Pang S, Li J, Liu C, et al. Activation of ferrate by carbon nanotube for enhanced degradation of bromophenols: Kinetics, products, and involvement of Fe(V)/Fe(IV). *Water Research*. 2019;**156**:1-8. DOI: 10.1016/j.watres.2019.02.057

[27] Li G, Wang N, Liu B, Zhang X. Decolorization of azo dye Orange II by ferrate(VI)-hypochlorite liquid mixture, potassium ferrate(VI) and potassium permanganate. *Desalination*. 2009;**249**:936-941. DOI: 10.1016/j.desal.2009.06.065

[28] Xu GR, Zhang YP, Li GB. Degradation of azo dye active brilliant red X-3B by composite ferrate solution. *Journal of Hazardous Materials*. 2009;**161**:1299-1305. DOI: 10.1016/j.jhazmat.2008.04.090

[29] Turkay O, Barışçı S, Dimoglo A. Kinetics and mechanism of methylene

- blue removal by electrosynthesized ferrate(VI). *Separation Science and Technology*. 2016;**51**:1924-1931. DOI: 10.1080/01496395.2016.1182189
- [30] Wu S, Li H, Li X, He H, Yang C. Performances and mechanisms of efficient degradation of atrazine using peroxymonosulfate and ferrate as oxidants. *Chemical Engineering Journal*. 2018;**353**:533-541. DOI: 10.1016/j.cej.2018.06.133
- [31] Chen Y, Xiong Y, Wang Z, Chen Y, Chen G, Liu Z. UV/ferrate(VI) oxidation of profenofos: Efficiency and mechanism. *Desalination and Water Treatment*. 2015;**55**:506-513. DOI: 10.1080/19443994.2014.917987
- [32] Liu H, Pan X, Chen J, Qi Y, Qu R, Wang Z. Kinetics and mechanism of the oxidative degradation of parathion by ferrate(VI). *Chemical Engineering Journal*. 2019;**365**:142-152. DOI: 10.1016/j.cej.2019.02.040
- [33] Liu H, Chen J, Wu N, Xu X, Qi Y, Jiang L, et al. Oxidative degradation of chlorpyrifos using ferrate(VI): Kinetics and reaction mechanism. *Ecotoxicology and Environmental Safety*. 2019;**170**: 259-266. DOI: 10.1016/j.ecoenv.2018.11.132
- [34] Sharma VK, Mishra SK, Ray AK. Kinetic assessment of the potassium ferrate(VI) oxidation of antibacterial drug sulfamethoxazole. *Chemosphere*. 2006;**62**:128-134. DOI: 10.1016/j.chemosphere.2005.03.095
- [35] Sharma VK, Mishra SK. Ferrate(VI) oxidation of ibuprofen: A kinetic study. *Environmental Chemistry Letters*. 2006;**3**:182-185. DOI: 10.1007/s10311-005-0002-5
- [36] Ma Y, Gao N, Li C. Degradation and pathway of tetracycline hydrochloride in aqueous solution by potassium ferrate. *Environmental Engineering Science*. 2012;**29**:357-362. DOI: 10.1089/ees.2010.0475
- [37] Wang Y, Liu H, Liu G, Xie Y, Gao S. Oxidation of diclofenac by potassium ferrate (VI): Reaction kinetics and toxicity evaluation. *Science of the Total Environment*. 2015;**506-507**:252-258. DOI: 10.1016/j.scitotenv.2014.10.114
- [38] Jiang JQ, Zhou Z, Patibandla S, Shu X. Pharmaceutical removal from wastewater by ferrate(VI) and preliminary effluent toxicity assessments by the zebrafish embryo model. *Microchemical Journal*. 2013; **110**:239-245. DOI: 10.1016/j.microc.2013.04.002
- [39] Wang S, Hu Y, Wang J. Strategy of combining radiation with ferrate oxidation for enhancing the degradation and mineralization of carbamazepine. *Science of the Total Environment*. 2019; **687**:1028-1033. DOI: 10.1016/j.scitotenv.2019.06.189
- [40] Barişçi S, Ulu F, Sillanpää M, Dimoglo A. The usage of different forms of ferrate (VI) ion for amoxicillin and ciprofloxacin removal: Density functional theory based modelling of redox decomposition. *Journal of Chemical Technology and Biotechnology*. 2016;**91**:257-266. DOI: 10.1002/jctb.4625
- [41] Yang B, Ying GG, Zhao JL, Liu S, Zhou LJ, Chen F. Removal of selected endocrine disrupting chemicals (EDCs) and pharmaceuticals and personal care products (PPCPs) during ferrate(VI) treatment of secondary wastewater effluents. *Water Research*. 2012;**46**: 2194-2204. DOI: 10.1016/j.watres.2012.01.047
- [42] Zhou Z, Jiang JQ. Treatment of selected pharmaceuticals by ferrate(VI): Performance, kinetic studies and identification of oxidation products. *Journal of Pharmaceutical and*

Biomedical Analysis. 2015;**106**:37-45.
DOI: 10.1016/j.jpba.2014.06.032

[43] Johnson MD, Hornstein BJ. The kinetics and mechanism of the ferrate (VI) oxidation of hydroxylamines. *Inorganic Chemistry*. 2003;**42**: 6923-6928. DOI: 10.1021/ic020705x

[44] Lee Y, Zu C. Ferrate (Fe(VI)) application for municipal wastewater treatment: A novel process for simultaneous micropollutant oxidation and phosphate removal. *Environmental Science & Technology*. 2009;**38**:3831-3838

[45] Lee Y, Um I. Arsenic (III) oxidation by iron (VI) (ferrate) and subsequent removal of arsenic (V) by iron (III) coagulation. *Environmental Science & Technology*. 2003;**37**:5750-5756

[46] Lee Y, Um I, Yoon J. Ferrate (VI) oxidation of arsenite (III) and subsequent removal of arsenate (V) by iron (III) coagulation. *Environmental Science & Technology*. 2003;**37**:3-5

[47] Lan B, Wang Y, Wang X, Zhou X, Kang Y, Li L. Aqueous arsenic (As) and antimony (Sb) removal by potassium ferrate. *Chemical Engineering Journal*. 2016;**292**:389-397. DOI: 10.1016/j.cej.2016.02.019

[48] Sylvester P, Rutherford LA, Gonzalez-Martin A, Kim J, Rapko BM, Lumetta GJ. Ferrate treatment for removing chromium from high-level radioactive tank waste. *Environmental Science & Technology*. 2001;**35**:216-221. DOI: 10.1021/es001340n

[49] Tiwari D, Sailo L, Pachuau L. Remediation of aquatic environment contaminated with the iminodiacetic acid metal complexes using ferrate(VI). *Separation and Purification Technology*. 2014;**132**:77-83. DOI: 10.1016/j.seppur.2014.05.010

[50] Sailo L, Pachuau L, Yang JK, Lee SM, Tiwari D. Efficient use of ferrate(VI) for the remediation of wastewater contaminated with metal complexes. *Environmental Engineering Research*. 2015;**20**:89-97. DOI: 10.4491/eer.2014.079

[51] Yngard R, Damrongsiri S, Osathaphan K, Sharma VK. Ferrate(VI) oxidation of zinc-cyanide complex. *Chemosphere*. 2007;**69**:729-735. DOI: 10.1016/j.chemosphere.2007.05.017

[52] Lee SM, Tiwari D. Application of ferrate(VI) in the treatment of industrial wastes containing metal-complexed cyanides: A green treatment. *Journal of Environmental Sciences*. 2009;**21**:1347-1352. DOI: 10.1016/S1001-0742(08)62425-0

[53] Osathaphan K, Tiyanont P, Yngard RA, Sharma VK. Removal of cyanide in Ni(II)-cyanide, Ni(II)-cyanide-EDTA, and electroplating rinse wastewater by ferrate(VI). *Water, Air, and Soil Pollution*. 2011;**219**: 527-534. DOI: 10.1007/s11270-010-0725-1

[54] Pachuau L, Lee SM, Tiwari D. Ferrate(VI) in wastewater treatment contaminated with metal(II)-iminodiacetic acid complexed species. *Chemical Engineering Journal*. 2013; **230**:141-148. DOI: 10.1016/j.cej.2013.06.081

[55] Jiang JQ, Panagouloupoulos A, Bauer M, Pearce P. The application of potassium ferrate for sewage treatment. *Journal of Environmental Management*. 2006;**79**:215-220. DOI: 10.1016/j.jenvman.2005.06.009

[56] Rai PK, Lee J, Kailasa SK, Kwon EE, Tsang YF, Ok YS, et al. A critical review of ferrate(VI)-based remediation of soil and groundwater. *Environmental Research*. 2018;**160**:420-448. DOI: 10.1016/j.envres.2017.10.016

- [57] Lee Y, Zimmermann SG, Kieu AT, Von Gunten U. Ferrate (Fe(VI)) application for municipal wastewater treatment: A novel process for simultaneous micropollutant oxidation and phosphate removal. *Environmental Science & Technology*. 2009;**43**:3831-3838. DOI: 10.1021/es803588k
- [58] Lim M, Kim MJ. Removal of natural organic matter from river water using potassium ferrate(VI). *Water, Air, and Soil Pollution*. 2009;**200**:181-189. DOI: 10.1007/s11270-008-9902-x
- [59] Gombos E, Barkács K, Felföldi T, Vértes C, Makó M, Palkó G, et al. Removal of organic matters in wastewater treatment by ferrate (VI)-technology. *Microchemical Journal*. 2013;**107**:115-120. DOI: 10.1016/j.microc.2012.05.019
- [60] Jiang JQ. Research progress in the use of ferrate(VI) for the environmental remediation. *Journal of Hazardous Materials*. 2007;**146**:617-623. DOI: 10.1016/j.jhazmat.2007.04.075
- [61] Nguema PF, Jun M. Application of ferrate (VI) as disinfectant in drinking water treatment processes: A review. *International Journal of Microbiology Research*. 2016;**7**:53-62. DOI: 10.5829/idosi.ijmr.2016.53.62
- [62] Gilbert MB, Waite TD, Hare C. Analytical notes — an investigation of the applicability of ferrate ion for disinfection. *Journal of American Water Works Association*. 1976;**68**(9):495-497
- [63] Hjelmsø MH, Hellmér M, Fernandez-Cassi X, Timoneda N, Lukjancenko O, Seidel M, et al. Evaluation of methods for the concentration and extraction of viruses from sewage in the context of metagenomic sequencing. *PLoS One*. 2017;**12**:e0170199. DOI: 10.1371/journal.pone.0170199
- [64] Kazama F. Respiratory inhibition of *Sphaerotilus* by potassium ferrate. *Journal of Fermentation and Bioengineering*. 1989;**67**:369-373. DOI: 10.1016/0922-338X(89)90042-1
- [65] Hu L, Page MA, Sigstam T, Kohn T, Mariñas BJ, Strathmann TJ. Inactivation of bacteriophage MS2 with potassium ferrate(VI). *Environmental Science & Technology*. 2012;**46**:12079-12087. DOI: 10.1021/es3031962
- [66] Heffron J, McDermid B, Mayer BK. Bacteriophage inactivation as a function of ferrous iron oxidation. *Environmental Science: Water Research & Technology*. 2019;**5**:1309-1317. DOI: 10.1039/c9ew00190e
- [67] Schink T, Waite TD. Inactivation of f2 virus with ferrate (VI). *Water Research*. 1980;**14**:1705-1717. DOI: 10.1016/0043-1354(80)90106-2
- [68] Ma J, Liu W. Effectiveness and mechanism of potassium ferrate(VI) preoxidation for algae removal by coagulation. *Water Research*. 2002;**36**:871-878. DOI: 10.1016/S0043-1354(01)00282-2
- [69] Deng Y, Wu M, Zhang H, Zheng L, Acosta Y, Hsu TTD. Addressing harmful algal blooms (HABs) impacts with ferrate(VI): Simultaneous removal of algal cells and toxins for drinking water treatment. *Chemosphere*. 2017;**186**:757-761. DOI: 10.1016/j.chemosphere.2017.08.052

Application of Advanced Oxidation Process in the Food Industry

Zhaoran Xin and Lars Rehmann

Abstract

Wastewater in the food industry contains recalcitrant organic compounds and a certain degree of toxicity. Present wastewater treatment plants are insufficient in dealing with the increasing complexity of effluents from modern food industries. Improperly treated wastewaters can lead to soil spoilage and are threats to aquatic life. The reaction of these recalcitrant chemicals with reactive radicals is an efficient treatment strategy. Researchers have proposed advanced oxidation processes (AOPs) that generate reactive radicals including ozonation, UV irradiation, (photo-) Fenton process, etc. This chapter reviews laboratory-scale and pilot-scale AOPs to incorporate with conventional pre-treatment methods and to evaluate their effectiveness and factors including operation condition and catalysts to optimize the process. Further research related to novel catalyst synthesis and cost evaluation of pilot-scale study is suggested.

Keywords: advanced oxidation processes (AOPs), food industry wastewaters, physicochemical methods, biodegradability improvement, combined treatment

1. Introduction

Water is a widely used resource in the food industry such as sanitary water for food processing, as a raw material, and for equipment cleaning. The large consumption of water leads to a corresponding generation of wastewater. Wastewater treatment from a diverse industry is technically more challenging than the treatment of domestic wastewater whose characteristics are largely similar. The various utilizations of water in the industries result in complex compositions of the resulting wastewater [1], which is often a threat to human, plant, and aquatic life [2].

The complexity of wastewaters from the food industry is a more severe issue than its amount. The effluents typically include large total load of organic pollutants such as colored and recalcitrant compounds with high organic loads (chemical oxygen demand, COD), proteins or fat, and chemicals used during processing [1], some with considerable levels of toxicity [3]. Current municipal wastewater treatment plants with the remaining capacity for population growth are not designed to handle the characteristics of such influent loading [4], creating a demand of complementary technologies in addition to traditional treatments.

Advanced oxidation processes (AOPs) generate highly reactive radical (**Table 1**). As one of the most active oxidizing agents, hydroxyl radical is generally

Oxidizing agent	Relative oxidation activity
Positively charged hole on titanium dioxide, TiO_2^+	2.35
Hydroxyl radical	2.05
Atomic oxygen	1.78
Ozone	1.52
Hydrogen peroxide	1.31
Permanganate	1.24
Hypochlorous acid	1.1
Chlorine	1

Table 1.
Relative oxidation activity of some oxidizing agents [5].

Organic compound	Rate constant [$\text{M}^{-1} \text{s}^{-1}$]	
	O_3	HO
Alcohols	10^{-2} -1	10^8 - 10^9
Aromatics	1- 10^2	10^8 - 10^{10}
Chlorinated alkenes	10^3 - 10^4	10^9 - 10^{11}
Ketones	1	10^9 - 10^{10}
N-containing organics	10- 10^2	10^8 - 10^{10}
Phenols	10^3	10^9 - 10^{10}

Table 2.
Reaction rate constants for ozone and hydroxyl radical for organic compounds [7].

used in AOPs. It reacts nonselectively with organic compounds [6] which are resistant to conventional oxidation methods as high reaction rate (**Table 2**).

AOPs are widely used in winery wastewater, olive oil mill wastewater, and slaughterhouse wastewater. In addition to degradation of extra chemical compounds directly, AOPs are used to degrade cellular contents to disinfect wastewater with high organic nature in the dairy industry [8].

However, AOPs are capital-intensive since they include the use of expensive reagents such as ozone and hydrogen peroxide, as well as the cost of equipment including sources of ultraviolet light. Hence AOPs are often combined with traditional treatments to overcome this drawback. The combination technologies reduce toxicity and increase the biodegradability of wastewater effluent after AOPs, which is more suitable for inexpensive biological process.

As a complementary of previous reviews [1, 9], this review categorizes relevant AOP applications in the food sector into winery, olive oil mill, meat industries, dairy, and food dye sections. This work summarizes state-of-the-art wastewater treatment technologies in food industries by AOPs both at laboratory-scale and pilot-scale after 2016. Current treatment technologies are also introduced.

2. Introduction to current wastewater treatment technologies in the food industry

Current wastewater treatment in the food industry is evolving from traditional treatments by focusing on the degradation of excessive organic matters, the

recovery of profitable by-products, and water reusability. Typically wastewater treatment consists of three common stages: primary treatment such as physicochemical treatments partially removing solids; secondary treatment aimed at removing biodegradable organics and suspended solids using biological methods including aerobic and anaerobic processes; and tertiary treatments designed to remove residual compounds of particular concern to the given plant. Current technology alternatives to AOPs for wastewater treatment in the food industry are introduced briefly.

2.1 Evaporation

Natural evaporation during summer can be applied to olive oil mill wastewater (OMW) stored in lagoons, which reduces the volume of waste but results in odor and soil pollution. Alternatively, vacuum evaporation can reduce the volume of wastewater at low temperature and pressure; two streams including distillate and concentrate are separated which can then easily be handled with common treatments [10].

2.2 Land application

The application of wastewater as organic fertilizers has been investigated. High organic loadings in wastewater provide nutrients for soil but can also result in soil contamination. For lower amounts of wastewater, soil can act as biofilter of OMW degradation [11]. In contrary to direct application, composting is more applicable due to the elimination of phenols [12].

2.3 Physicochemical treatments

Colloidal particles in wastewater result in filtering devices clog. To prevent the malfunction of equipment for biological treatment and to meet the discharge requirement, technologies called physicochemical treatments are in demand to eliminate these particles.

The addition of flocculation destabilizes colloidal dispersions which count for the majority of the total dispersed solids (TDS), turbidity, and part of COD. Moreover, lime treatment and adsorption are also practical technologies [13]. Such treatments increase biodegradability during biological treatment and reduce residual components including organic load, color, and metal content after biological treatment [14]. For further study, alternative coagulants are promising to achieve higher removal efficiency, less pollution, and lower health risks [15].

2.4 Membrane technologies

Membrane technology is applied when phytotoxic recalcitrant pollutants invalidate biological treatment [16] or for recovery of valuable products [17]. With the advantage of high efficiency, simple equipment, and convenient operation, membrane technologies are beneficial to small plants that cannot afford high investments. However, membrane fouling needs to be reduced to increase economic feasibility. Pulido et al. reviewed current membrane technologies addressing the efforts of decreasing fouling issues in OMW [16].

According to the comprehensive review papers of winery wastewater treatment, membrane bioreactors are competitive considering water reuse [14, 15].

2.5 Summary

The choice of treatment solution is based on the specific characteristic of wastewater. The combination of complementary treatments is promising to achieve discharge regulation. More detailed current technologies and their comparison are reviewed elsewhere [18].

The advances in wastewater treatment in the food industry are driven by the rising awareness of environment protection in the public. At present, for example, various reactors are being designed for olive mill wastewater treatment, while most of them were not treated before 2004 in the EU [10]. However, the remaining challenges after current treatment call for extra treatment technologies in future research, which might be addressed through AOPs.

3. Application of AOPs in the food industry

3.1 Wineries

In 2016, the worldwide total alcohol consumption was equal to 6.4 liters of pure alcohol per person aged 15 years and older [19]. Accordingly, winery wastewater originates from multiple steps in the production process. One of the origins is fresh water used for cleaning, including washing of equipment and facilities [20], while other streams are directly related to wine, such as the effluent from filtration units and off products [15].

Winery wastewater contains organic matters such as ethanol, sugars, organic acids, phenolic compounds, etc. [15]. Moreover, there are toxic compounds from pesticides used on grapes [22]. Winery wastewater discharged without any treatment would result in soil pollution. General sewage treatment facilities are not sufficient to process the wastewater which leads to acid pH and high COD [27]. The treatment for winery wastewater has to be specific due to the differences between each winery, such as the type of wine, unique component and volume of the wastewater, etc. [28]. Even in the same winery, the effluent is unstable according to the operation period and season [29].

A recent review [15] summarizes the processes currently applied and/or tested for the treatment including physicochemical, biological, membrane filtration and separation, advanced oxidation processes, and combined biological and advanced oxidation processes. Physicochemical processes (i.e., coagulation/flocculation, EC) can be used as pre-treatment to lower TSS. Biological treatment processes using membrane bioreactors (MBR) are promising and are efficient in reducing organic load, while AOPs, especially photo-Fenton as post-treatment in combination with other treatment, show higher efficiency in reducing COD. Mechanism and restriction of each method are reviewed elsewhere [30], also providing a guidance for choosing suitable method according to different matrices. Applications of AOPs in the winery industry since 2016 are summarized in **Table 3**.

The combined electro-Fenton processes and photolysis processes showed higher efficiency in degradation rate and energy consumption because of synergetic effect. Such processes can be implemented in separate steps or can be integrated together. Díez et al. proposed different sequential reactors which are divided into two sections. Wastewater processed in the electro-Fenton section generates Fe complexes, which are decomposed by light radiation in the photolysis section. They initially proposed a two-chamber cubic reactor, which suffered from foam formation during aeration. The foam reduces the irradiation volume; hence the reactor was changed

Winery wastewater origin	Treatment process	Observations	Reference
Simulated winery wastewater (SWW) from commercial wine. COD 14.43 g/L, TOC 3.726 g/L, maximum wavelength 522 nm, color intensity (CI) 1.31, browning index (BI) 0.55, pH 3.9	Photo-electro-Fenton process	TOC reduced to 61% (mercury lamp) and 65% (LED lamp). DC, CI, and BI reduced totally. (optimized condition: electrode gap, 2 cm electric field 15 V; reaction time, 180 min) TOC: 68.14% (RWW1), 68.77% (RWW2)	[21]
Simulated (SE1, SE2) and real (RE) COD 10,940 mg/L TOC 4427 mg/L pH 3.2 COD; TOC of SE2 is about 8 times of SE1 (82,050, 33,200). pH 2.9 COD (86100) of real WW (60100) is similar to SE2; TOC is twofolds of SE2. pH 3.4	Photo-electro-Fenton process	SE1(200 min) Color: 97.49% TOC: 53.01% G-PTFE cathode, flow rate: 2 ml/min SE2: Color: 93% TOC: 65.7% RE: Color: 60% TOC: 51% 5 V, reaction time 1.3 h	[22]
local white wine producer (Spain) pH 4.08 TOC 55 g L ⁻¹	Sequential two-column electro-Fenton-photolytic reactor	Color: 65% TOC: 67%, 64% ^P COD: 77%, 74% ^P IC ₅₀ : 76.5%, 41% ^P M Na ₂ SO ₄ , 75 mg L ⁻¹ of Fe ³⁺ , pH 2 and 5 V Reaction time: 12 h ^P : with pesticides	[22]
Undurraga® Winery Company (Talagante, Santiago de Chile) COD 3490 mg/L TOC 1320 mg/L NTU 15.2	Anodic oxidation	Eliminate COD, TOC, and NTU totally 50 mM of NaCl or Na ₂ SO ₄ and apply higher-density currents (60 mA /cm ²) Reaction time 420 min pH 8.30 ± 0.20	[23]
Douro red wine diluted samples COD 513 mg/L TOC 143 mg/L pH 4.0	Solar radiation-assisted sulfate radical-based advanced oxidation processes (SR-AOP)	TOC: around 50% COD: 75% (pH 4.5, PMS, Fe (II)) Reaction time 3 h	[24]
Wine cellar in the Douro region in the north of Portugal pH = 4.37, COD 600 mg/L, BOD ₅ 145 mg/L, BOD ₅ /COD 0.24. TOC 166 mg/L	UV-C assisted sulfate radical-based advanced oxidation processes (SR-AOP)	COD 96%, TOC 71% Reaction time 240 min. pH 7. Consumed 25 mM S ₂ O ₈ ²⁻ UV-C = 254 nm	[25]
pH = 3.8, COD 2.128 g/L, BOD ₅ 974 mg/L, TOC 825 mg/L	Adsorption and photo-Fenton process Ca-smectite as adsorbent and catalyst support	TOC reduced 90% in total, by 54% (adsorption) and 36% (photo-Fenton) pH = 4, H ₂ O ₂ 98 MM, catalyst 6 g/L	[26]

Table 3.
 Recent application of AOPs in the winery industry.

into two divided columns. The economic efficiency was increased by decreasing the voltage from 15 to 5 V [21, 22]. In order to minimize the electrode gap, the reactor system is designed in two columns connected vertically. The efficiency for

degradation of TOC and decreasing color increased in treating real winery wastewater compared to initial laboratory studies.

Both studies investigating simulated winery wastewater using column reactors eliminate color totally. Other than color, TOC reduction rates are both nearly 65%. However, the efficiency reduced with an increased concentration of TOC, which reduces $\cdot\text{OH}$ from UV radiation, and accumulated carboxylic acids inhibit regeneration of Fe(II) by reacting with Fe(III) [22].

Anodic oxidation with boron-doped diamond (BDD) electrode is able to process real effluents with high concentration of COD (3490 mg/L), TOC (1320 mg/L), and more than 40 organic compounds [23]. The addition of electrolytes including NaCl and Na_2SO_4 and the application of high-density currents (60 mA/cm^2) increased the efficiency of oxidation, leading to total mineralization in 400 min. The higher efficiency of this process results from the larger number of radicals which have two origins: (i) $\text{HO}\cdot$ radicals are weakly bounded on BDD electrode with high O_2 -overpotential; (ii) addition of salt generates other radicals such as $\text{S}_2\text{O}_8^{2-}$ and active chlorine species.

Solar-driven sulfate radical is also a promising tertiary treatment [24]. This process has the advantage of independence from pH. The addition of transition metal as catalyst including Fe(II) and Co(II) shows that Fe(II) performs best when considering environmental implications and efficacy. Furthermore, the reduction of TOC could be enhanced from around 50–71% by combination of UV radiation and thermally activated persulfate (TAP) [25]. It indicates higher efficiency of $\text{S}_2\text{O}_8^{2-}$ than H_2O_2 for removal of COD (96%) and organic matters, as the UV-C/ $\text{S}_2\text{O}_8^{2-}$ process generates two kinds of radicals, $\text{HO}\cdot$ and $\text{SO}_4^{\cdot-}$, where the yield of $\text{SO}_4^{\cdot-}$ is higher and $\text{SO}_4^{\cdot-}$ can be converted into $\text{HO}\cdot$.

Natural Ca-smectite can be used for removal [26]. It works both as adsorbent and catalyst support saturated with Fenton. The adsorption capacity can be predicted by Jovanovich isothermal model. For photo-Fenton process' operation condition regarding pH, H_2O_2 concentration and catalyst dosage were optimized, yielding 90% of TOC removal with 54% due to adsorption and 36% due to the photo-Fenton process. However, catalyst regeneration analysis in three consecutive cycles shows reduction to 57%.

Based on the complex organic components and toxicity of winery wastewater, each method aims at increasing the effective radicals. Further study related to reactor optimization, utilization of multiple radicals, and novel catalyst synthesis is worthwhile.

3.2 Olive oil mills

The high demand of water in olive oil production processes results in large amounts of wastewater ranging from 0.5 to 1.68 m^3 per ton with large amounts of semisolid or slurry wastes.

Factors influencing the characteristics of olive oil mill wastewater (OMW) include (i) composition of vegetation water, (ii) olive oil extraction process, and (iii) storage time [30]. Moreover, phenolic compounds result in toxicity of the effluents. However, properly treated OMW produces nutrients (N, P, K) for plants [31]. Therefore, pre-treatment steps are necessary to economically increase the efficiency of the following treatment steps, as summarized in **Table 4**.

A photo-Fenton with medium pressure UV-lamp process was developed for mixture of real OMW [32]. This process showed the ability of fast degradation of pollutants (>90% in 30 mins). The wavelength of UV light did not influence the reduction rates. Another factor is the concentration of H_2O_2 . The total nitrogen content removal rate is not related to the concentration of H_2O_2 but the reaction

Olive oil mill wastewater origin	Treatment process	Observations	Reference
Olive oil mill in the province of Seville (Spain) mixture of WOW (olives washing) and WOOW (olive oil washing) pH 5.98; COD 7060 mg/L; TOC 918 mg/L; BOD ₅ 685 mg/L; turbidity (FTU) 1390	Photo-Fenton	Nitrogen content removed 62.5–75.5%, COD = 95.7 ± 0.53%, TOC 96.3%, total phenolic compounds = 93.6 ± 2.5%, total carbon = 94.0 ± 1.2%, total organic carbon = 96.3 ± 0.6%, total nitrogen = 74.9 ± 6.8%, turbidity = 92.5 ± 1.9%. pH = 3, T = 20°C, catalyst = 3 g/L, reaction time 5–30 min, agitation rate = 600 rpm	[32]
Adjusted olive oil mill (mean value) samples from Cyprus, Israel, Jordan, and Portugal. pH 5.2 EC 12.5 mS/cm COD 25.0 g/L BOD ₅ 5.1 g/L DOC 6 g/L TSS 24 g/L TP 4.2 g/L TPh 4.2 g/L	Coagulation/flocculation followed by solar photo-Fenton oxidation	Coagulation/flocculation TSS 90%, COD 40%, DOC 11% Solar photo-Fenton oxidation COD 94%, DOC 43%, BOD ₅ 86%, TSS 96%, TPh 99.8% Reaction time 70 min	[17]
Badajoz (Spain) pH 4.9 COD 6450 mgO ₂ /L TN 42 mg/L TP 21 mg/L TSS 3190 mg/L BOD ₅ 2130 mg O ₂ /L BOD ₅ /COD 0.33	Coagulation/flocculation followed by Fenton oxidation and biological treatment (only industry)	Lab Coagulation/flocculation COD 38% + 75% TSS 40% Industry COD 95% Flow rate 1.5m ³ h ⁻¹ Reaction time 60 days	[33]
COD 1344 ± 22 mg/L; TN 22.4 ± 1.4 mg/L; total phosphate 19.1 ± 1.6 mg/L; phenols 5.89 ± 0.8 mg/L; pH 6.9; conductivity 1260 ± 32 μS/cm Color, expressed as Pt/Co units 2310 ± 9 Olive Oil washing wastewater after filtration Mersin, Turkey	Combined electrocoagulation (ECR)-photocatalytic (PCR) degradation system	ECR + PCR COD 88% Phenol (ECR: 88%) 100% Color 100% Reaction time PCR + ECR COD 78% Phenol 93.2% (PCR: 40.7%) ECR: voltage, 12.5 V; CD, 12.9 A/m ² ; pH, 6.9; reaction time, 120 min; electrode type, Al PCR: catalyst loading, 1 g/L; catalyst type, ZnO; pH, 7.7; reaction time, 120 min; light source, (UVA)	[34]
COD 33927 ± 200 mg/L DOC 10120 mg/L Phenol 164 ± 13 mg/L Color 13,350 ± 120 (Pt-Co) Acid-cracked wastewater from olive production factory. Kahramanmaras, Turkey	Combined ozone/Fenton process	Color 51.6% +21% DOC 27.9% + 49% CODs 58% +22% Phenol 100%	[35]

Olive oil mill wastewater origin	Treatment process	Observations	Reference
TOC 23231–34,050 mgL ⁻¹ COD 62400–82,400 mgL ⁻¹ Color 369 Pt-Co pH 4.5 BOD ₅ /COD 0.144 100 times diluted sample wastewater from olive production factory. Gemlik region, Turkey	Microwave (MW) activated persulfate	TOC 100% COD 63.38% Color 94.85% Optical density 121.7% PS: 266 g L ⁻¹ Reaction time 23.58 min Power level 567 W Initial pH 2	[36]

Table 4.
Recent application of AOPs on OMW.

time. The removal efficiency decreased with longer reaction time since more N₂ is fixed with abundant CO₂. The conversion rates of TOC have all reached more than 90% and increased slightly with increasing H₂O₂ concentrations.

Solar photo-Fenton oxidation pretreated by coagulation/flocculation achieved 90% TSS removal at optimal dose of FeSO₄·7H₂O [17]. After coagulation, solar photo-Fenton oxidation removed up to 94% of COD. In this process, Fe²⁺ should be chosen to promote the regeneration of Fe(II). Otherwise, at higher Fe(II) concentration, the penetration efficiency of light decreases. At lower Fe(II) concentration, it accelerates consumption of H₂O₂ without the generation of ·OH, which also explained the low efficiency in high H₂O₂ concentration. Furthermore, the solar photo-Fenton-treated effluents contained fewer toxic matters and lead to higher nutrient uptake by plant. It appears to an efficient and economic technology for plants which can take advantage of sunshine. A similar technology was applied without solar photocatalysis, and the removal efficiency of COD decreased to 75% [33]. However, it increased to 95% after 60 days biological treatment since the process increases the biodegradability. Similar effects for different dosages of Fe²⁺ were observed. Scale-up experiment in industry indicates that adjusting the reagent dosages by monitoring the concentration of COD is necessary to optimize efficiency and cost. Compared with lab scale, decreased efficiency of degradation might be a result of the complexity of real matrices.

Optimal operation condition for electrocoagulation (ECR) and photocatalytic (PCR) process were investigated [34]. For ECR, neutral pH and higher current density are chosen to optimize the solubility of aluminum hydroxide, which enhances electrocoagulation of COD, phenol, and color. For PCR, different types of catalyst, including ZnO and TiO₂, had similar removal efficiency of COD and color. But ZnO has higher efficiency in phenol removal while also having a cost advantage. Sequential application of ECR before PCR results in higher degradation in COD and phenol.

Fenton process followed by ozonation has also been optimized [35]. Considering removal efficiency and cost of ozone, 90 min was found to be the optimal reaction time. However, subsequent biological treatment processes are needed to meet regulatory guidelines for COD and color.

Oxidation of OMW by microwave (MW)-activated persulfate is a promising pre- or post-treatment step [36]. Based on dielectric heating principle, MW irradiation is efficient in heating, which activates persulfate and breaks down phenolic compounds which have dark brown color. Hence MW counts for main removal of TOC, operating cost, and a portion of color reduction, while pH is the dominant factor in reducing color.

Rich in nutrient and color, more OMW is degraded by Fenton process in combination with pre-treatment technologies after 2016, compared with previous

comprehensive literature review [13]. Factors involved in Fenton process are investigated extensively, including dosage of reactants and catalyst, pH, and reaction time. For further study, different combination of conventional pre-treatment methods and Fenton process can be analyzed. In addition, great effort for scale-up study and cost evaluation is needed.

3.3 Meat processing industry

The meat processing industry produces large volumes of slaughterhouse wastewater (SWW). SWW contains elevated amount of organic matter, suspended solids, oil, grease, and toxic matters [37]. Anaerobic treatment is efficient in removing organic matter with low costs in addition to the generation of methane. However, complementary treatment is necessary for the effluents to meet the required discharge limits [38]. As post-treatment method, AOPs are a promising supplementary for the entire process in removing non-biodegradable organics and inactivated microorganisms producing hazardous by-products [37] as summarized in **Table 5**.

UV/H₂O₂ has been applied to degrade slaughterhouse effluents pretreated by anaerobic baffled reactor (ABR) and an aerobic activated sludge (AS) reactor connected sequentially [37]. RSM was used to optimize the operation condition in order to maximize removal efficiency of TOC and TN and CH₄ yield, as well as minimize H₂O₂ in effluent.

This process can be enhanced by silver-doped TiO₂ nanoparticles as photocatalyst [42]. Electrons captured by silver react with oxygen more efficiently than those combined with electron hole in TiO₂. However, application of silver and further treatment for separation of photocatalyst make it an uneconomic technology for practical use.

The combined UV-C/H₂O₂-VUV was studied with the similar method used by Bustillo-Lecompte, but a Box-Behnken design was used instead of the CCD [39]. The combined process removed more TOC and minimized H₂O₂ simultaneously compared with individual processes. Furthermore, this technology performs better if applied after biological treatment, since the respirometry analyses indicated low biodegradable degree. Wastewater pretreated by anaerobic digestion can yield up to 90% COD removal but remains yellow in color after 30 days [41]. Further treatment is necessary to remove more COD and eliminate color compounds, which can be achieved by SPEF with BDD anode. SPEF results in higher decline of absorbance and COD than photolysis only and less cost compared with electron-Fenton (EF) [42] and Fenton process only [40].

Compared with conventional disinfection methods, cold plasma technology has the advantage of less by-product and high removal efficiency [43]. This technology achieved high removal efficiency of pathogens, organics, and inorganic pollutants at the same time with enough hydraulic retention time. Furthermore, other operation condition for cold plasma can be investigated.

Various AOPs combined with biological treatment methods have been applied. Treatment of wastewater from meat processing industry meets specific challenge including methane production. Different experiment strategies are performed to study the factors. Cost evaluation in scale-up plant is needed considering both removal efficiency and overall economy, including cost and profits of CH₄.

3.4 Dairy wastewater

The consumption of dairy production in Canada increases gradually. Correspondingly, more wastewaters need to be treated. Dairy industries' wastewaters come from processing milk and system management and typically contain large

Meat processing plants wastewater origin	Treatment process	Observations	Reference
BOD 1209 mg/L COD 4221 mg/L TN 427 mg/L TOC 546 mg/L TP 50 mg/L TSS 1164 mg/L pH 6.95 Slaughterhouse effluents in Ontario, Canada	An anaerobic baffled reactor (ABR), followed by an aerobic activated sludge (AS) reactor, and a UV/H ₂ O ₂ photoreactor (ABR-AS-UV/H ₂ O ₂ processes)	TOC 97.8% H ₂ O ₂ residual 1.3% TOC 50 mg/L, flow rate 15 mL/min, H ₂ O ₂ dosage 344 mg/L, pH 7.2	[37]
Slaughterhouse effluents in Ontario, Canada	Combined UV-C/H ₂ O ₂ -VUV	TOC 46.19% H ₂ O ₂ residual 1.05% TOC 213 mg/L H ₂ O ₂ dosage 450 mg/L Irradiation time 9 min	[39]
pH 7–8.3 COD 25–32 g/L Volatile solid (VS) 3.31–9 g/L TS 5.32–11.5 g/L Total coliforms MPN/100 mL 90x10 ⁵ Fecal coliforms MPN/100 mL 20 × 10 ⁵ EC 550–900 μS/cm TDS 0.9–1 g/L Color 800–1197 Pt/Co SVI 900–950 mL/g	Fenton process	TS 50% VS 61% COD 53% Color 61% pH = 3 Reaction time 150 min c(H ₂ O ₂) = 4000 mg/L	[40]
TOC 132 mg/L COD 480 mg/L BOD ₅ 267 mg/L Slaughterhouse in Puente Alto, Santiago, Chile	Anaerobic digestion followed by solar photoelectron-Fenton (SPEF)	COD 97% Turbidity and solids total removal CH ₄ accumulation 90 mL pH 3 Fe ²⁺ 1 mM Reaction time 180 min	[41]
pH 6.687 BOD 1078.45 mg/L COD 2024.5 mg/L N 74.8 mg/L Slaughterhouse effluent from Lahore, Pakistan	Photocatalytic oxidation assisted with TiO ₂ and silver-doped TiO ₂ nanoparticles	BOD 95% COD 87% N 74% Ag-TiO ₂ -H ₂ O ₂ under UV (400 Watt)	[42]
COD 7.4 g/L TN 609.9 mg/L TP 44.1 mg/L T-Fe 66.9 mg/L Toxic unit (TU) 13.8 Total coliforms 267,000 CFU/ml Slaughterhouse effluent from Nonsan, Korea (average)	Cold plasma	COD 78–93% TN 51–92% TP 35–83% T-Fe 93% Bacteria 98% TU 96%	[43]

Table 5. Recent application of AOPs on meat processing industry.

amounts of organic materials, suspended solids, oils, salts, and fats [44]. The following AOPs (**Table 6**) are studied to degrade excessive pollutants.

Kinetic models describing the COD degradation of flotation/ozonation processes have been developed and compared [45]. The highest kinetic constant can be achieved for ozonation at acidic medium. The results imply that pre-treatment is necessary to remove the scavengers of HO· in milk. Moreover, participation of casein at low pH might also contribute to the removal of COD. The process could be enhanced further by the addition of H₂O₂ [46], which was then optimized via a CCD (pH, dosage of H₂O₂, ozone, and catalyst). Ozonation is also efficient in decomposing antibiotic in milk based on electrophilic attack by O₃ rather than generated HO· [52].

RSM has been applied to optimize the operation condition of electro-Fenton process with iron electrodes [47]. In order to maximize the removal rate of color and COD, five factors are investigated, including reaction time, current density, pH, H₂O₂/DW (mL/L), and molar ratio. The results reveal strong interactions between pH and molar ratio, as well as between pH and current density. Increasing the current density below the optimal point accelerates Fe²⁺ regenerated from Fe³⁺, but higher current density results in the generation of O₂ and H₂. Longer reaction times increase removal efficiency, while high pH results in iron ion precipitation, and low pH affects H₂O₂ decomposition into ·OH. Similar process analyzed via RSM was done for Fenton only processes [48]. The electro-Fenton process has the advantage of less consumption of chemicals. Besides removal of chemicals, disinfection of dairy effluent has also been studied [51]. The electrocoagulation process followed by electro-Fenton (EF) or UVA-assisted photoelectro-Fenton (PEF) is suitable for this objective. The results show that EF and PEF are more efficient in inactivation. PEF is better than EF because of UVA radiation.

TiO₂ has also been used as a catalyst to disinfect dairy wastewater [8] which is used as an irrigation water resource. The results show that disinfection efficiency is higher with the addition of TiO₂ and that oxygen accelerates the photocatalysis process. The removal efficiencies of COD, BOD, and SS increased with TiO₂ as photocatalyst illuminated by UV light combined with biological treatment compared with photocatalytic UV reactor only [49].

AOPs in dairy wastewater often operate with biological treatment methods. The operation conditions are optimized by RSM and well explained. Other than elimination of general TOC, COD, and BOD, dairy wastewater treatment also requires disinfection for further application.

3.5 Miscellaneous food industry wastewaters

The diversity of the food industry results in a multitude of wastewater effluents. They are often rich in refractory organics and color compounds. The following table presents existing technologies in other types of food industries (**Table 7**). AOPs have also shown capability for degradation of these effluents.

Molasses used in the production of baker's yeast result in dark color and high organic load of wastewater. The color compound is recalcitrant to aerobic and anaerobic processing. Ultrasonic irradiation assisted by TiO₂-ZnO decolorized the effluent by 25% [53] after optimization (factors: reaction temperature, catalyst composite and calcination temperature, and catalyst load). However, the COD did not change because ultrasonic irradiation transformed organics into smaller intermediate.

In beverage production, 1.72 L wastewater is produced for every 1 L beverage [54]. Photocatalytic processes have been used to degrade synthesized beverage wastewater effluent [54], showing advantages of cerium doped ZnO and favorable

Dairy wastewater origin	Treatment process	Observations	Reference																					
COD 2000 mg/L Simulate WW: whole milk + distilled water	Flotation/ozonation	More than 80%	[45]																					
COD 2000 mg/L Simulate WW: whole milk + distilled water	Flotation followed by O ₃ /H ₂ O ₂ and O ₃ /Mn ²⁺	64.5% O ₃ 42.9 mg/L H ₂ O ₂ 1071.5 mg/L pH 10.9	[46]																					
COD 2527 mg/l Color 100 pH 6.27 Conductivity 210 µs/cm TDS 981 mg/L	electro-Fenton process	<table border="1"> <thead> <tr> <th>Factors</th> <th>COD</th> <th>Color</th> </tr> </thead> <tbody> <tr> <td>Removal</td> <td>91.76</td> <td>95.22</td> </tr> <tr> <td>Current density (mA/cm²)</td> <td>56</td> <td>55.1</td> </tr> <tr> <td>Reaction time (min)</td> <td>90</td> <td>86</td> </tr> <tr> <td>pH</td> <td>7.52</td> <td>7.48</td> </tr> <tr> <td>Molar ratio H₂O₂/Fe²⁺</td> <td>3.965</td> <td>3.987</td> </tr> <tr> <td>H₂O₂/DW (mL/L)</td> <td>0.898</td> <td>0.907</td> </tr> </tbody> </table>	Factors	COD	Color	Removal	91.76	95.22	Current density (mA/cm ²)	56	55.1	Reaction time (min)	90	86	pH	7.52	7.48	Molar ratio H ₂ O ₂ /Fe ²⁺	3.965	3.987	H ₂ O ₂ /DW (mL/L)	0.898	0.907	[47]
Factors	COD	Color																						
Removal	91.76	95.22																						
Current density (mA/cm ²)	56	55.1																						
Reaction time (min)	90	86																						
pH	7.52	7.48																						
Molar ratio H ₂ O ₂ /Fe ²⁺	3.965	3.987																						
H ₂ O ₂ /DW (mL/L)	0.898	0.907																						
COD 6055 mg/L TS 11900 mg/L TSS 1320 mg/L Color (Pt-Co) 1700 pH 5.7 Conductivity 6 mS/cm Wastewater treatment plant produces milk, yogurt, and butter	Electro-Fenton process	electro-Fenton COD 72% Orthophosphate 88% SS 92% Color removal efficiencies 92.5% H ₂ O ₂ /COD ratio 2, current density 32 mA/cm ² , pH 2.4 and reaction time 45 min	[48]																					
pH 6.5–7.5 Turbidity 2–5 NTU DO 6.5–7.5 mg/L Microbes 2300e2900 CFU·mL ⁻¹ Dairy wastewater after treated by activated sludge process (extended aeration)	Solar photocatalysis (ph-C S) concentrated solar photocatalysis (ph-C CS) solar photolysis (ph-L S) concentrated solar photolysis (ph-L CS) TiO ₂ as catalyst	Disinfection efficiency ph-C S 41% ph-C CS 97% ph-L S 10.5% ph-L CS 68.9% Reaction time 30 min	[8]																					
COD 876 ± 255 mg/L BOD 33 ± 10 mg/L SS 580 ± 159 mg/L Conductivity 1.6 ± 0.4 mS/cm pH 7.9 DO 1.8 ± 0.3 mg/L Dairy effluent after a three-step piggery wastewater treatment (TPWT) system, involving (1) solid/liquid separation, (2) anaerobic treatment, and (3) aerobic	Photocatalytic UV reactor (UVR) followed by bioreactor	Photocatalytic + biological COD 72% BOD 98% SS 79% UV only COD 53% BOD 62% SS 62%	[49]																					

Dairy wastewater origin	Treatment process	Observations	Reference
treatment (activated sludge basin with a final clarifier)			
Wastewater after anaerobic and aerobic ponds	Ultraviolet/persulfate (UV/PS) oxidation		[50]
pH 5.7 ± 0.2 Conductivity 2.95 ± 0.12 mS/cm TOC 1416 ± 24 mg C L ⁻¹	Electrocoagulation (EC) with Fe electrodes followed by electro-Fenton (EF) or UVA-assisted photoelectro-Fenton (PEF) with BDD or RuO ₂ -based anode	Not available	[51]

Table 6.
 Recent application of AOPs in the dairy industry.

Wastewater origin	Treatment process	Observations	Reference
Absorbance at 400 nm 0.3–0.4 pH 5–6 COD 4800–5400 mg/L Baker's yeast factory effluent (Turkey)	Ultrasonic irradiation TiO ₂ -ZnO as sonocatalyst	Decolorization 25% COD 22.4% (no reduction by ultrasound) Ultrasonic irradiation 20 kHz, 200 W TiO ₂ /ZnO 4:1 molar ratio (0.15 g/L) 700°C for 60 min	[53]
COD (mg/L) 500–3000 pH 4.7 EC ($\mu\text{s}/\text{cm}^2$) 1845 Turbidity (NTU) 100 Total dissolved solids (TDS) (mg/L) 850 Synthesized beverage industry effluent	UV and solar illumination assisted by synthesized catalyst, immobilized cerium doped ZnO	Photodegradation efficiency* Catalyst dosage 1–5% 35.33–51.56% (UV) 19.86–32.45% (visible light) COD initial concentration 500–3000 mg/L 65.14–21.9% (UV) 42.13–10.12% (visible light) Reaction time 120 min	[54]
COD 15290 ± 855 mg/L TSS 14950 ± 2400 mg/L Palm oil mill effluent (POME) from Rantau, Malaysia	Coagulation by chitosan, addition of ferrous sulfate (FeSO ₄), chitosan with hydrogen peroxide (H ₂ O ₂), and chitosan with Fenton oxidation	COD $82.82 \pm 1.71\%$ TSS $89.92 \pm 0.48\%$ Chitosan (2500 mg/L) with H ₂ O ₂ (500 mg/L) pH 7 Reaction time 15 min mixing +1 h sedimentation	[55]
pH 3.6–4.5 Conductivity ($\mu\text{S}/\text{cm}$ 20 C) 450–550 TSS (mg/L) 240–280 COD (mg/L) 10,000 BOD ₅ (mg/L) 4246–5252 DOC (mg/L) 4218–4260 NTU 130–160 Color 450–100 BOD ₅ /COD 0.43–0.53 Diluted citrus effluents from Cuba	1. Ozone-based processes (O ₃ , O ₃ /OH ⁻ , O ₃ /UV, O ₃ /H ₂ O ₂ , and O ₃ /UV/H ₂ O ₂) 2. Solar photo-Fenton treatment	1. Ozone-based processes COD 15.7% DOC 10.9% pH 7 Ozone 1.9 g/L UV 254 nm Reaction time 150 min H ₂ O ₂ 1017 mg/L 1. Solar photo-Fenton treatment COD 77% DOC 53%	[56]

*Calculation based on adsorption reading through spectrophotometry.

Table 7.
 Recent application of AOPs in miscellaneous food industries.

effect of an acidic environment. Large amounts of wastewater effluents result from the fast growth of the palm oil industry [55]. AOPs utilizing FeSO_4 or H_2O_2 and the contribution of chitosan as flocculant have been investigated for such water. Process optimization revealed opposite fluctuation of removal efficiency for COD and TSS with different combination of reagents. Furthermore, chitosan (2500 mg/L) with H_2O_2 (500 mg/L) results in the best removal efficiency as post-treatment of anaerobically digested POME [55].

The effluents of citrus fruit processing facilities are characterized by acidity, presence of essential oils, and toxicity. Diluted real citrus juice wastewater was investigated with various ozonation process, and it was found that the solar-Fenton process is better both in removal efficiency and economic perspective [56].

In the coffee industry, wastewater effluent treatments have recently been reviewed elsewhere [57]. The main characteristics of these streams are the presence of various color compounds and macromolecules. AOPs have been proven to be efficient in combination with biological treatment [58]. However, considering the nature of color compounds, ion exchange is a more promising field.

Wastewater treatment for different food or beverages should be adjusted according to the characteristics of different effluents such as complex color compounds (yeast and coffee) or low pH (juice). Pre-treatment such as coagulation or anaerobic digestion is favorable.

3.6 Food dyes

Apart from wastewater effluents from food processing factories directly, municipal wastewater contains some refractory compounds from food industries. Food dyes are extensively used in fruit juices and sweets products as food additives. The colored effluents from such industries need to be treated carefully before discharge. Otherwise they will lead to issues such as pollution on esthetic grounds and interference of light transmission [59].

Food dye	Treatment process	K_{app}	Reference
Ponceau 4R	Electro-oxidation 1. Electrogenerated H_2O_2 (EO- H_2O_2) 2. Electro-Fenton (EF) 3. Photoelectro-Fenton (PEF)	$(10^{-2} \text{ min}^{-1})$ 1. 2.72 ± 0.41 2. 12.31 ± 0.53 3. 13.35 ± 0.66 (real water matrices)	[61]
Amaranth food dye (AM)	Heterogeneous E-Fenton process with synthesized $\text{Fe}_3 - \text{xCu}_x\text{O}_4$ ($0 \leq x \leq 0.25$) NPs	$4.2 \times 10^{-2} \text{ min}^{-1}$ ($x = 0.25$)	[62]
Brilliant blue FCF (BBF)	Fe_3O_4 - TiO_2 (FTNs) assisted with different UV light	0.059 min^{-1} (FTNs/UVA/PMS)	[63]
Carmoisine (E22)	UVA-LEDs/PMS/ Fe^{2+}	0.1553 min^{-1}	[64]
Tartrazine	Visible light photo-Fenton oxidation with three bismuth oxyhalide catalysts	$0.0026\text{--}0.06 \text{ min}^{-1}$ Temperature from $30\text{--}70^\circ\text{C}$	[65]
Sunset yellow FCF (SY)	Electrochemical assisted with palladium-ruthenium nanoparticles incorporated with carbon aerogel (Pd-Ru/CA)	0.295 s^{-1}	[66]
Tartrazine yellow (TT) and brilliant blue (BB)	Photocatalytic process	0.016 min^{-1}	[67]

Table 8. Recent application of AOPs in food dyes.

Azo compounds are widely used in food industries because of its brilliant shades, relative low cost, and simple manufacture [60]. However, azo compounds are resistant to conventional treatment due to one or more azo bonds [61]. Hence the following AOPs (**Table 8**) are applied to degrade specific food dyes.

Fenton process is widely used. Thiam et al. proposed the routes for ponceau 4R degradation. The Fenton process was found to provide fast $\cdot\text{OH}$ production and stability despite the interference of real water matrices [61].

Fenton processes can be enhanced by various catalysts. In order to circumvent the pH limitation of Fenton processes, catalysts with immobilized iron ions are synthesized to avoid precipitation. The combination of magnetite (Fe_3O_4) and copper presents high specific surface area and synergic effects between $\text{Cu}^{2+}/\text{Cu}^+$ and $\text{Fe}^{3+}/\text{Fe}^{2+}$. Moreover, it is easy to separate [62]. Similarly, $\text{Fe}_3\text{O}_4\text{-TiO}_2$ (FTNs) [63] as well as metal doped bismuth oxyhalide catalysts (BiOCl , Cu-BiOCl , and Fe-BiOCl) have been used to degrade BBF [65].

Compared with conventional UVA, UVA-LED are more efficient and cost beneficial. The implementation of UVA-LED accelerates the regeneration of radicals. [64]. Zazouli et al. also suggest that UVC, a high energy UV source, is more efficient in decomposing PMS into $\cdot\text{OH}$ and $\text{SO}_4^{\cdot-}$ than UVA [63]. The replacement of batch reactors by flow reactors is another promising modification [67].

In dealing with a specific food dye, catalysts are synthesized to assist AOPs. The operation conditions such as catalyst dosage and UV source have to be considered. Further studies are required related to economic catalyst development and ease of separation and recovery.

4. Practical application of AOPs

Wastewater treatment in the food industry with AOPs is a flourishing field. Nevertheless, pilot-scale plants are not widely studied. A number of studies implement AOPs in sequential approaches with a complete solution for the treatment and reuse of a complex wastewater from food industries.

Yalılı Kılıç et al. investigated the pilot-scale treatment of olive oil mill wastewater [68]. The combination of physicochemical treatment, ultrafiltration, and $\text{O}_3/\text{H}_2\text{O}_2/\text{UV}$ presented the most favorable results of pollutant removal. However, cost evaluation indicates that the absence of ozone is more economic without removal efficiency diminishment. Another study applied Fenton process in a CSTR at pilot scale [69]. The results highlight the importance of operation condition optimization in actual plant condition. However, such a process is not affordable for small facilities generating large amount of pollutants.

In the winery wastewater treatment field, ozone-based AOPs (O_3/UV and $\text{O}_3/\text{UV}/\text{H}_2\text{O}_2$) at pilot-scale bubble column reactors have shown high efficiency in TOC removal. Moreover, addition of H_2O_2 is favorable considering overall costs [70]. One of the origins of winery wastewater is cork boiling water. AOPs including solar photo-Fenton and ozone have been applied to the effluents pre-treated by physicochemical methods. [71] The pre-treatment reduces the additional benefits of AOPs such as increased biodegradability and toxicity reduction. Further assessments of overall costs remain to be investigated.

5. Conclusion

In the food industry, wastewater effluents including complex organics are generated from various food processing steps and equipment maintenance procedures.

Moreover, the concentration of contaminants varies according to the type of food. This situation leads to an urgent demand for AOPs as complementary technologies to traditional wastewater treatment which is insufficient to process excess pollutants. The effluents from AOPs are more biodegradable for biological treatments, and hence the addition of AOPs as pre-treatment or post-treatment is a promising and economical solution for processing various wastewaters in the food industry.

Further research on catalysts that increase the amounts of effective radicals, simple separation procedure, and high recovery rates is suggested. Reactor design and optimization is another promising field. Due to the small number of practical applications, additional pilot-scale studies with AOPs are also recommended. Large-scale studies can provide overall cost evaluation including capital cost, operation cost, and possible profits from by-products. Such integrated economic assessment in real plants will be valuable guidance for future research.

IntechOpen

Author details

Zhaoran Xin and Lars Rehmann*

Department of Chemical and Biochemical Engineering, Western University
London, ON, Canada

*Address all correspondence to: lrehmann@uwo.ca

IntechOpen

© 2020 The Author(s). Licensee IntechOpen. Distributed under the terms of the Creative Commons Attribution - NonCommercial 4.0 License (<https://creativecommons.org/licenses/by-nc/4.0/>), which permits use, distribution and reproduction for non-commercial purposes, provided the original is properly cited. 

References

- [1] Krzemińska D, Neczaj E, Borowski G. Advanced oxidation processes for food industrial wastewater decontamination. *Journal of Ecological Engineering*. 2015;**16**:61-71
- [2] Ghosh Ray S, Ghangrekar MM. Comprehensive review on treatment of high-strength distillery wastewater in advanced physico-chemical and biological degradation pathways. *International Journal of Environmental Science and Technology*. 2019;**16**: 527-546
- [3] Lima VN, Rodrigues CSD, Borges RAC, et al. Gaseous and liquid effluents treatment in bubble column reactors by advanced oxidation processes: A review. *Critical Reviews in Environmental Science and Technology*. 2018;**48**: 949-996
- [4] Water and Wastewater Monitoring Report. Region of Waterloo [online]. Available from: <https://www.regionofwaterloo.ca/en/living-here/resources/Documents/water/reports/WS2019WaterAndWastewaterMonitoringReport.pdf>
- [5] The UV/Oxidation Handbook, Solarchem Environmental Systems. Markham, Ontario; 1994
- [6] Staehelin J, Holgné J. Decomposition of ozone in water: Rate of initiation by hydroxide ions and hydrogen peroxide. *Environmental Science & Technology*. 1982;**16**:676-681
- [7] Carey JH. An introduction to advanced oxidation processes (AOP) for destruction of organics in wastewater. *Water Quality Research Journal*. 1992;**27** (1):1-22
- [8] Afsharnia M, Kianmehr M, Biglari H, et al. Disinfection of dairy wastewater effluent through solar photocatalysis processes. *Water Science and Engineering*. 2018;**11**:214-219
- [9] Heponiemi A, Lassi U. Advanced oxidation processes in food industry wastewater treatment – A review. In: *Food Industrial Processes - Methods and Equipment*. London, UK: InTech; 2012
- [10] Azbar N, Bayram A, Filibeli A, et al. A review of waste management options in olive oil production. *Critical Reviews in Environmental Science and Technology*. 2004;**34**:209-247
- [11] Union PO of the E. Survey on current activity on the valorization of by-products from the olive oil industry
- [12] Galliou F, Markakis N, Fountoulakis MS, et al. Production of organic fertilizer from olive mill wastewater by combining solar greenhouse drying and composting. *Waste Management*. 2018; **75**:305-311
- [13] Elkacmi R, Bennajah M. Advanced oxidation technologies for the treatment and detoxification of olive mill wastewater: A general review. *Journal of Water Reuse and Desalination*. 2019;**9**: 463-505
- [14] Lofrano G, Meric S. A comprehensive approach to winery wastewater treatment: A review of the state-of-the-art. *Desalination and Water Treatment*. 2016;**57**:3011-3028
- [15] Ioannou LA, Puma GL, Fatta-Kassinos D. Treatment of winery wastewater by physicochemical, biological and advanced processes: A review. *Journal of Hazardous Materials*. 2015;**286**:343-368
- [16] Pulido JMO. A review on the use of membrane technology and fouling control for olive mill wastewater treatment. *Science of the Total Environment*. 2016;**563–564**:664-675
- [17] Ioannou-Ttofa L, Michael-Kordatou I, Fattas SC, et al. Treatment efficiency

and economic feasibility of biological oxidation, membrane filtration and separation processes, and advanced oxidation for the purification and valorization of olive mill wastewater. *Water Research*. 2017;**114**:1-13

[18] European IPPC Bureau. Best Available Techniques Reference document on food, drink and milk industries. 2019. Available from: http://eippcb.jrc.ec.europa.eu/reference/bref/download/download_FDM.cfm

[19] WHO. Total alcohol per capita (15+ years) consumption, in litres of pure alcohol. WHO

[20] Petruccioli M, Duarte JC, Federici F. High-rate aerobic treatment of winery wastewater using bioreactors with free and immobilized activated sludge. *Journal of Bioscience and Bioengineering*. 2000;**90**:381-386

[21] Díez AM, Iglesias O, Rosales E, et al. Optimization of two-chamber photo electro Fenton reactor for the treatment of winery wastewater. *Process Safety and Environment Protection*. 2016;**101**: 72-79

[22] Díez AM, Rosales E, Sanromán MA, et al. Assessment of LED-assisted electro-Fenton reactor for the treatment of winery wastewater. *Chemical Engineering Journal*. 2017;**310**:399-406

[23] Candia-Onfray C, Espinoza N, Sabino da Silva EB, et al. Treatment of winery wastewater by anodic oxidation using BDD electrode. *Chemosphere*. 2018;**206**:709-717

[24] Rodríguez-Chueca J, Amor C, Mota J, et al. Oxidation of winery wastewater by sulphate radicals: Catalytic and solar photocatalytic activations. *Environmental Science and Pollution Research*. 2017;**24**:22414-22426

[25] Amor C, Rodríguez-Chueca J, Fernandes JL, et al. Winery wastewater

treatment by sulphate radical based-advanced oxidation processes (SR-AOP): Thermally vs UV-assisted persulphate activation. *Process Safety and Environment Protection*. 2019;**122**: 94-101

[26] Guimarães V, Lucas MS, Peres JA. Combination of adsorption and heterogeneous photo-Fenton processes for the treatment of winery wastewater. *Environmental Science and Pollution Research*. 2019;**26**:31000-31013

[27] Malandra L, Wolfaardt G, Zietsman A, et al. Microbiology of a biological contactor for winery wastewater treatment. *Water Research*. 2003;**37**: 4125-4134

[28] Artiga P, Ficara E, Malpei F, et al. Treatment of two industrial wastewaters in a submerged membrane bioreactor. *Desalination*. 2005;**179**:161-169

[29] Bustamante MA, Moral R, Paredes C, et al. Agrochemical characterisation of the solid by-products and residues from the winery and distillery industry. *Waste Management*. 2008;**28**:372-380

[30] Amor C, Marchão L, Lucas MS, et al. Application of advanced oxidation processes for the treatment of recalcitrant agro-industrial wastewater: A review. *Water*. 2019;**11**(2):205

[31] Mekki A, Dhouib A, Sayadi S. Review: Effects of olive mill wastewater application on soil properties and plants growth. *International Journal of Recycling of Organic Waste in Agriculture*. 2013;**2**:15

[32] García CA, Hodaifa G. Real olive oil mill wastewater treatment by photo-Fenton system using artificial ultraviolet light lamps. *Journal of Cleaner Production*. 2017;**162**:743-753

[33] Amaral-Silva N, Martins RC, Nunes P, et al. From a lab test to industrial

application: Scale-up of Fenton process for real olive mill wastewater treatment. *Journal of Chemical Technology and Biotechnology*. 2017;**92**:1336-1344

[34] Ates H, Dizge N, Cengiz YH. Combined process of electrocoagulation and photocatalytic degradation for the treatment of olive washing wastewater. *Water Science and Technology*. 2017;**75** (1):141-154

[35] Kirmaci A, Duyar A, Akgul V, et al. Optimization of combined ozone/Fenton process on olive mill wastewater treatment. *Aksaray University Journal of Science and Engineering*. 2018;**2**: 52-62

[36] Genç N, Durna E, Kayapinar C, Cigün HK. Response surface modeling and optimization of microwave-activated Persulfate oxidation of olive oil mill wastewater. *Clean: Soil, Air, Water*. 2020;**48**:1-11

[37] Bustillo-Lecompte C, Mehrvar M, Quiñones-Bolaños E. Slaughterhouse wastewater characterization and treatment: An economic and public health necessity of the meat processing industry in Ontario, Canada. *International Conference on Environmental Pollution and Public Health*. 2016;**2016**:175-186

[38] Bustillo-Lecompte CF, Mehrvar M. Treatment of an actual slaughterhouse wastewater by integration of biological and advanced oxidation processes: Modeling, optimization, and cost-effectiveness analysis. *Journal of Environmental Management*. 2016;**182**: 651-666

[39] Naderi KV, Bustillo-Lecompte CF, Mehrvar M, et al. Combined UV-C/H₂O₂-VUV processes for the treatment of an actual slaughterhouse wastewater. *Journal of Environmental Science and Health Part B Pesticides Food Contaminants and Agricultural Wastes*. 2017;**52**:314-325

[40] Masoumi Z, Shokohi R, Atashzaban Z, et al. Stabilization of excess sludge from poultry slaughterhouse wastewater treatment plant by the Fenton process. *Avicenna Journal of Environmental Health Engineering*. 2015;**2**:3239-3239

[41] Vidal J, Huiliñir C, Salazar R. Removal of organic matter contained in slaughterhouse wastewater using a combination of anaerobic digestion and solar photoelectro-Fenton processes. *Electrochimica Acta*. 2016;**210**:163-170

[42] Bukhari K, Ahmad N, Sheikh IA, et al. Effects of different parameters on Photocatalytic oxidation of slaughterhouse wastewater using TiO₂ and silver-doped TiO₂ Nanoparticles. *Polish Journal of Environmental Studies*. 2019;**28**:1591-1600

[43] Kim HJ, Won CH, Kim HW. Pathogen deactivation of glow discharge cold plasma while treating organic and inorganic pollutants of slaughterhouse wastewater. *Water, Air, and Soil Pollution*. 2018;**229**:1-10

[44] Sánchez IMR, Ruiz JMM, López JLC, et al. Effect of environmental regulation on the profitability of sustainable water use in the agro-food industry. *Desalination*. 2011;**279**:252-257

[45] Carvalho MCS, Borges AC, Pereira MDS, et al. Degradation kinetics of organic matter in dairy industry wastewater by flotation/ozonation processes. *Bioscience Journal*. 2018;**34**: 587-594

[46] Maroneze MM, Zepka LQ, Vieira JG, et al. A tecnologia de remoção de fósforo: Gerenciamento do elemento em resíduos industriais. *Revista Ambiente & Água*. 2018;**9**:445-458

[47] Davarnejad R, Nikseresht M. Dairy wastewater treatment using an electrochemical method: Experimental and statistical study. *Journal of*

Electroanalytical Chemistry. 2016;**775**: 364-373

[48] Akkaya GK, Erkan HS, Sekman E, et al. Modeling and optimizing Fenton and electro-Fenton processes for dairy wastewater treatment using response surface methodology. *International Journal of Environmental Science and Technology*. 2019;**16**:2343-2358

[49] Su JC, Wang YL, Su JJ. Photocatalytic oxidation of dairy effluent with UV lamp or UV light-emitting diode module and biological treatment processes. *International Journal of Environmental Science and Technology*. 2019;**16**:1047-1056

[50] Pramanik BK, Hai FI, Roddick FA. Ultraviolet/persulfate pre-treatment for organic fouling mitigation of forward osmosis membrane: Possible application in nutrient mining from dairy wastewater. *Separation and Purification Technology*. 2019;**217**:215-220

[51] Bruguera-Casamada C, Araujo RM, Brillas E, et al. Advantages of electro-Fenton over electrocoagulation for disinfection of dairy wastewater. *Chemical Engineering Journal*. 2019; **376**:119975

[52] Alsager OA, Alnajrani MN, Abuelizz HA, et al. Removal of antibiotics from water and waste milk by ozonation: Kinetics, byproducts, and antimicrobial activity. *Ecotoxicology and Environmental Safety*. 2018;**158**:114-122

[53] Yilmaz E, Fındık S. Sonocatalytic treatment of baker's yeast effluent. *Journal of Water Reuse and Desalination*. 2017;**7**:88-96

[54] Vakili B, Shahmoradi B, Maleki A, et al. Synthesis of immobilized cerium doped ZnO nanoparticles through the mild hydrothermal approach and their application in the photodegradation of synthetic wastewater. *Journal of Molecular Liquids*. 2019;**280**:230-237

[55] Parthasarathy S, Gomes RL, Manickam S. Process intensification of anaerobically digested palm oil mill effluent (AAD-POME) treatment using combined chitosan coagulation, hydrogen peroxide (H₂O₂) and Fenton's oxidation. *Clean Technologies and Environmental Policy*. 2016;**18**:219-230

[56] Guzmán J, Mosteo R, Sarasa J, et al. Evaluation of solar photo-Fenton and ozone based processes as citrus wastewater pre-treatments. *Separation and Purification Technology*. 2016;**164**: 155-162

[57] Ijanu EM, Kamaruddin MA, Norashiddin FA. Coffee processing wastewater treatment: A critical review on current treatment technologies with a proposed alternative. *Applied Water Science*. 2020;**10**:1-11

[58] Ibarra-Taquez HN, GilPavas E, Blatchley ER, et al. Integrated electrocoagulation-electrooxidation process for the treatment of soluble coffee effluent: Optimization of COD degradation and operation time analysis. *Journal of Environmental Management*. 2017;**200**:530-538

[59] Shaikh IA, Munir S, Ahmed F, et al. Advanced oxidative removal of C.I. food red 17 dye from an aqueous solution. *Pakistan Journal of Nutrition*. 2014;**13**: 631-634

[60] Thiam A, Brillas E. Treatment of a mixture of food color additives (E122, E124 and E129) in different water matrices by UVA and solar photoelectro-Fenton. *Water Research*. 2015;**81**:178-187

[61] Thiam A, Brillas E, Garrido JA, et al. Routes for the electrochemical degradation of the artificial food azo-colour Ponceau 4R by advanced oxidation processes. *Applied Catalysis B: Environmental*. 2016;**180**:227-236

[62] Barros WRP, Steter JR, Lanza MRV, et al. Catalytic activity of Fe₃-xCu_xO₄

($0 \leq x \leq 0.25$) nanoparticles for the degradation of Amaranth food dye by heterogeneous electro-Fenton process. *Applied Catalysis B: Environmental*. 2016;**180**:434-441

[63] Zazouli MA, Ghanbari F, Yousefi M, et al. Photocatalytic degradation of food dye by Fe₃O₄-TiO₂ nanoparticles in presence of peroxymonosulfate: The effect of UV sources. *Journal of Environmental Chemical Engineering*. 2017;**5**:2459-2468

[64] Ahmadi M, Ghanbari F, Alvarez A, et al. UV-LEDs assisted peroxymonosulfate/Fe²⁺ for oxidative removal of carmoisine: The effect of chloride ion. *Korean Journal of Chemical Engineering*. 2017;**34**:2154-2161

[65] Tekin G, Ersöz G, Atalay S. Visible light assisted Fenton oxidation of tartrazine using metal doped bismuth oxyhalides as novel photocatalysts. *Journal of Environmental Management*. 2018;**228**:441-450

[66] Thirumalraj B, Rajkumar C, Chen SM, et al. Carbon aerogel supported palladium-ruthenium nanoparticles for electrochemical sensing and catalytic reduction of food dye. *Sensors and Actuators B: Chemical*. 2018;**257**:48-59

[67] Júnior WJ, Júnior N, Aquino RVS, et al. Development of a new PET flow reactor applied to food dyes removal with advanced oxidative processes. *Journal of Water Process Engineering*. 2019;**31**:100823

[68] Yahılı Kılıç M, Yonar T, Kestioğlu K. Pilot-scale treatment of olive oil mill wastewater by physicochemical and advanced oxidation processes. *Environmental Technology*. 2013;**34**:1521-1531

[69] Hodaifa G, Ochando-Pulido JM, Rodriguez-Vives S, et al. Optimization of continuous reactor at pilot scale for olive-oil mill wastewater treatment by

Fenton-like process. *Chemical Engineering Journal*. 2013;**220**:117-124

[70] Lucas MS, Peres JA, Li PG. Treatment of winery wastewater by ozone-based advanced oxidation processes (O₃, O₃/UV and O₃/UV/H₂O₂) in a pilot-scale bubble column reactor and process economics. *Separation and Purification Technology*. 2010;**72**:235-241

[71] De Torres-Socías E, Fernández-Calderero I, Oller I, et al. Cork boiling wastewater treatment at pilot plant scale: Comparison of solar photo-Fenton and ozone (O₃, O₃/H₂O₂). Toxicity and biodegradability assessment. *Chemical Engineering Journal*. 2013;**234**:232-239

Catalytic Ozone Oxidation of Petrochemical Secondary Effluent: Mechanism, Application and Future Development

Yu Tan, Liya Fu, Changyong Wu, Yanan Li, Xiumei Sun and Yuexi Zhou

Abstract

Petrochemical secondary effluent contains toxic and refractory organic compounds, which are difficult to be further treated by traditional biological process. In China, most of the advanced treatment units have been built recently by catalytic ozone oxidation process to achieve the high-quality effluent. In this chapter, the mechanism and reaction process of catalytic ozone oxidation of petrochemical secondary effluent will be introduced in detail. With the operation of the catalytic ozone oxidation tank, a series of problems which are not taken into account at the beginning of the design have arisen. The chapter will talk about the problems concerning the biological flocs, colloidal macromolecule organic compounds, ozone mass transfer, and catalysts based on practical applications. In the last part of the chapter, the development trends of catalytic ozone oxidation of petrochemical secondary effluent will also be discussed.

Keywords: ozone, petrochemical wastewater, reaction mechanism, biological flocs, trends

1. Introduction

As an important part of the chemical industry, the petrochemical industry is one of the pillar industries in China and has a large proportion in the national economy. According to China Industrial Research Network, the total output value of China's petrochemical industry in 2014 has exceeded 13 trillion CNY, ranking second in the world. In 2016, the total discharge of petrochemical wastewater reached 2 billion tons, accounting for more than 10% of the national industrial wastewater discharge. The organic pollution wastewater generated during the operation of petrochemical enterprises is an important part of China's industrial wastewater. Types of pollutants, large concentration, high toxicity, as well as containing many refractory biodegradation organic substances make water quality of the petrochemical wastewater complex; its governance has become a bottleneck restricting the development of the petrochemical industry.

Complex water quality features have spawned new water treatment processes. Advanced oxidation processes (AOPs) can produce hydroxyl radicals ($\bullet\text{OH}$) with strong oxidizing ability under the reaction conditions of electricity, sound, photo, catalyst, and others. Hydroxyl radical ($\bullet\text{OH}$) is an important reactive oxygen species with a standard oxidation–reduction potential of +2.8 V, which is second only to fluorine in nature [1]. It can successfully decompose most pollutants including refractory organics in water and oxidize macromolecule refractory organic matter into low-toxic or nontoxic small molecular substances.

The catalytic ozone oxidation process is a kind of advanced oxidation process, which has the following characteristics: (a) it produces strong oxidizing $\bullet\text{OH}$, and the oxidation process is fast, reaching 10^6 to $10^{10}\text{L}/(\text{mol}\cdot\text{s})$; (b) it performs excellently in removing refractory organic matter with no secondary pollutants, which means the process is green and efficient; and (c) the process runs economically. Taking a petrochemical integrated sewage treatment plant in northern China as an example, ozone can directly use air as raw material by ozone generator without adding auxiliary materials, and the earliest used catalyst has been running normally for 5 years, which still has high catalytic activity now. Therefore, catalytic ozone oxidation process is widely used in the advanced treatment of petrochemical wastewater. Especially after July 1, 2015, the Ministry of Ecology and Environment began to implement the *Petrochemical industry pollutant discharge standards (GB 31571-2015)* to replace the *Integrated Wastewater Discharge Standard (GB 8978-1996)*, which improves the direct drainage's COD limit of sewage treatment plant in petrochemical industrial park from 100 to 60 mg/L and adds 60 indicators of characteristic organic pollutants. Catalytic ozone oxidation process is increasingly popular in wastewater treatment due to the advantage of high efficiency, low consumption, energy saving, and environmental protection.

2. Research progress of catalytic ozone oxidation

Due to the excellent performance of catalytic ozone oxidation process in industrial wastewater treatment, substantial researches on the development of new catalysts and catalytic processes have been carried out. But so far the mechanism of catalytic ozone oxidation has not been unified in the academia, even the mechanisms proposed in many published literature are contradictory, which has largely limited the promotion of catalytic ozone oxidation process as an efficient, green technology. Several possible mechanisms on the catalytic ozone oxidation process will be introduced in the following.

According to the state of the catalyst, the catalytic ozone oxidation process can be divided into homogeneous and heterogeneous catalytic oxidation.

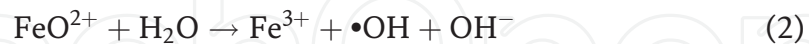
2.1 Homogeneous catalytic oxidation

Some transition metal cations have been shown to improve ozonation efficiency; among the most widely used are Mn(II), Fe(III), Fe(II), Co(II), Cu(II), Zn(II), and Cr(III) [2–4]. In simple terms, homogeneous catalytic oxidation is to let the transition metal ion decompose ozone or assist organics to be more easily oxidation. Two major mechanisms of homogeneous catalytic ozone oxidation can be found in the published research papers:

1. Ozone decomposes under the action of the catalyst to generate free radicals [5–7].

2. A complex coordination reaction occurs between the catalyst and the organic matter or ozone to promote the reaction between ozone and organic matter [2, 8, 9].

The free radical mechanism is similar to the Fenton reaction, and the electron transfer is achieved by oxidation and reduction of the valence metal ions. Based on the early work of Logager et al. [10], Sauleda et al. [7] explained the formation of hydroxyl radicals in the presence of Fe(II) ions:



Another mechanism is proposed by Pines and Reckhow [8] on the research catalytic ozone oxidation of oxalic acid in the presence of Co(II) ions. In general, hydroxyl radicals are more likely to be produced under alkaline conditions. However, experiments have shown that the reaction became inefficient with the increase of pH. Moreover in the presence of t-butanol (a radical scavenger), the reaction rate was also found not to change. These suggest that the free radical mechanism is not responsible for mineralization of oxalate in the Co(II)/O₃ system. So the hypothesis illustrated in **Figure 1** is proposed to explain the experimental phenomenon. Mineralization of oxalate is achieved by forming complexes with Co(II) ions.

Other metal ions have also been found to have similar catalytic effects. However, once metal ions are used as catalysts to promote ozone oxidation, the question on how to separate catalysts from the treated water should take into consideration. Therefore, there have been few reports on its research recently.

2.2 Heterogeneous catalytic oxidation

Among the most widely used catalysts in heterogeneous catalytic ozone oxidation are [11]:

- Metal oxides (MnO₂, TiO₂, Al₂O₃, and FeOOH).
- Metals (Cu, Ru, Pt, Co) on supports (SiO₂, Al₂O₃, TiO₂, CeO₂, and activated carbon).
- Activated carbon.

Adsorption is the key word in heterogeneous catalytic ozone oxidation. There are three possible ways which could be the general mechanism of heterogeneous catalytic ozone oxidation (**Figure 2**) [12]:

- Ozone is adsorbed on the surface of the catalyst.
- Organic molecule is adsorbed on the surface of the catalyst.
- Both, ozone and organic molecule, are adsorbed on the catalyst surface.

A lot of research work has been carried out for different catalysts.

2.2.1 Metal oxides

A variety of metal oxides have been shown to be effective in heterogeneous catalytic oxidation, such as MnO₂, Al₂O₃, TiO₂, and FeOOH. All published articles

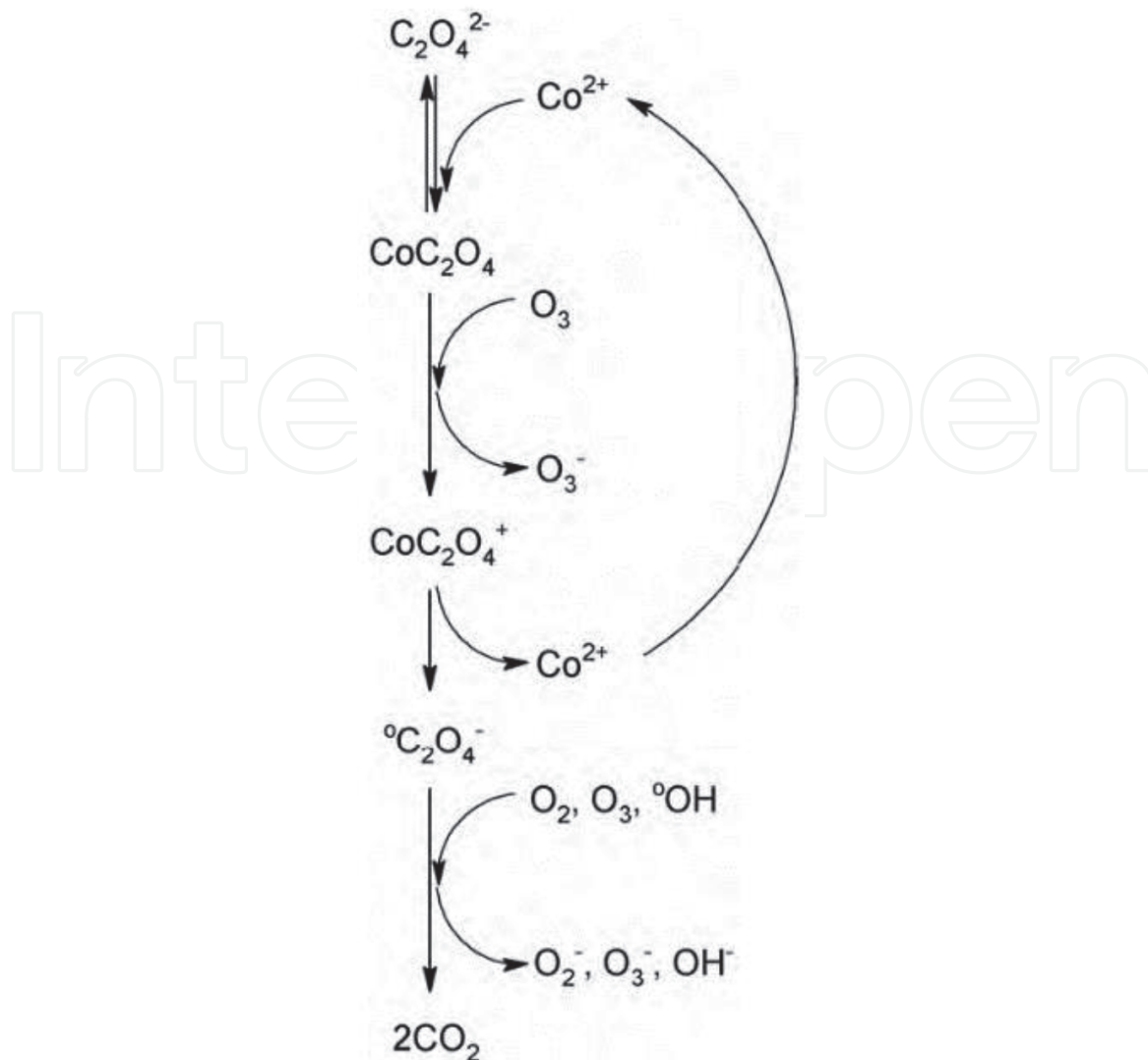


Figure 1.

Mechanism of oxalic acid oxidation in the presence of Co(II) ions proposed by Pines and Reckhow (modified from [8]).

have indicated that the mechanism of catalysis has a tight affinity with the surface chemistry of the oxides. More specifically, metal oxides as catalysts are surrounded by water in wastewater treatment. There is no doubt that the surface is covered by hydroxyls which have ion-exchange properties. Some of the oxides may also have Lewis acid centers which are considered as another adsorption site on their surfaces. In addition, hydrophobic sites can also be spotted on the surface on some metal oxides to explain the adsorption of organic molecules. **Table 1** lists the metal oxides commonly used as catalysts in the research and target organics for removal.

2.2.1.1 MnO_2

In the research of the catalytic mechanism of MnO_2 , Andreozzi et al. [33] first found in the study that the catalytic activity of MnO_2 to degrade oxalic acid was the highest when $pH = 3.2$. This result, however, is contradictory with what we have known: the optimum pH for dissociating ozone to produce $\bullet OH$ is 5–6. This means during the process $\bullet OH$ is not the dominated factor for removing oxalic acid. According to Tong et al. [58], adsorption of organic molecule on the surface of MnO_2 and subsequent attack of ozone on adsorbed organic molecule are responsible for catalytic activity.

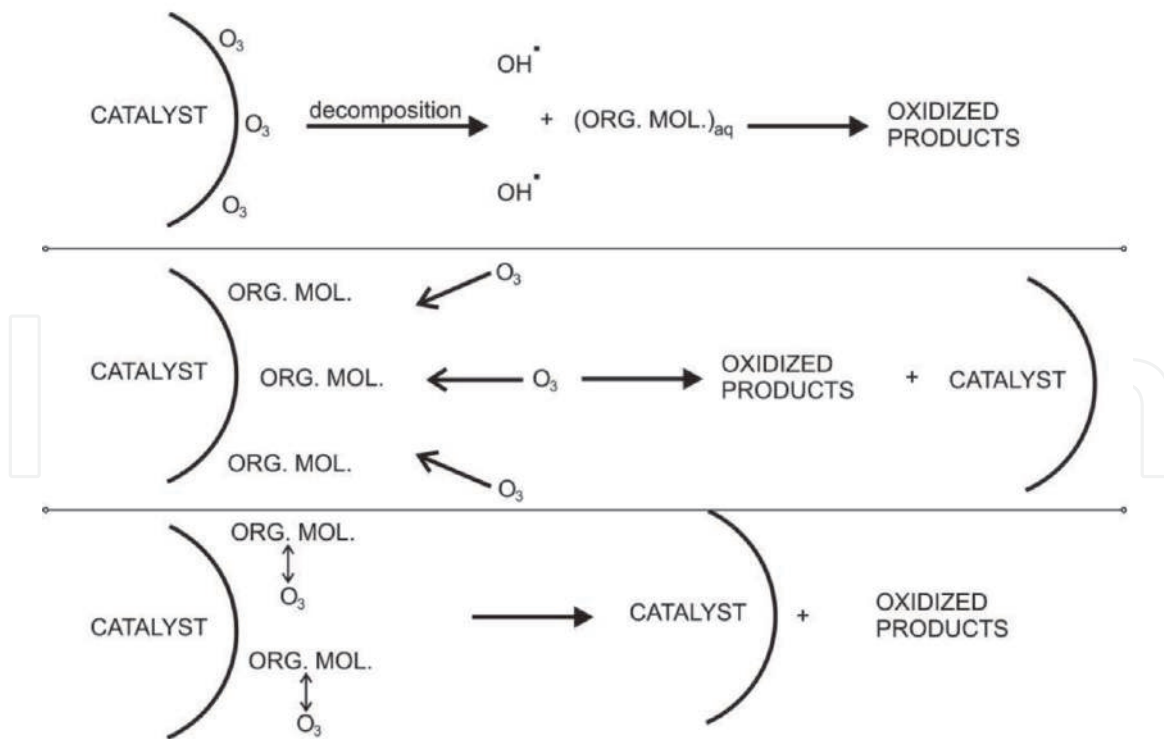


Figure 2.
 Three possible cases of heterogeneous catalysis [12].

On the other hand, when atrazine was used as the characteristic pollutant, adding in t-butanol could inhibit the catalytic activity of MnO_2 [14]. If atrazine is replaced with nitrobenzene, t-butanol has light effect on catalytic activity of MnO_2 [59]. From the research, we can draw a conclusion that the catalytic mechanism of MnO_2 catalyzed ozone oxidation to degrade organic matter in water varies depending on the type of organic matter, including the mechanism of free radicals produced by decomposing ozone, the surface coordination mechanism of organic matters, and the combination of both.

2.2.1.2 Al_2O_3

Al_2O_3 is another metal oxide that is widely used as a catalyst. There is a lot of controversy about research of the catalytic mechanism of Al_2O_3 . The researches of Kasprzyk-Hordern and Nawrocki had found that in the presence of Al_2O_3 , there was no catalytic activity for the removal of aromatic hydrocarbons and ethers. However, in the latter experiments, it was detected that the decomposition rate of ozone is twice that of ozonation alone [60–62]. In Kasprzyk-Hordern [19] another experiment, high catalytic activity was demonstrated when the substrate is natural organic matter (NOM) in the presence of alumina. The key factor to explain this contrast is the capacity of the surface to adsorb different organic molecules, as both hydrocarbons and ethers do not adsorb on alumina from aqueous solutions while alumina revealed high adsorption capacity toward NOM. These could be the evidence of the hypothesis that the catalytic activity of Al_2O_3 depends on the surface absorption of the substrate. However, Ernst et al. [20] reported that the adsorption of organic molecules is detrimental to the catalytic activity of $\gamma-Al_2O_3$. The research showed it was the high adsorption of oxalic acid on the surface that caused the lower efficiency. Obviously, the mechanism is remained to be discussed further and deeper.

Catalyst	Target organics	References
MnO ₂	Carboxylic acids (oxalic, pyruvic, sulfosalicylic, propionic, glyoxylic), N-methyl-p-aminophenol, atrazine	[3, 8, 13–17]
Al ₂ O ₃	Carboxylic acids (oxalic, acetic, salicylic, succinic), 2-chlorophenol, chloroethanol, NOM, dimethyl phthalate	[18–23]
TiO ₂	Oxalic acid, carbamazepine, naproxen, nitrobenzene, clofibrac acid	[24–27]
FeOOH	p-Chlorobenzoic acid, NOM	[28–32]
TiO ₂ , Al ₂ O ₃ , Ni ₂ O ₃ , CuO, MoO ₃ , CoO, Fe ₂ O ₃	m-Dinitrobenzene	[33]
ZnO	p-Chlorobenzoic acid	[34, 35]
TiO ₂ (2.5%)/α-Al ₂ O ₃	NOM	[36–38]
TiO ₂ (10%)/Al ₂ O ₃ , Fe ₂ O ₃ (10%)/Al ₂ O ₃	Oxalic acid, chloroethanol, chlorophenol	[19]
TiO ₂ /Al ₂ O ₃	Fulvic acids	[38]
TiO ₂ (15%)/γ-Al ₂ O ₃	Oxalic acid	[39]
MnO ₂ (10%)/TiO ₂	Phenol	[2]
MnO _x (10.8%)/AC	Nitrobenzene	[40]
β-Al ₂ O ₃	Pyruvic acid	[41]
γ-Al ₂ O ₃	Methylisoborneol	[42]
γ-ALOOH, α-Al ₂ O ₃	2,4,6-trichloroanisole	[43]
MnO ₂	Phenol, NMO	[44, 45]
CeO ₂	Aniline, sulfanilic acid, dyes	[46]
Co ₃ O ₄ /Al ₂ O ₃	Pyruvic acid	[41]
CuO/Al ₂ O ₃	Alachlor, oxalic acid, substituted phenols	[3, 47, 48]
Co(OH) ₂	p-Chloronitrobenzene	[49]
TiO ₂ / AC	Methylene blue	[50]
NiO/Al ₂ O ₃	Oxalic acid	[51]
NiO/CuO	Dichloroacetic acid	[52]
MnO _x /Al ₂ O ₃	Phenazone, ibuprofen, phenytoin, diphenhydramine	[53]
MgO	Dye	[54]
CoO _x /ZrO ₂	2,4-D	[55]
Co/CeO, Ag/CeO, Mn/CeO	Phenolic wastewater	[56, 57]

Table 1. Common catalyst components and target organics for removal (modified from [11]).

2.2.1.3 TiO₂

TiO₂ is usually used as a photocatalyst [63–68], which also has a good catalytic effect when degrading organic matter in wastewater. The catalytic mechanism of TiO₂ has close affinity with the construction of TiO₂.

TiO₂, which is often used as a catalyst, is classified into rutile type and anatase type. Yang et al. [69] used rutile TiO₂ for catalytic ozone oxidation research and found that the efficiency of removing organic matter decreased after adding TBA to the reaction system. This implies that the free radical mechanism dominates the reaction process. On the contrary, Ye et al. [70] studied the degradation of

4-chloronitrobenzene (CNB) during catalytic and photocatalytic ozone oxidation in the presence of TiO_2 . The result of the experiment is that the TOC is higher under UV condition, which does not correspond with the free radical mechanism. So far, the difference in this mechanism is still lacking in-depth explanation.

2.2.1.4 FeOOH

The mechanism of FeOOH is similar to the mechanism of homogeneous catalytic oxidation. The difference between them is that the decomposition and oxidation happen in bulk water in homogeneous catalytic oxidation, while for FeOOH, the process occurs on the surface.

1. The process satisfies the hydroxyl radical mechanism. As is illustrated in **Figure 3**, the ozone molecule first forms a surface ring with the hydroxyl group on the surface of the catalyst and then decomposes to produce Fe-OH-O^- and O_2 . Finally, Fe-OH-O^- is directly attacked by ozone to form $\bullet\text{OH}$ and $\text{O}_2^{\bullet-}$, and the water molecules complex on the surface of FeOOH to form a new hydroxyl group.
2. Organic compounds form complexes on the surface of FeOOH and are then directly oxidized by ozone molecules to degrade organic matter [72].

2.2.2 Metals on supports

Metals on supports are a type of catalysts which use supports (SiO_2 , Al_2O_3 , TiO_2 , CeO_2 , and activated carbon) to load metals (Cu, Ru, Pt, Co). They have been observed to have a high catalytic activity in catalytic ozone process.

Two main routes have been proposed to explain the catalytic mechanism [73] (**Figure 4**):

1. The metal supported on the catalyst has a constant valence state in the catalytic reaction and only functions as a coordination.
2. The metals are attacked by the ozone to generate hydroxyl radicals. Then, through the adsorption and desorption of organic matter on the surface of the catalyst, electron transfer is completed to achieve metal reduction and oxidation of organic matter.

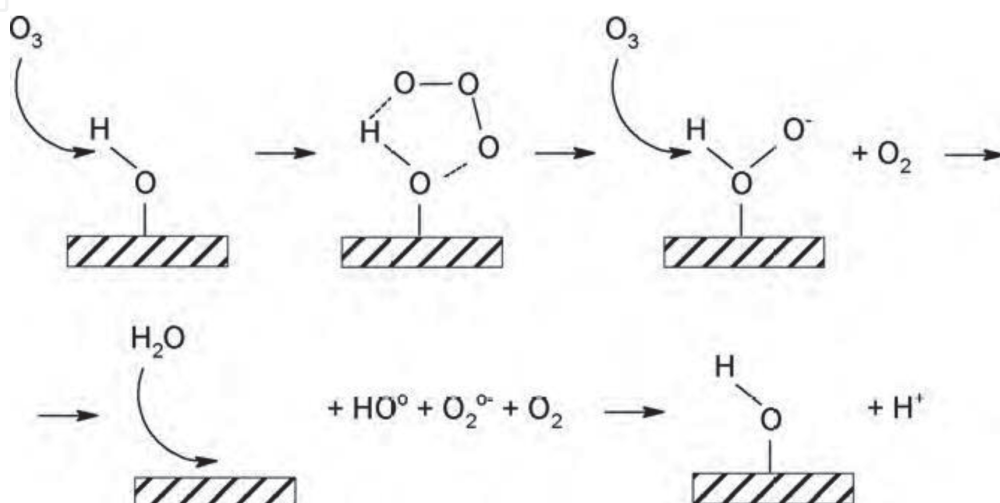


Figure 3.
Mechanism of hydroxyl radical generation in the presence of FeOOH [71].

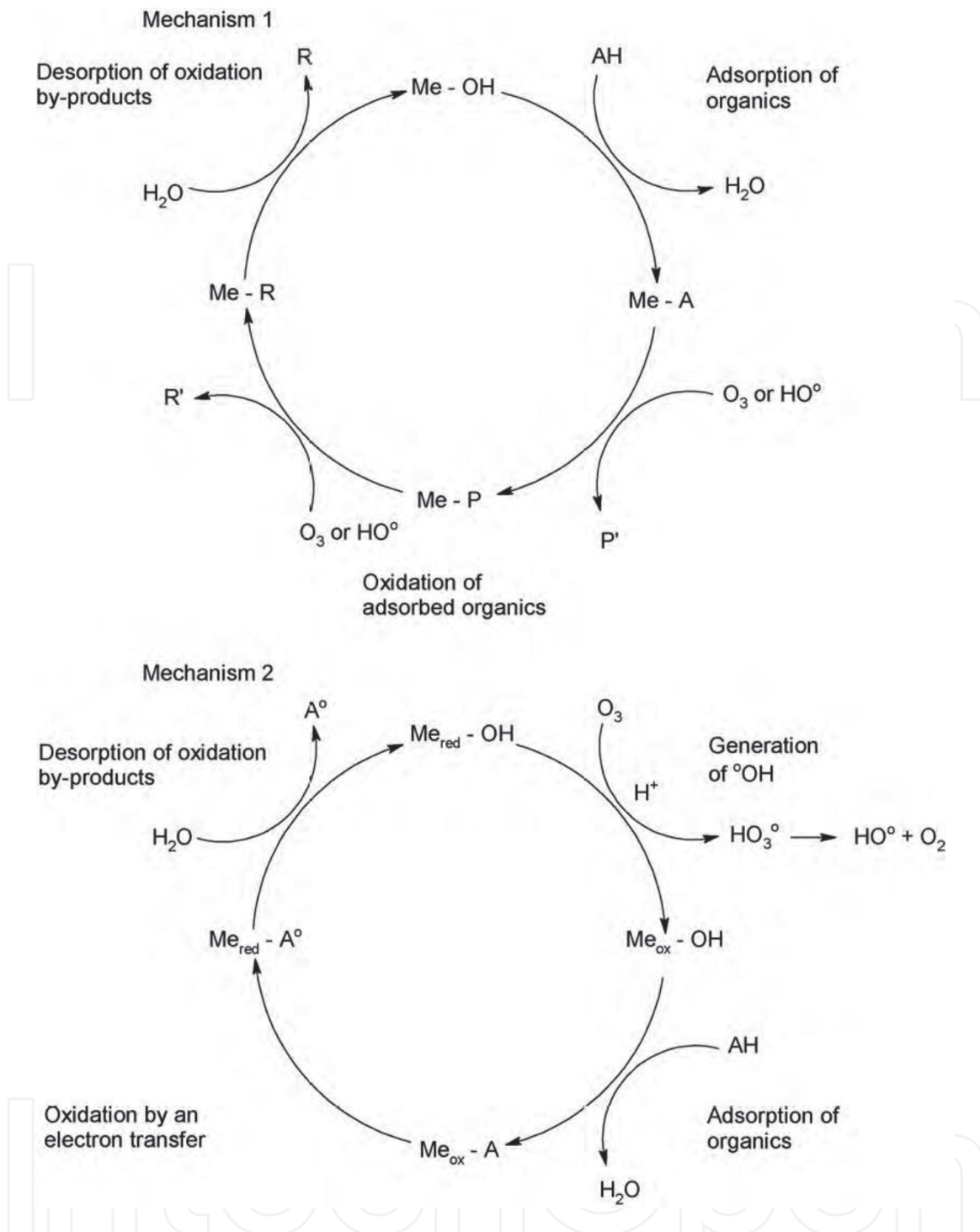


Figure 4. Mechanisms of catalytic ozone oxidation in the presence of metals on supports (AH (organic acid); P, R (adsorbed primary and final by-products); P, R (primary and final)) [73].

2.2.3 Activated carbon

Activated carbon is also used as a catalyst for catalytic ozone oxidation as a relatively cheap and durable material. The surface properties of activated carbon are different from metals' and cannot coordinate with organic matter in water. So most of the research focused on how ozone decomposes on the surface of activated carbon. In general, there are two catalytic paths for activated carbon: (i) increasing the surface reaction area and (ii) decomposing ozone on the surface to produce $\cdot\text{OH}$ radicals.

3. Research on catalytic ozone oxidation in petrochemical secondary effluent

The mechanism described above is part of the research progress on the mechanism of catalytic ozone oxidation in recent years and plays a decisive role in the theoretical development of the process. However, the main research ideas of these studies are to use target pollutants to explore the mechanism of related catalysts. Whether it is possible to maintain high treatment efficiency in the face of actual wastewater with complex water quality is not clear at present; moreover some catalysts have high cost which restrains to implement in practical engineering applications.

In China, ozonation/catalytic ozone oxidation has been widely used in the advanced treatment of petrochemical wastewater. The proportion of applications is estimated to be as high as approximately 64%. Thus, it is necessary to carry out research on the mechanism of catalytic ozone oxidation which is instructive for practical engineering.

The research team of the author is based on a petrochemical wastewater treatment plant (WWTP) which uses catalytic ozone oxidation process as an advanced treatment in the north of China. All the water samples and catalysts in the experiment are obtained from the WWTP, instead of choosing the target pollutants to do in-depth researches, which break through the traditional ways of exploring the mechanism and mean a lot to the practical engineering applications.

In terms of the petrochemical secondary effluent (PSE) treatment, the research on the mechanism of catalytic ozone oxidation and existing problems in the treatment of petrochemical wastewater when using catalytic ozone oxidation process has achieved certain results, which is at the domestic leading level. The research will be generally introduced below.

3.1 Research ideas

The catalysts used in the WWTP are commercial material which mainly comprises alumina-supported copper oxide (ACO). It has been demonstrated that the adsorption of organics on alumina was associated with hydrophilicity of organics [74]. The catalytic activity of dissolved organic matters (DOM) is extremely correlative to their physicochemical properties (e.g., aromaticity, polarity, hydrophobicity-hydrophilicity, acidity-alkaline, molecular weight) [31, 75–77]. Due to the differences of hydrophobicity-hydrophilicity and acidity-alkaline, resin fraction can be an appropriate way to isolate DOM from wastewater [78]. Moreover, the specific effects of ozonation/catalytic ozone oxidation on DOM with different characteristics can be observed from the changes of different DOM fraction. Therefore, the research team innovatively used the resin classification method to divide the DOM in PSE into four components: hydrophobic acids (HoA), hydrophobic bases (HoB), hydrophobic neutrals (HoN), and hydrophilic substances (HI). Herein, HI included hydrophilic acid (HiA), hydrophilic base (HiB), and hydrophilic neutral (HiN). The effect of the three common ozone treatment processes, single ozonation, ozone/H₂O₂ (representing homogeneous catalytic oxidation technology), and catalytic ozone oxidation with a commercial ACO (representing heterogeneous catalytic oxidation technology), on different fractions, was investigated. Then the catalytic ozone oxidation mechanism of the major fractions is systematically elaborated.

3.2 Results and discussion

3.2.1 The characteristic of catalyst

In the study, as the catalyst is commercial and obtained from the practical industrial application, we only investigate the characteristics related to the mechanism proposed. SEM images of commercial catalyst used were presented in **Figure 5**. The catalyst was spherule of 2–4 mm. It possessed mesoporous surface with packed lamellar layer. The structure is very important for the organic pollutant removal. The BET surface area, pore volume, and average size were listed in **Table 2**. The pH_{pzc} of ACO was found to be (pH_{pzc}) of 8.0 ± 0.2 . The pH of sample was about 7.5 ($\text{pH} < \text{pH}_{\text{pzc}} = 8.0$). ACO will be positively charged and adsorb anions from aqueous solution. The surface hydroxyl group density was $2.7 \times 10^{-5} \text{ M/m}^2$. The FTIR spectra of catalyst before and after catalytic ozone oxidation were shown in **Figure 6**. The adsorption peaks at 3450 and 1635 cm^{-1} attributed to the surface hydroxyl groups of catalyst and adsorbed water, respectively. The bands at 1525 and 1385 cm^{-1} were likely to attribute to surface acid functional group of catalyst. After catalytic ozone oxidation, the hydroxyl groups at 3450 cm^{-1} broadened may be formed from adsorbed water by hydrogen binding because the catalyst interacted with ozone.

X-ray photoelectron spectroscopy (XPS) is a surface-sensitive quantitative spectroscopic technique that detects information on the composition and content of various compounds, chemical state, molecular structure, and chemical bonds. As shown in **Figure 7**, obvious O 1s and Al 2p and weak Cu 2p signals are observed in the survey region. The signal corresponding to Al 2p was found at 73.7 eV. The content of Cu was minor. The weak signal related to Cu 2p at around 932 eV could be identified in the narrow region. The signal of O 1s was displayed at 530.3 eV corresponding to the adsorbed hydroxyl.

3.2.2 The effect of ozonation and catalytic ozone oxidation on fraction distribution of the PSE

For the selection study of the optimal wastewater treatment method, Fu et al. compared the reactivity characteristics of DOM in single ozone, ozone/ H_2O_2 , and

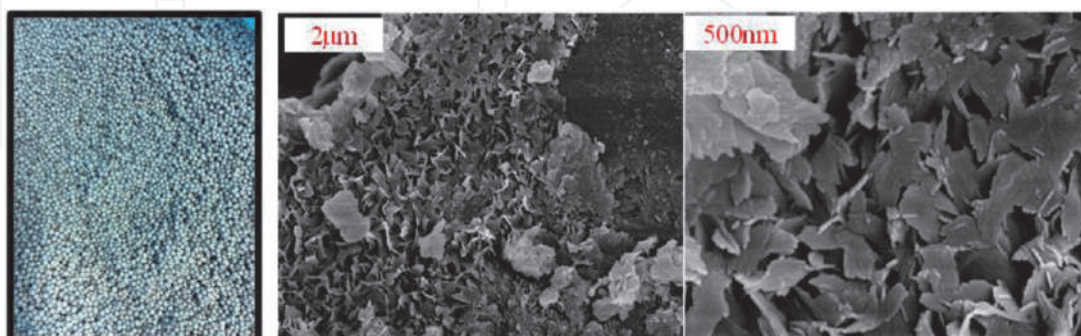


Figure 5.
SEM images for catalyst.

Items	BET surface area (m^2/g)	Pore volume (cm^3/g)	Average pore diameter (nm)	pH_{pzc}	Surface hydroxyl group density (M/m^2)
Average value	169.28	0467	11.0	8.0 ± 0.2	2.7×10^{-5}

Table 2.
Surface characteristics e of commercial catalyst.

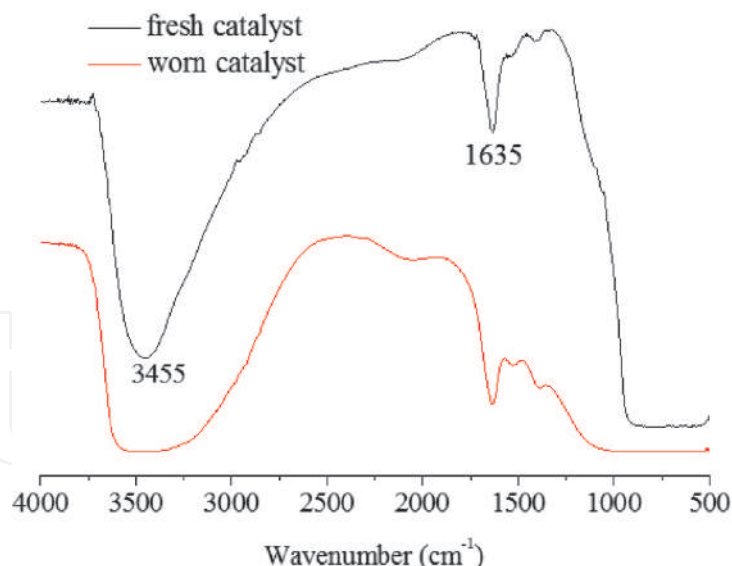


Figure 6.
The FTIR spectra of original and worn catalyst.

ozone/catalyst systems [79]. The highest removal efficiency (42.8%) of TOC was achieved in the ozone/catalyst system, followed by the ozone/H₂O₂ (23.8%) and single ozone (4.7%) systems. This implied that homogeneous catalysis (ozone/H₂O₂) has obvious lower DOM removal rate (~20%) than heterogeneous catalysis when the ozone dosage and contact time were the same treating PSE.

In order to investigate the specific changes of each component, Sun et al. [80] first isolated four fractions (HiA, HiB, HiN, and HI) and operated the ozonation experiment on separate fraction system. They measured the values of DOC and SUVA₂₅₄ of raw water and its fractions before and after ozonation and catalytic ozone oxidation, which present in **Figure 8**. As shown in **Figure 8a**, HI and HoA were the dominated fractions in PSE with relatively high percentage of total DOC. SUVA₂₅₄, the value of UV₂₅₄ divided by itself DOC, has been reported to act as an indicator of active aromatic structure and unsaturated bonds (carbon-carbon and carbon-oxygen) from organic matters [81]. In **Figure 8b**, HoA had the largest SUVA₂₅₄ value among other fractions, indicating HoA had the most containing aromatic and unsaturated bond organic matters, while the SUVA₂₅₄ of HI is the smallest. The results are entirely in accordance with the results of the previous studies [77, 78].

The fraction distribution changed significantly after ozonation and catalytic ozone oxidation. **Figure 8a** manifested that the DOC of HoA remarkably decreased by ozonation. However, the DOC of HI had slight reduction after ozonation. This result indicated that ozonation could be more readily to oxidize HoA than HI. Under the same condition, catalytic ozone oxidation exhibited higher DOC removal than ozonation for all fractions, in particular HI. It is well known that ozone is prone to react with compounds containing electrophilic groups [82]. As can be seen in **Figure 8b**, ozonation decreased significantly the SUVA₂₅₄ of all fractions. On the contrary, catalytic ozone oxidation showed less changes on the reduction of SUVA₂₅₄ than ozonation for all fractions. This suggested UV-absorbing matters are susceptible to electrophilic groups which are easily attacked by ozone. Thus, ozonation reacting easily with HoA is likely to be the highest SUVA₂₅₄.

In a high complex circumstance, Fu et al. evaluated specific changes; six fractions in both raw wastewater and ozonized wastewater instead separate isolated fractions in previous study [80]. Fu et al. specified that HiN (belongs to HI) were one dominant DOM fractions with the highest TOC contents in the effluent of the three ozonation systems, accounting for 24.8–53.6% of the total TOC contents (**Figure 9a**). From the changes in TOC distributions ($\text{TOC}_{\text{effluent}} - \text{TOC}_{\text{influent}}$)

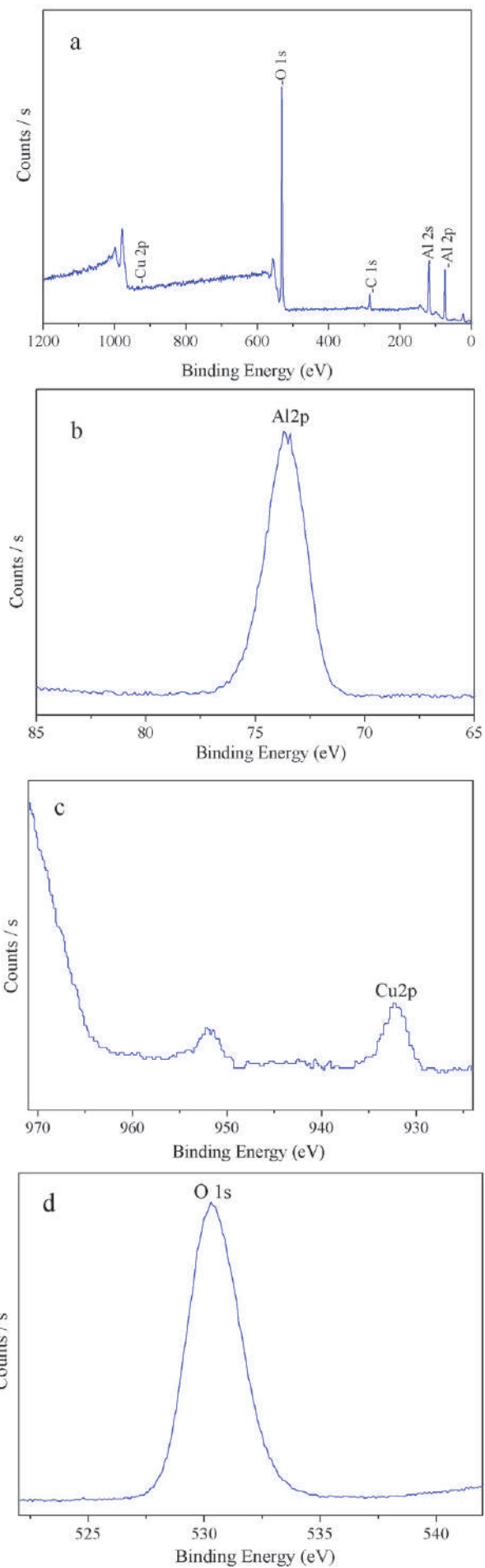


Figure 7. XPS spectra of catalyst: (a) wide-range survey, (b) Al 2p region, (c) Cu 2p region, and (d) O 1s.

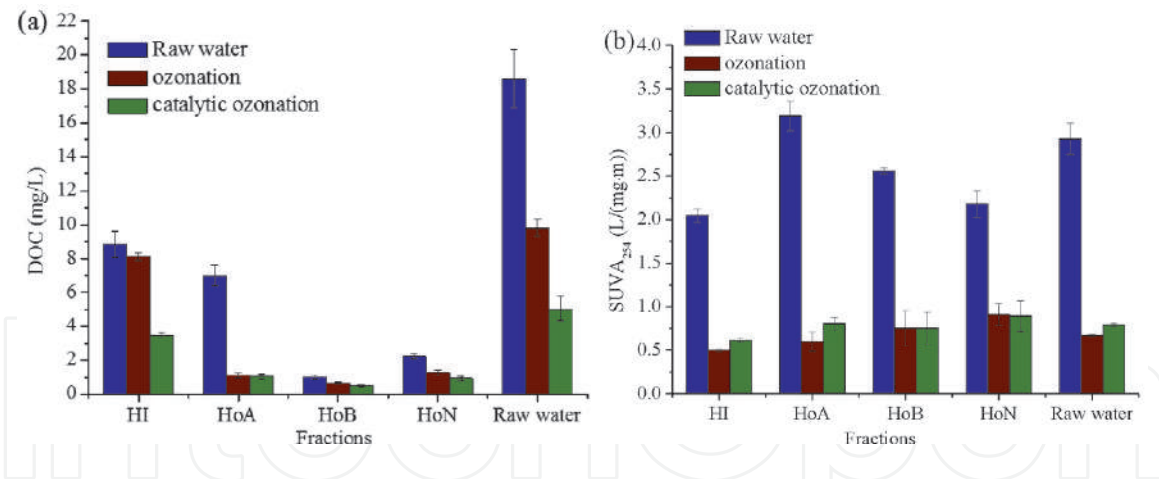


Figure 8. The DOC (a) and SUVA₂₅₄ (b) of raw water and its fractions before and after ozonation and catalytic ozone oxidation. Experiment conditions: initial concentration, 19.0 ± 2.0 mg/L; initial pH, 7.5; ozone dose, 1.0 mg/min; reaction time, 120 min; catalyst dose, 500 g.

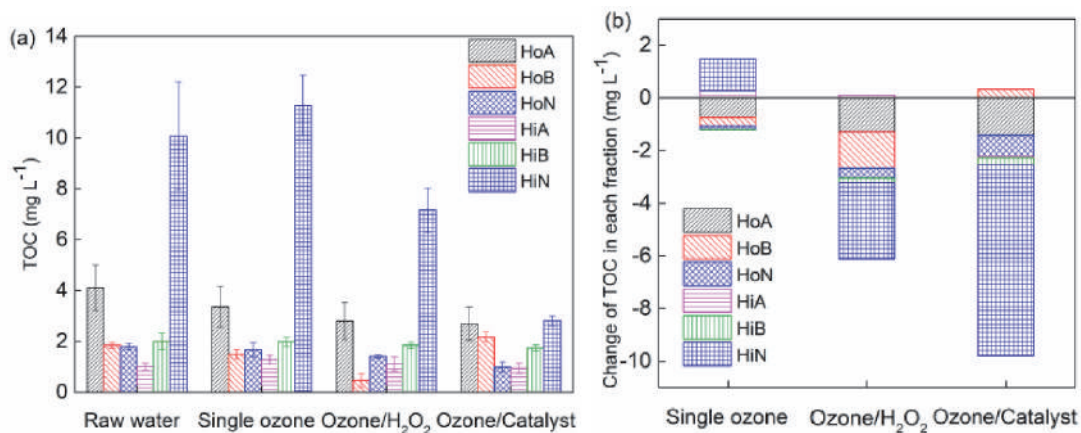


Figure 9. TOC distribution of the DOM fractions before and after ozonation via single ozone, ozone/H₂O₂, and ozone/catalyst treatment: (a) TOC content and (b) change in TOC content.

(Figure 9b), for the single ozone system, the mass balance of TOC content was maintained after single ozone treatment (Figure 9b), and the sum of the increased TOC content (contributed by HiA and HiN) was 38.8%, which approximately equaled the sum of the decreased TOC content contributed by the other four fractions (44.8%). In the single ozone system, HoA showed the highest TOC removal, decreasing by 18.1%, whereas HiN exhibited the lowest TOC removal content, increasing by 12.0% in the effluent conversely. Thus, it is reasonable to think that the single ozone system transformed hydrophobic components (e.g., HoB, HoN, and HoA) into hydrophilic compounds (e.g., HiA and HiN). In addition, for ozone/H₂O₂ treatment, HiA was hard to remove, while HoB was easy to remove.

3.2.3 Transformation of DOM fractions during the ozonation process

The specific fluorescence excitation-emission matrix (EEM) spectroscopy volume could be used to rapidly identify the fluorescent compounds present in the DOM and reflect the compositional and structural characteristics of DOM. The ratio of the cumulative volume (Φ_i) to the TOC (Φ_i/TOC) of the DOM fractions is further compared (Figure 10) [79]. HiA and HiN had the lowest Φ_i/TOC ratios among other fractions in raw water, indicating that non-fluorescent compounds contributed a large portion of TOC in these two fractions. The FTIR adsorption spectrum of HiA and HiN also suggested that the spectral fine structure and

adsorption patterns of the reactive functional groups, such as the stretching vibration of $C=O$, $O-H$ of the carboxylates, were not as significant as those for the other fractions. The HiN presented the smallest changes in Φ_i/TOC ratio after single ozone treatment, implying that the portion of non-fluorescent and fluorescent substances did not change much when reacted with single ozone, and HiN may mainly consist of ozone-resistant compounds.

After treatment by the ozone/ H_2O_2 and ozone/catalyst systems, the Φ_i/TOC ratios of HiN in raw water increased significantly (**Figure 10**), showing that compounds with little fluorescence but large TOC contents were removed. Therefore, it could be assumed that the HiN in the raw water may consist of compounds with unsaturated bonds and low molecular weights, which have short conjugation lengths and could readily react with H_2O_2 or catalyst in the presence of ozone [83, 84]. As shown in **Figure 10**, Φ_i/TOC ratio of HiN did not change substantially in the single ozone system, but increased gradually in the ozone/ H_2O_2 and ozone/catalyst systems. This also demonstrated that HiN was principally responsible for the DOM removal in the ozone/ H_2O_2 system and especially in ozone/catalyst system. Because HiN is the dominant fraction in the sample and was ozone resistant, for the better treatment of petrochemical wastewater, efficient HiN removal is necessary.

3.2.4 The proposed mechanism of catalytic ozone oxidation

1. *HoA removal and transformation.* Sun et al. have proven that HoA is a group of DOM which contains activated aromatic rings or double bonds in their research (**Figure 11**). Those electrophilic groups easily react with ozone molecule [85]. It benefits the contact of HoA and ozone molecule. The study also confirmed that HoA transformed into HI with ozonation. $\bullet OH$ quenching test also proved that ozone molecule and partial $\bullet OH$ reaction are the main pathways.
2. *HI removal.* Higher adsorption rate (22% for HI) on the catalyst of alumina-supported copper oxide (ACO) was observed than that of other studies [74]. The adsorption of catalyst plays a key role during catalytic ozone oxidation. Higher adsorption rate led to the enrichment of organics on ACO, and concentration of HI adsorbed is much higher than that of in the bulking solution. In addition, that adsorbed ozone decomposed into $\bullet OH$ on the surface of

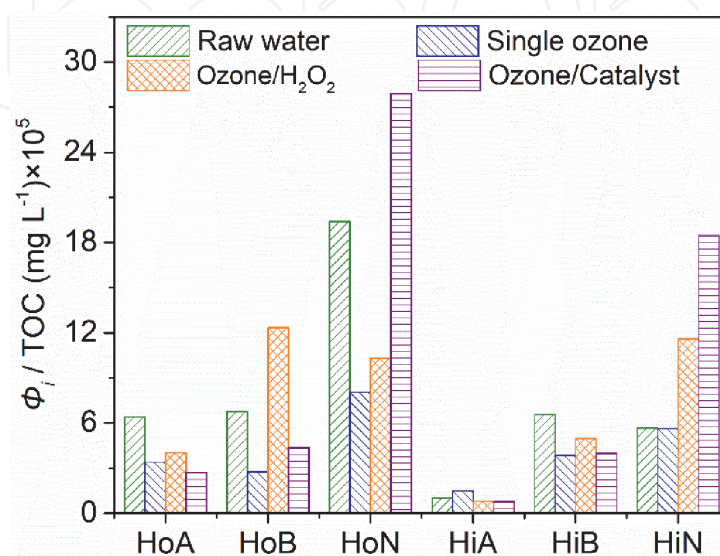


Figure 10. Ratio of Φ_i to TOC in the wastewater fractions (Φ_i/TOC (mg/L) $\times 10^4$ for HiN).

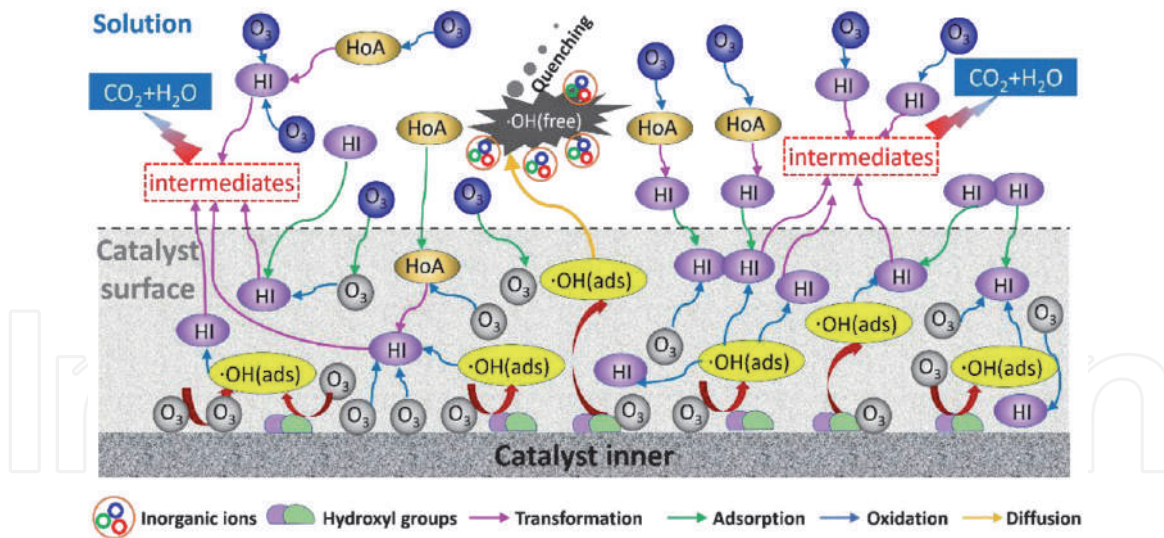


Figure 11.
 The proposed reaction mechanism of HoA and HI during catalytic ozone oxidation treating PSE.

catalyst accelerated the mineralization of adsorbed HI, and the reduction of HI on the catalysts' surface would promote the further adsorption of HI from the bulking. Thus, the adsorption role on catalytic ozone oxidation kept a dynamic balance process between ozonation and re-adsorption, triggering a cyclic reaction to reduce the concentration of HI.

3. *OH quenching protection.* Survival time of $\cdot\text{OH}$ is just about 10 ms [86]. If the generated $\cdot\text{OH}$ on the surface of catalyst are spread into the bulking solution, it can be immediately consumed by high concentration of inorganic salts, such as Cl^- (359.5–380.0 mg/L) and SO_4^{2-} (908.0–955.9 mg/L) with their low affinity for adsorption on the surface of catalyst [87]. Our previous study also found that homogeneous catalysis ($\text{H}_2\text{O}_2/\text{O}_3$) has obvious lower DOM removal rate ($\sim 20\%$) than heterogeneous catalysis when the ozone dosage and contact time were the same treating PSE [79, 88]. It is proven that the quenching of $\cdot\text{OH}$ cannot be ignored during catalytic ozone oxidation of PSE. The adsorption of organic on the surface of catalyst and simultaneous $\cdot\text{OH}$ generation in the solid-liquid interface can guarantee the high consumption of $\cdot\text{OH}$ reacting with HI, preventing the emission of $\cdot\text{OH}$ into the bulking solution. Solid-liquid interface provides dominant reaction site between ozone molecule and $\cdot\text{OH}$ with organics. It is the $\cdot\text{OH}$ quenching protection.

3.3 Problems on catalytic ozone oxidation in the PSE

3.3.1 The effect of flocs on catalytic ozone oxidation

The toxicity of petrochemical wastewater is higher than that of ordinary urban sewage, which has an adverse effect on the biological treatment system of wastewater, causing the concentration of suspended solids (SS) (mainly organic flocs) in effluent generally beyond 25 mg/L [89]. Generally, SS and colloidal substances in PSE account for 15–20% of the total organic matter in the wastewater. The main components are microbial residues, microbial secretions (such as extracellular polymeric substances, EPSs), soluble microbial metabolites (SMPs), adsorbed proteins, sugars, and other macromolecular organics or inorganic substances such as heavy metals [90]. The presence of flocs in PSE system will have the following adverse effects on the catalytic ozone oxidation unit:

1. An increase in ozone consumption: According to the research, more than 75% of SS in the PSE are small pieces of activated sludge that does not completely separate from the water. The average particle size is about 30–60 μm [91]. Researches discover when catalytic ozone oxidation process is adopted to treat the PSE, the removal of per unit COD will consume more ozone with the increase of SS. The reason is bioflocs in the wastewater can react with O_3 , causing the grow of ozone consumption [89]. The research of Zucker et al. [92] shows O_3 has a tendency to react with particulate matter at a high rate even in the first second of the reaction. Our researchers used catalytic ozone oxidation process to treat the PSE. It was found that when the influent SS concentration ranged from 0 to 10 mg/L, the depletion of COD was 1.17 $\text{gO}_3/\text{g COD}$. When the concentration range of SS rose to 30–35 mg/L, the depletion of COD grew to 2.31 $\text{gO}_3/\text{g COD}$. Zhang et al. [90] suggested that when the ozone dosage was less than 10 mg/L, the ozone basically did not react with the flocs in the PSE. Once the dosage was beyond 10 mg/L, ozone can react rapidly with flocs, following the order of dissolved organic matter, outer layer loosely bound EPS (LB-EPS), and inner layer tightly bound EPS (TB-EPS).
2. The flocs covering the catalyst surface hinder the mass transfer of ozone and dissolved organic matters to the catalyst surface, thereby reducing the reaction efficiency. Studies have shown that catalytic ozone oxidation can affect the distribution of the floc particle size in wastewater. It can enhance the flocculation of the flocs, causing the particles to aggregate as larger flocs [92], which are trapped in the catalyst bed. In actual engineering application, if there are no actions being taken to the SS in the PSE before discharging into the unit of catalytic ozone oxidation, the treatment effect will be significantly reduced even within 7 h. Backwashing can effectively improve the situation; however, frequent backwashing strengthens the friction and shear between the catalysts, resulting in the loss of active components of the catalyst, reducing the service life of the catalyst, and invisibly increasing the application cost of the process.
3. Detrimental effects on the removal of characteristic organic matter in the PSE. The research of Zhang et al. [93] indicates that esters, alcohols, olefins, ketones, and nitrogen-containing organic compounds in the PSE can be effectively removed by catalytic ozone oxidation. Twelve main characteristic organic pollutants are detected in the influent, about six kinds of them can be degraded by catalytic ozone oxidation. But the target characteristic pollutants in the effluent can be reduced to three, if the PSE is filtered by 0.45 μm membrane before catalytic ozone oxidation.

3.3.2 The effect of colloidal macromolecular organic matters

Due to the characteristics of small size, light weight, and large specific surface area, the colloidal substance adsorbs a large amount of ions on the surface so that the colloids are mutually repulsive to keep stable state. Colloidal macromolecular substances cannot be settled by their own gravity. So it is necessary to add chemicals in water to make the colloids destabilize and for sedimentation. Studies have shown that colloidal organic matters accounted for about 9%–15% of COD in the PSE [94]. Because of the large molecular weight, such substances will affect the treatment of catalytic ozone oxidation. Adding 25 mg/L poly-aluminum chloride (PAC) coagulant to the PSE to remove the colloidal organic matters before performing catalytic ozone oxidation, compared with the direct use of catalytic

ozone oxidation for the PSE, the removal rate of COD can be increased by about 11%. This is because the presence of colloidal macromolecular organics in the PSE affects the rate of ozone decomposition in the initial stage ($t < 30$ s), thereby reducing the production efficiency of hydroxyl radicals ($\bullet\text{OH}$) [95]. Many studies have also shown that in the advanced treatment of sewage, colloidal macromolecular organic matters mainly had effect on the removal of characteristic organic matters during the catalytic ozone oxidation.

3.3.3 The effect on the mass transfer of ozone

Ozone oxidation of organic pollutants in water depends on ozone transferring from the gas phase to the liquid phase, reacting with the target pollutants after diffusion. The mass transfer efficiency of ozone shifting into the liquid phase directly affects the effect of ozone oxidation [96]. The total ozone mass transfer coefficient is mainly influenced by many factors, for example, the degree of gas-liquid two-phase turbulence, the scale and quantity of ozone bubbles, the area of the two-phase contact, and the kinetics of ozonation reaction. The process rate is usually limited by the procedure in which ozone is transferred from the gas phase to the liquid phase [97]. At the same gas flow rate, the smaller bubble size is, the larger phase boundary area will be. Broadening the gas-liquid two-phase boundary area is beneficial not only to increase the total mass transfer rate of the process but also to improve the utilization of ozone [98]. At present, there is still a lack of relevant reports at home and abroad.

4. Conclusions

Flocs and colloidal macromolecular organic matter in the PSE increase the consumption of ozone as well as make the operation unstable. The configuration and operation mode of the catalytic ozone oxidation reactor are not optimized enough, causing the gas-liquid-solid three-phase mass transfer efficiency relatively low. These problems are common problems in the WWTP that are already operating catalytic ozone oxidation processes in China. As a kind of advanced oxidation process, catalytic ozone oxidation has attracted much attention because of its green, high-efficiency and energy-saving characteristics.

People have never stopped exploring its catalytic mechanism; the main research ideas of these studies are to use target pollutants and mixed water to explore the mechanism of related catalysts. Whether it is possible to maintain high treatment efficiency in the face of actual wastewater with complex water quality is not clear at present.

This manuscript first reviews and summarizes the progress and current status of ozonation/catalytic ozone oxidation mechanism research and secondly provides a relatively unique research idea: the DOM in raw water is divided into four fractions, HI, HoA, HoN, and HoB, according to the difference in chemical characteristics. The possible mechanism of ozonation/catalytic ozone oxidation is studied by observing the changes of each fraction. What's more, the common problems that may exist in the actual ozonation/catalytic ozone oxidation process are proposed and summarized. The matching point between mechanism research and practical engineering application is found, which provides direction for future research.

Future research should be carried on further with actual wastewater in the following aspects: (1) Fractional. It is a marvelous research idea to divide the substances in the water into different fractions for the specific research. (2) Microscopic. Future research should focus on microscopic scales, such as phase interface;

it can be combined with orbital theory to discuss the catalytic dynamics in-depth. (3) Whole process. The horizon of researches should be extended to the entire process to explore the effects of the surrounding environment on the catalytic process and mechanism, such as the specific effects of flocs and colloidal molecules on the process. In other words, although we have achieved some results in the study of catalytic ozone oxidation, there is still a lot of work that we need to continue.

IntechOpen

Author details

Yu Tan¹, Liya Fu¹, Changyong Wu^{1*}, Yanan Li¹, Xiumei Sun^{1,2} and Yuexi Zhou^{1*}

1 State Key Laboratory of Environmental Criteria and Risk Assessment, Chinese Research Academy of Environmental Sciences, Beijing, China

2 College of Water Science, Beijing Normal University, Beijing, China

*Address all correspondence to: changyongwu@126.com and zhouyuexi@263.net

IntechOpen

© 2020 The Author(s). Licensee IntechOpen. Distributed under the terms of the Creative Commons Attribution - NonCommercial 4.0 License (<https://creativecommons.org/licenses/by-nc/4.0/>), which permits use, distribution and reproduction for non-commercial purposes, provided the original is properly cited. 

References

- [1] Liao LH. Application of advanced oxidation technology in water supply and wastewater treatment. *Chemical Engineering and Equipment*. 2018;**08**: 279-281 +259
- [2] Beltran FJ, Rivas FJ, Montero-de-Espinosa R. Iron type catalysts for the ozonation of oxalic acid in water. *Water Research*. 2005;**39**:3553-3564
- [3] Pli Y, Ernst M, Schrotter J-CH. Effect of phosphate buffer upon CuO/Al₂O₃ and Cu(II) catalyzed ozonation of oxalic acid solution. *Ozone: Science and Engineering*. 2003;**25**:393-397
- [4] Abd El-Raady AA, Nakajima T. Decomposition of carboxylic acids in water by O₃, O₃/H₂O₂, and O₃/catalyst. *Ozone: Science and Engineering*. 2005; **27**:11-18
- [5] Gracia R, Aragues JL, Ovelleiro JL. Study of the catalytic ozone oxidation of humic substances in water and their ozonation Byproducts. *Ozone: Science and Engineering*. 1996;**18**:195-208
- [6] Piera E, Calpe JC, Brillas E, Domenech X, Peral J. 2,4-Dichlorophenoxyacetic acid degradation by catalyzed ozonation: TiO₂/UVA/O₃ and Fe(II)/UVA/O₃ systems. *Applied Catalysis B: Environmental*. 2000;**27**:169-177
- [7] Sauleda R, Brillas E. Mineralization of aniline and 4-chlorophenol in acidic solution by ozonation catalyzed with Fe²⁺ and UVA light. *Applied Catalysis B: Environmental*. 2001;**29**:135-145
- [8] Pines DS, Reckhow DA. Effect of dissolved cobalt (II) on the ozonation of oxalic acid. *Environmental Science and Technology*. 2002;**36**:4046-4051
- [9] Beltran FJ, Rivas FJ, Montero-de-Espinosa R. Ozone-enhanced oxidation of oxalic acid in water with cobalt catalysts. 2. Heterogeneous catalytic ozone oxidation. *Industrial & Engineering Chemistry Research*. 2003; **42**:3210-3217
- [10] Logager T, Holeman J, Sehested K, Pedersen T. Oxidation of ferrous ions by ozone in acidic solutions. *Inorganic Chemistry*. 1992;**31**:3523-3529
- [11] Nawrocki J, Kasprzyk-Hordern B. The efficiency and mechanisms of catalytic ozone oxidation. *Applied Catalysis B: Environmental*. 2010;**99**:27-42
- [12] Nawrocki J. Catalytic ozone oxidation in water: Controversies and questions. Discussion paper. *Applied Catalysis B: Environmental*. 2013; **142-143**:465-471
- [13] Beltrán Fernando J, Rivas FJ, Montero-de-Espinosa R. Ozone-enhanced oxidation of oxalic acid in water with cobalt Catalysts.1. Homogeneous catalytic ozone oxidation. *Industrial & Engineering Chemistry Research*. 2003;**42**(14):3210-3217
- [14] Ma J, Graham NJD. Degradation of atrazine by manganese-catalysed ozonation: Influence of humic substances. *Water Research*. 1999;**33**(3):785-793
- [15] Sánchez-Polo M, Rivera-Utrilla J. Ozonation of 1,3,6-naphthalenetrisulfonic acid in presence of heavy metals. *Journal of Chemical Technology & Biotechnology*. 2004; **79**(8):8
- [16] Ma J, Graham NJD. Preliminary investigation of manganese-catalyzed ozonation for the destruction of atrazine. *Ozone Science & Engineering*. 1997;**19**(3):227-240
- [17] Andreatti R, Casale MSL, Marotta R, et al. N-methyl-p-aminophenol(metol) ozonation in aqueous solution: Kinetics, mechanism

- and toxicological characterization of ozonized samples. *Water Research*. 2000;**34**(18):4419-4429
- [18] Cooper C, Burch R. Mesoporous materials for water treatment processes. *Water Research*. 1999;**33**(18):3689-3694
- [19] Kasprzyk-Hordern B, Raczyk-Stanisławiak U, S'wietlik J, Nawrocki J. Catalytic ozone oxidation of natural organic matter on alumina. *Applied Catalysis B: Environmental*. 2006;**62**:345-358
- [20] Ernst M, Lurot F, Schrotter JC. Catalytic ozone oxidation of refractory organic model compounds in aqueous solution by aluminum oxide. *Applied Catalysis B: Environmental*. 2004;**47**(1):15-25
- [21] Yunrui Z, Wanpeng Z, Fudong L, et al. Catalytic activity of Ru/A₁₂O₃ for ozonation of dimethyl phthalate in aqueous solution. *Chemosphere*. 2007;**66**(1):145-150
- [22] Ni CH, Chen JN. Heterogeneous catalytic ozone oxidation of 2-chlorophenol aqueous solution with alumina as a catalyst. *Water Science & Technology*. 2001;**43**(2):213
- [23] Beltrán FJ, Rivas FJ, Montero-De-Espinosa R. Catalytic ozone oxidation of oxalic acid in an aqueous TiO slurry reactor. *Applied Catalysis B: Environmental*. 2002;**39**(3):221-231
- [24] Rosal R, Rodríguez A, Gonzalo MS, et al. Catalytic ozone oxidation of naproxen and carbamazepine on titanium dioxide. *Applied Catalysis B: Environmental*. 2008;**84**(1):48-57
- [25] Rosal R, Gonzalo MS, Rodríguez A, et al. Ozonation of clofibric acid catalyzed by titanium dioxide. *Journal of Hazardous Materials*. 2009;**169**(1):411-418
- [26] Rosal R, Gonzalo MS, Boltes K, et al. Identification of intermediates and assessment of ecotoxicity in the oxidation products generated during the ozonation of clofibric acid. *Journal of Hazardous Materials*. 2009;**172**(2):1061-1068
- [27] Zhang T, Lu J, Ma J, et al. Fluorescence spectroscopic characterization of DOM fractions isolated from a filtered river water after ozonation and catalytic ozone oxidation. *Chemosphere*. 2008;**71**(5):911-921
- [28] Park JS, Choi H, Ahn KH. The reaction mechanism of catalytic oxidation with hydrogen peroxide and ozone in aqueous solution. *Water Science & Technology*. 2003;**47**(1):179
- [29] Park JS, Choi H, Ahn KH, et al. Removal mechanism of natural organic matter and organic acid by ozone in the presence of goethite. *Ozone Science & Engineering*. 2004;**26**(2):141-151
- [30] Park JS, Choi H, Cho J. Kinetic decomposition of ozone and para-chlorobenzoic acid (CBA) during catalytic ozone oxidation. *Water Research*. 2004;**38**(9):2285-2292
- [31] Zhang T, Lu J, Ma J, et al. Comparative study of ozonation and synthetic goethite-catalyzed ozonation of individual NOM fractions isolated and fractionated from a filtered river water. *Water Research*. 2008;**42**(6):1563-1570
- [32] Trapido M, Veressinina Y, Munter R, et al. Catalytic ozone oxidation of m-dinitrobenzene. *Ozone Science & Engineering*. 2005;**27**(5):359-363
- [33] Andreozzi R, Insola A, Caprio V, et al. The use of manganese dioxide as a heterogeneous catalyst for oxalic acid ozonation in aqueous solution. *Applied Catalysis A: General*. 1996;**138**(1):75-81

- [34] Muruganandham M, Wu JJ. Synthesis, characterization and catalytic activity of easily recyclable zinc oxide nanobundles. *Applied Catalysis B: Environmental*. 2008;**80**(1):32-41
- [35] Gracia R, Cortés S, Sarasa J, et al. Heterogeneous catalytic ozone oxidation with supported titanium dioxide in model and natural waters. *Ozone Science & Engineering*. 2000;**22**(5): 461-471
- [36] Gracia R, Cortés S, Sarasa J, et al. Catalytic ozone oxidation with supported titanium dioxide. The stability of catalyst in water. *Ozone Science & Engineering*. 2000;**22**(2): 185-193
- [37] Gracia R, Cortes S, Sarasa J, et al. TiO₂-catalysed ozonation of raw Ebro river water. *Water Research*. 2000; **34**(5):1525-1532
- [38] Volk C, Roche P, Joret JC, et al. Comparison of the effect of ozone, ozone-hydrogen peroxide system and catalytic ozone on the biodegradable organic matter of a fulvic acid solution. *Water Research*. 1997;**31**(3): 650-656
- [39] Beltrán FJ, Rivas FJ, Montero-De-Espinosa R. A TiO₂/Al₂O₃ catalyst to improve the ozonation of oxalic acid in water. *Applied Catalysis B: Environmental*. 2004;**47**(2):101-109
- [40] Ma J, Sui MH, Chen ZL, et al. Degradation of refractory organic pollutants by catalytic ozone oxidation—Activated carbon and Mn-loaded activated carbon as catalysts. *Ozone Science & Engineering*. 2004;**26**(1):3-10
- [41] Álvarez PM, Beltrán FJ, Pocostales JP, et al. Preparation and structural characterization of Co/Al₂O₃ catalysts for the ozonation of pyruvic acid. *Applied Catalysis B: Environmental*. 2007;**72**(3):322-330
- [42] Chen L, Qi F, Xu B, et al. The efficiency and mechanism of γ -alumina catalytic ozone oxidation of 2-methylisoborneol in drinking water. *Water Science & Technology: Water Supply*. 2006; **6**(3):43
- [43] Qi F, Xu B, Chen Z, et al. Catalytic ozone oxidation for degradation of 2,4,6-trichloroanisole in drinking water in the presence of gamma-ALOOH. *Water Environment Research*. 2009; **81**(6):592
- [44] Dong Y, Yang H, He K, et al. β -MnO₂ nanowires: A novel ozonation catalyst for water treatment. *Applied Catalysis B: Environmental*. 2009;**85**(3): 155-161
- [45] Faria PCC, Monteiro DCM, Órfão JJM, et al. Cerium, manganese and cobalt oxides as catalysts for the ozonation of selected organic compounds. *Chemosphere*. 2009;**74**(6): 818-824
- [46] Faria PCC, Órfão JJM, Pereira MFR. Activated carbon and ceria catalysts applied to the catalytic ozone oxidation of dyes and textile effluents. *Applied Catalysis B: Environmental*. 2009;**88**(3): 341-350
- [47] Qu J, Li H, Liu H, et al. Ozonation ofalachlor catalyzed by Cu/Al₂O₃ in water. *Catalysis Today*. 2004;**89**(3):291-296
- [48] Udrea I, Bradu C. Ozonation of substituted phenols in aqueous solutions over CuO-Al₂O₃ catalyst. *Ozone Science & Engineering*. 2003; **25**(4):335-343
- [49] Xu ZZ, Chen ZL, Joll C, et al. Catalytic efficiency and stability of cobalt hydroxide for decomposition of ozone and-chloronitrobenzene in water. *Catalysis Communications*. 2009;**10**(8): 1221-1225

- [50] Jie Z, Lee KH, Cui L, et al. Degradation of methylene blue in aqueous solution by ozone-based processes. *Journal of Industrial & Engineering Chemistry*. 2009;**15**(2): 185-189
- [51] Avramescu SM, Bradu C, Udrea I, et al. Degradation of oxalic acid from aqueous solutions by ozonation in presence of Ni/Al₂O₃ catalysts. *Catalysis Communications*. 2008;**9**(14): 2386-2391
- [52] Qin W, Li X, Qi J. Experimental and theoretical investigation of the catalytic ozone oxidation on the surface of NiO–CuO nanoparticles. *Langmuir: The ACS Journal of Surfaces & Colloids*. 2009;**25**(14):8001-8011
- [53] Yang L, Hu C, Nie Y, et al. Catalytic ozone oxidation of selected pharmaceuticals over mesoporous alumina-supported manganese oxide. *Environmental Science & Technology*. 2009;**43**(7):2525-2529
- [54] Moussavi G, Mahmoudi M. Degradation and biodegradability improvement of the reactive red 198 azo dye using catalytic ozone oxidation with MgO nanocrystals. *Chemical Engineering Journal*. 2009;**152**(1):1-7
- [55] Hu C, Xing S, Jiuhui Qu A, et al. Catalytic ozone oxidation of herbicide 2,4-D over cobalt oxide supported on mesoporous zirconia. *Journal of Physical Chemistry C*. 2008;**112**(15):5978-5983
- [56] Sui M, Sheng L, Lu K, et al. FeOOH catalytic ozone oxidation of oxalic acid and the effect of phosphate binding on its catalytic activity. *Applied Catalysis B: Environmental*. 2010;**96**(1):94-100
- [57] Rui CM, Quinta-Ferreira RM. Catalytic ozone oxidation of phenolic acids over a Mn-Ce-O catalyst. *Applied Catalysis B: Environmental*. 2009;**90**(1): 268-277
- [58] Tong S-P, Liu W-P, Leng W-H, Zhang Q-Q. Characteristics of MnO₂ catalytic ozone oxidation of sulfosalicylic acid and propionic acid in water. *Chemosphere*. 2003;**50**:1359-1364
- [59] Ma J, Sui M, Zhang T, et al. Effect of pH on MnO_x/GAC catalyzed ozonation for degradation of nitrobenzene. *Water Research*. 2005;**39**(5):779-786
- [60] Kasprzyk B, Nawrocki J. Preliminary results on ozonation enhancement by a perfluorinated bonded alumina phase. *Ozone: Science and Engineering*. 2002;**24**:63-68
- [61] Kasprzyk-Hordern B, Nawrocki J. The feasibility of using a perfluorinated bonded alumina phase in the ozonation process. *Ozone: Science and Engineering*. 2003;**25**:185-194
- [62] Kasprzyk-Hordern B, Andrzejewski P, Dąbrowska A, Czaczyk K, Nawrocki J. MTBE, DIPE, ETBE and TAME degradation in water using perfluorinated phases as catalysts for ozonation process. *Applied Catalysis B: Environmental*. 2004;**51**:51-66
- [63] Han F, Kambala VSR, Srinivasan M, Rajarathnam D, Naidu R. Tailored titanium dioxide photocatalysts for the degradation of organic dyes in wastewater treatment: A review. *Applied Catalysis A: General*. 2009;**359**:25-40
- [64] Gaya UI, Abdullah AH. Heterogeneous photocatalytic degradation of organic contaminants over titanium dioxide: A review of fundamentals, progress and problems. *Journal of Photochemistry and Photobiology C: Photochemistry Reviews*. 2008;**9**:1-12
- [65] Chatterjee D, Dasgupta S. Visible light induced photocatalytic degradation of organic pollutants. *Journal of Photochemistry and Photobiology C: Photochemistry Reviews*. 2005;**6**:186-205

- [66] Suty H, de Traversay C, Cost M. Applications of advanced oxidation processes: Present and future. *Water Science and Technology*. 2004;**49**: 227-233
- [67] Bhatkhande DS, Pangarkar VG. Photocatalytic degradation for environmental applications-a review *Journal of Chemical Technology and Biotechnology*. 2002;**77**:102-116
- [68] Chong MN, Jin B, Chow Christopher WK, Saint C. Recent developments in photocatalytic water treatment technology: A review. *Water Research*. 2010;**44**(10): 2997-3027
- [69] Yang Y, Ma J, Qin Q, Zhai X. Degradation of nitrobenzene by nano-TiO₂ catalyzed ozonation. *Journal of Molecular Catalysis A: Chemical*. 2007; **267**:41-48
- [70] Ye M, Chen Z, Liu X, Ben Y, Shen J. Ozone enhanced activity of aqueous titanium dioxide suspensions for photodegradation of 4-chloronitrobenzene. *Journal of Hazardous Materials*. 2009;**167**: 1021-1027
- [71] Zhang T, Ma J. Catalytic ozone oxidation of trace nitrobenzene in water with synthetic goethite. *Journal of Molecular Catalysis A: Chemical*. 2008; **279**:82-89
- [72] Ma J, Zhang T, Chen ZL. The mechanism of ozone decomposition and oxidation of trace nitrobenzene catalyzed by ferric hydroxide in water. *Environmental Science*. 2005;**26**(2): 78-82
- [73] Legube B, Karpel Vel Leitner N. Catalytic ozone oxidation: A promising advanced oxidation technology for water treatment. *Catalysis Today*. 1999; **53**(1):61-72
- [74] Ikhlaq A, Brown DR, Kasprzyk-Hordern B. Catalytic ozone oxidation for the removal of organic contaminants in water on alumina. *Applied Catalysis B: Environmental*. 2015;**165**:408-418
- [75] Qi F, Chen ZL, Xu BB, Shen JM, Ma J, AnnaHeitz CJ. Influence of surface texture and acid-base properties on ozone decomposition catalyzed by aluminum (hydroxyl) oxides. *Applied Catalysis B: Environmental*. 2008;**84**: 684-690
- [76] Qian FY, Sun XB, Liu YD. Effect of ozone on removal of dissolved organic matter and its biodegradability and adsorbability in biotreated textile effluents. *Ozone Science & Engineering*. 2013;**35**:7-15
- [77] Li CM, Wang DH, Xu X, Wang ZJ. Formation of known and unknown disinfection by-products from natural organic matter fractions during chlorination, chloramination, and ozonation. *Science of the Total Environment*. 2017;**587-588**:177-184
- [78] Gong JL, Liu YD, Sun XB. O₃ and UV/O₃ oxidation of organic constituents of biotreated municipal wastewater. *Water Research*. 2008;**42**:1238-1244
- [79] Fu LY, Wu CY, Zhou YX, Zuo JE, Song GQ, Tan Y. Ozonation reactivity characteristics of dissolved organic matter in secondary petrochemical wastewater by single ozone, ozone/H₂O₂, and ozone/catalyst. *Chemosphere*. 2019;**233**:34-43
- [80] Sun XM, Wu CY, Zhou YX, Han W. Using DOM fraction method to investigate the mechanism of catalytic ozonation for real wastewater. *Chemical Engineering Journal*. 2019; **369**:100-108
- [81] Ratpukdi T, Siripattanakul S, Khan E. Mineralization and biodegradability enhancement of

- natural organic matter by ozone—VUV in comparison with ozone, VUV, ozone—UV, and UV: Effects of pH and ozone dose. *Water Research*. 2010;**44**: 3531-3542
- [82] Hoigné J, Bader H. Rate constants of reactions of ozone with organic and inorganic compounds in water—I: Non-dissociating organic compounds. *Water Research*. 1983;**17**:173-183
- [83] Baker A. Fluorescence excitation–emission matrix characterization of some sewage-impacted rivers. *Environmental Science & Technology*. 2001;**35**:948-953
- [84] Chen W, Westerhoff P, Leenheer JA, Booksh K. Fluorescence excitation–emission matrix regional integration to quantify spectra for dissolved organic matter. *Environmental Science & Technology*. 2003;**37**:5701-5710
- [85] Van Sonntag C, Van Gunten U. *Chemistry of Ozone in Water and Wastewater Treatment*. London, UK: IWA Press; 2012
- [86] Wu JF, Su TM, Jiang YX, Xie XL, Qin ZZ, Ji HB. In situ DRIFTS study of O₃ adsorption on CaO, γ -Al₂O₃, CuO, γ -Fe₂O₃ and ZnO at room temperature for the catalytic ozone oxidation of cinnamaldehyde. *Applied Surface Science*. 2017;**412**:290-305
- [87] Petre AL, Carbajo JB, Rosal R, Garcia-Calvo E, Perdigón-Melón JA. CuO/SBA-15 catalyst for the catalytic ozone oxidation of mesoxalic and oxalic acids: Water matrix effects. *Chemical Engineering Journal*. 2013;**225**:164-173
- [88] Fu LY. The study of the operation and mechanism of an integrated ozone and biological aerated filter (BAF) advanced treatment for petrochemical wastewater [PhD dissertation]. Beijing, China: Tsinghua University; 2017
- [89] Wu C, Li Y, Zhou Y, Li Z. Upgrading the Chinese biggest petrochemical wastewater treatment plant: Technologies research and full scale application. *Science of the Total Environment*. 2018;**633**:189-197
- [90] Zhang SY, Wu CY, Zhou YX. Effects of bioflocs on advanced treatment of petrochemical secondary effluent by ozone catalytic oxidation. *Proceedings of the Annual Meeting of the Chinese Society of Environmental Sciences*. 2017:2869-2877
- [91] Wu C, Zhou Y, et al. Pretreatment of petrochemical secondary effluent by micro-flocculation and dynasand filtration: Performance and DOM removal characteristics. *Water Air & Soil Pollution*. 2016;**227**(11):415
- [92] Zucker I, Lester Y, Avisar D, et al. Influence of wastewater particles on ozone degradation of trace organic contaminants. *Environmental Science and Technology*. 2015;**9**:301-308
- [93] Zhang S, Wu C, Zhou Y, et al. Effect of wastewater particles on catalytic ozone oxidation in the advanced treatment of petrochemical secondary effluent. *Chemical Engineering Journal*. 2018;**345**:280-289
- [94] Rickert DA, Hunter JV. Colloidal matter in wastewaters and secondary effluents. *Journal of Water Pollution Control Federation*. 1972;**44**(1):134-139
- [95] Wert EC, Gonzales S, Dong MM, et al. Evaluation of enhanced coagulation pretreatment to improve ozone oxidation efficiency in wastewater. *Water Research*. 2011; **45**(16):5191-5199
- [96] Qin YJ, Qin WZ, Yang PF. Advances in enhanced ozone mass transfer. *Journal of Process Engineering*. 2017; **17**(2):420-426

[97] Li X, Lin C, Jiang Y. Effect of microporous distributor on mass transfer in photocatalytic ozonation reactor. *Journal of Environmental Engineering*. 2011;5(5):1101-1105

[98] Chu JY, Wu CD, Chen WJ. Ozone technology and its application. Beijing: Chemical Industry Press; 2002

IntechOpen

IntechOpen

Scale-Up and Optimization for Slurry Photoreactors

*Gianluca Li Puma, Fiderman Machuca-Martínez,
Miguel Mueses, José Colina-Márquez
and Ciro Bustillo-Lecompte*

Abstract

Several aspects of scale-up and optimization of heterogeneous photocatalytic reactors are detailed in the following chapter. The relevance of the dimensionless numbers, the critical factors of the photoreactor design, and the optimization methods are explored from an engineering point of view. The apparent optical thickness is the most crucial dimensionless parameter for photoreactor design and optimization; therefore, the study will be more focused on this topic. Moreover, a real case for a commercial application of the solar photocatalysis will be presented in this chapter. This full-scale plant is currently operating as an industrial wastewater treatment plant in a flexographic company located in Cali, Colombia.

Keywords: scale-up, heterogeneous photocatalysis, full-scale, advanced wastewater treatment

1. Introduction

For scaling-up heterogeneous photocatalytic reactors, it is necessary to consider the following key factors: kinetic law, UV radiation source, photoreactor type, catalyst type (suspended or fixed), and mass transfer phenomena. The performance of the photocatalytic reactor depends directly on the number of photons absorbed by the catalyst surface; and this is related to the geometry of the photoreactor, UV photons source, and how the catalyst interacts with the chemical species. Although the photoreactor models consider practically all these aspects, the use of dimensionless parameters is highly recommended for scaling-up purposes. The four dimensionless numbers needed for the scaling-up process are as follows [1]:

- Reynolds number (N_{Re}), which suggests the type of fluid regime to be considered for the reactor model.
- Damkohler number (N_{Da}), which expresses the ratio of the overall reaction rate, calculated at the inlet concentration and at maximum photon flux, to the maximum input mass flow rate of the reactant model (laminar or turbulent flow) to be included in the model. The values estimated for this dimensionless number allow identifying which can be the slower stage of the overall reaction rate.

- The optical thickness of the photoreactor (τ), corresponding to the degree of opacity of the photoreactor.
- The scattering albedo of the photocatalyst (ω), which depends on the optical properties of the catalyst.

The last two dimensionless numbers (optical thickness and scattering albedo) are the most relevant for scaling up photocatalytic reactors. Both help to describe the dynamics of the UV photon absorption and determine the level of difficulty of the scaling-up process. For example, some thin-film slurry (TFS) photoreactors (**Figure 1**) can exhibit very low values of scattering albedo ($\omega < 0.3$); thus, the rate of photon absorption (LVRPA) can be estimated by neglecting the scattering effect safely, and the scaling-up process can be more straightforward for this case; whereas, for TFS with higher scattering albedos or “geometrically thick” slurry photoreactors, such as compound parabolic collectors (CPC) and tubular reactors, the LVRPA needs to be modeled with more complex mathematical expressions due to the scattering effect cannot be neglected [1].

Although TFS reactors with low scattering albedos are easier to scale-up (regarding photonic effects calculations), they can result not so practical when they need to handle larger volumes of reaction, especially if the dimensionless numbers need to remain constant in the process of scaling-up. Several aspects of scale-up and optimization of heterogeneous photocatalytic reactors are detailed in the following sections of this chapter.

2. Scale-up of heterogeneous photocatalytic reactors

The dimensions of a full-scale TFS reactor can be challenging to handle if, for example, a large plate of several meters of length and width needs to be located in a reduced space. This is not the case for CPC or tubular photoreactors, which can be set up as modular units for larger reaction volumes. This advantage is more relevant when the photon source is the UV solar radiation since the photocatalytic reactors must be located outdoors, and the TFS reactors must have additional protection for weather phenomena. The solar CPC photoreactors, instead, are more robust, and there are several large-scale applications as it has been reported in the literature [1–5].

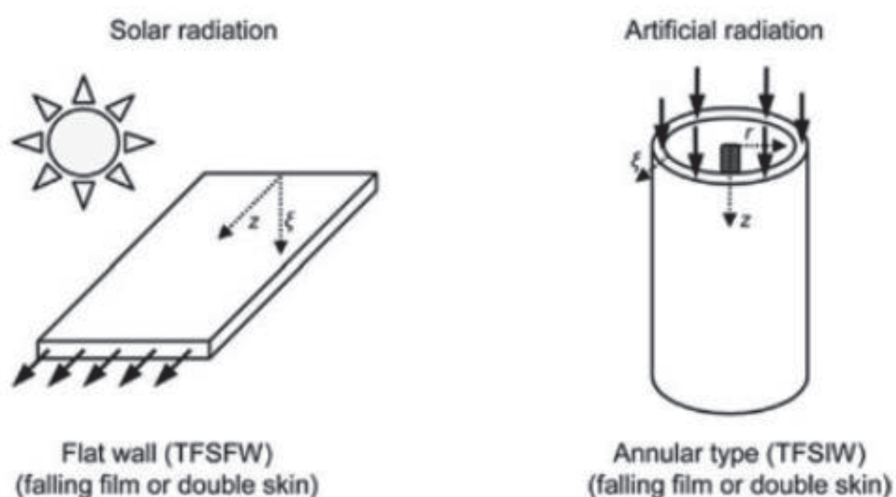


Figure 1. Thin-film slurry (TFS) photoreactors. © 2005 Elsevier Science Ltd. Originally published in Li Puma [1] under CC BY-NC-ND 4.0 license.

Nonetheless, other “geometrically thick” reactors can be considered as feasible options to be scaled-up, regarding the cost-benefit ratio.

The optical thickness, which depends on the catalyst load and the reactor thickness, may be manipulated in order to maximize the photon absorption by the catalyst. Consequently, it is necessary to observe how the LVRPA behaves with different values of optical thickness, considering that the type of reactor is relevant to the behavior of this parameter.

Figure 2 shows how the conversion of an ideal substrate varies with the optical thickness and the type of reactor: falling film laminar flow (FFLF), plug flow (PF), and slit flow (SF) reactors. It is also clear that the lower scattering albedos allow higher conversions of this ideal substrate.

The “optically thick” reactors ($\tau > 1.0$) exhibit lower conversions due to a high scattering effect although there are also high photon absorption rates due to the higher amounts of catalyst. For this kind of photoreactors, the optimization of the apparent optical thickness is strongly recommended in order to use the minimum amount of catalyst that ensures satisfactory performance of the photocatalytic reactor.

Other dimensionless numbers or parameters can be used. The dimensionless intensity of radiation at the entrance window of the reactor and the dimensionless LVRPA may be useful as well. The following expressions apply for TFS reactors ($\omega < 0.3$) [1]:

$$I_{\xi^*=0, z^*}^* = \frac{I_{\xi^*=0, z^*}^{\xi^*}}{\left(I_{\xi^*=0}^{max}\right)_{\omega=0}} \quad (1)$$

$$LVRPA^* = I_{\xi^*=0, z^*}^* \exp(-\tau_{app} \xi^*) \quad (2)$$

where $I_{\xi^*=0, z^*}^*$ is the dimensionless intensity at the entrance window ($\xi^* = 0$); $I_{\xi^*=0, z^*}^{\xi^*}$ is the actual intensity estimated at the entrance window; and $\left(I_{\xi^*=0}^{max}\right)_{\omega=0}$ is the maximum intensity of the radiation estimated in the absence of scattering effects.

The dimensionless LVRPA is easily estimated from the dimensionless intensity at the entrance window, the apparent optical thickness (τ), and the dimensionless

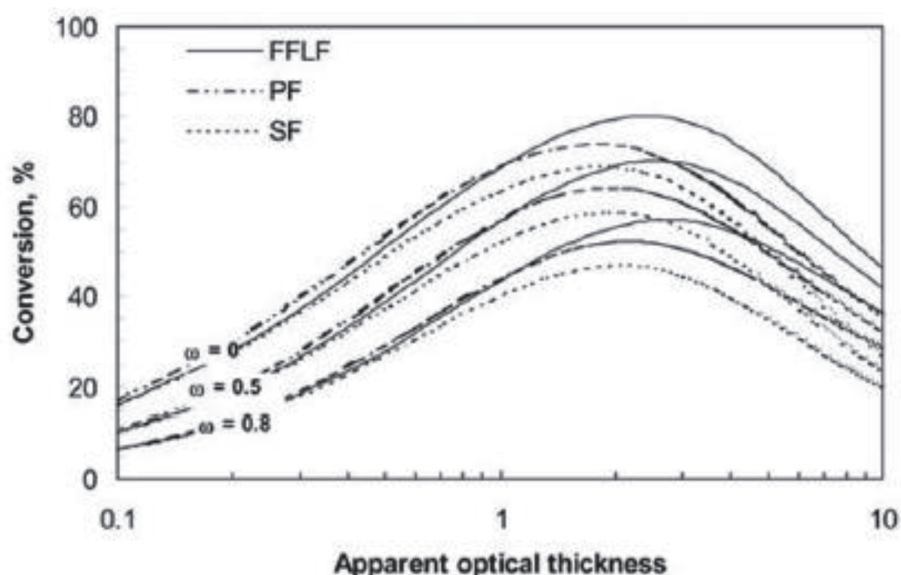


Figure 2. Model simulations for the conversion of a substrate as a function of the optical thickness and scattering albedo for different idealized flow conditions. © 2005 Elsevier Science Ltd. Originally published in Li Puma [1] under CC BY-NC-ND 4.0 license.

radial coordinate (ξ^*). As mentioned earlier, the problem with those expressions is that they are limited to cases where the scattering albedo is low. However, that is not the case for the commercial TiO_2 used in heterogeneous photocatalytic reactions, which exhibits higher values of ω [1].

The dimensionless intensity can be used when a photocatalytic reactor with artificial UV radiation source is going to be scaled-up. Nevertheless, this expression cannot be applied for solar photoreactors because of the variability of the solar incident radiation. For this case, the LVRPA must be calculated based on the solar radiation emission models, considering the location latitude, time, and date and the clearness factor (K_C) [2]. This K_C parameter depends on the number of clouds at the time of the photocatalytic reaction, which varies on the weather conditions [3].

3. Optimization methods

The optimization for photocatalytic reactors is usually intended for finding the operating conditions that ensure the best performance regarding the degradation of a specific substrate by photochemical oxidation. For the scaling-up process, this is a necessary step for making the heterogeneous photocatalysis a profitable and competitive technology.

The optimization can be carried out from the experimental data of pilot-scale photoreactors by using a simple empirical model. This model is built from a polynomial expression that involves the most relevant operating variables that affect the interest variable (e.g. relative degradation of the substrate).

Figure 3 shows an example where the surface response methodology was used for optimizing the decolorization of methylene blue (MB) with two bench-scale photoreactors [6].

In the reported study by Arias et al. [6], the tubular reactor corresponds to a 38 mm-ID borosilicate glass tube of 30 cm of length (**Figure 4a**), whereas the CPC reactor consists of the same glass tube but with a reflective collector that redistributes the reflected radiation (**Figure 4b**).

For each case, the slurry was recirculated during 30 min under darkness conditions, in order to achieve the adsorption equilibrium of the dye on the catalyst surface. In previous results, the adsorption removal of the dye was around 10–15%. It was possible to build the polynomial models from results of a full-composite experimental design, where the TiO_2 load and the initial pH of the slurry were selected as the controllable factors and the relative decolorization was the response variable. The optimization was made by using the first-derivative method for the

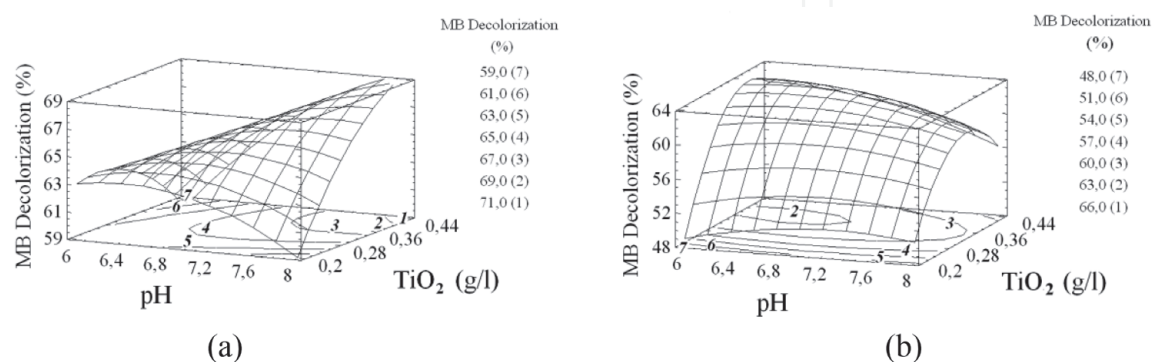


Figure 3. Surface response plots and contour lines for methylene blue (MB) TiO_2 -based photocatalytic degradation: (a) CPC reactor and (b) tubular reactor. © 2005 Walter de Gruyter & Co. Originally published in Arias et al. [6] under CC BY-NC-ND 4.0 license.

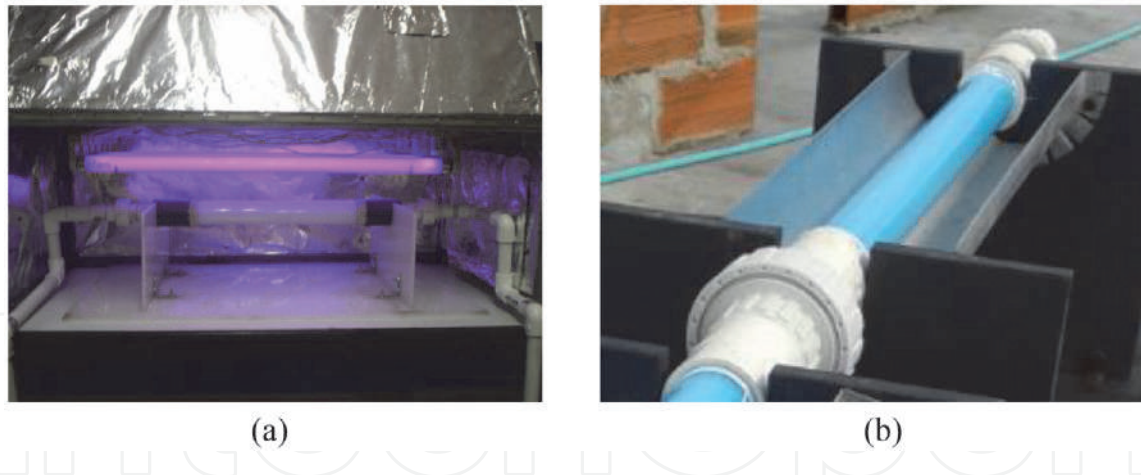


Figure 4. Bench-scale photoreactors used for MB decolorization; (a) tubular and (b) CPC.

obtained empirical expressions, and the optimal catalyst load and pH were found for each photoreactor [6].

This method allows finding optimums without a significant mathematical effort; however, its results only are scalable within the experimental conditions used for the pilot or bench-scale tests. Besides, the effects of mass transfer and the photon absorption effects are not considered in this empirical model. This leads to using of photoreactors of the same dimensional and hydrodynamic features than that used for the experimental tests. Therefore, this optimization method is limited because of its empirical nature, and it is necessary to consider a method that involves dimensionless numbers, more suitable for scaling-up.

The other method consists of optimizing the mathematical expressions of the photoreactor model. The first derivative (as optimization tool) might not be practical for finding the maximums or minimums of these mathematical expressions due to their intrinsic complexity, especially for “geometrically thick” photoreactors. Therefore, it is more recommendable to evaluate the property to be optimized in a wide range of the dependent variables. Despite the demanding calculation time of this type of optimization, this strategy is more applicable for the scaling-up process since the use of dimensionless numbers in the optimization ensures the similarity between scales.

The most suitable dimensionless parameter being used in the optimization is τ . Generally, the variable to be optimized is the volumetric rate of photon absorption (VRPA). However, the degradation of a specific substrate can be further used. **Figure 2** shows the behavior of a hypothetical conversion vs. the apparent optical thickness and the plots that exhibit an optimum.

From the LVRPA expression and supposing a constant UV radiation flux (I_0) of 30 W/m^2 , the following plots can be obtained in order to optimize the rate of photon absorption in the CPC or tubular reactors (**Figure 5**).

The plots shown in **Figure 6** describe the behavior of the VRPA/H with tubular and CPC reactors of 32 mm ID and AEROXIDE® P-25 as the catalyst. From the previous definitions, these reactors are considered “optically thick,” and the LVRPA must be calculated using the six-flux model (SFM) approach. It is important to note that these plots are only applicable to the conditions of radiation and the tube diameter specified [7]. Although for scaling-up modular photoreactors, such as the CPC or tubular, the tube diameter can remain constant in the process. In the case of different diameter (or different reactor thickness), τ is the most suitable parameter to be involved in the optimization. **Figure 6** shows a similar trend to the one shown in **Figure 2**. The presence of optimums in each case is because of the scattering increases with the optical thickness, generally associated to the high catalyst loads that do not permit a satisfactory light penetration inside the reactor bulk.

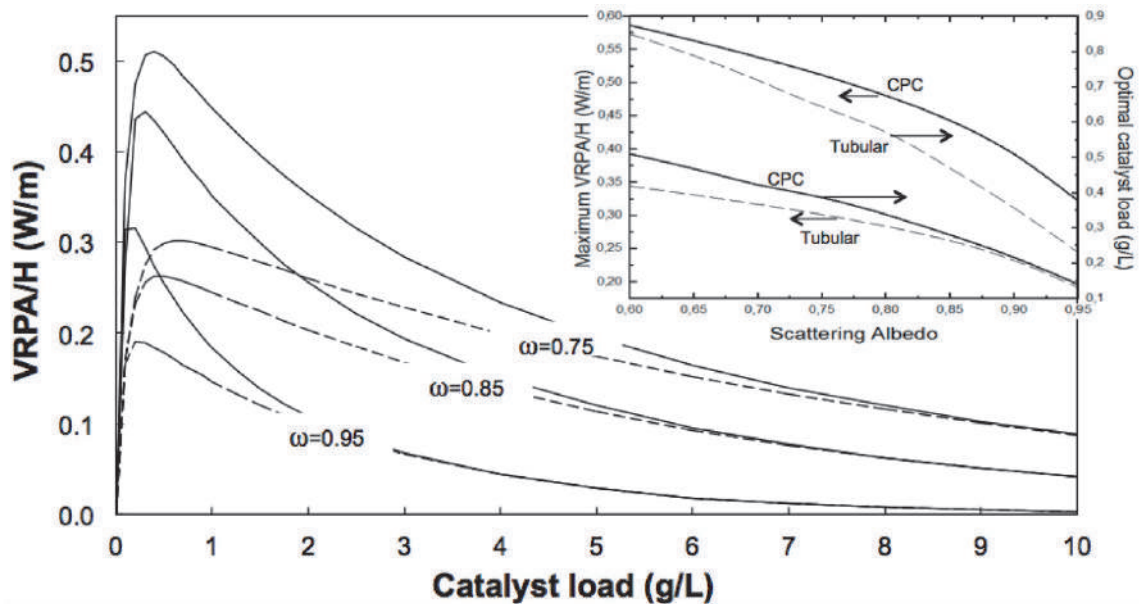


Figure 5. Volumetric rate of photon absorption per reactor length unit (VRPA/H) vs. TiO_2 catalyst load; dashed line, tubular, and solid line, CPC reactor, with 30 W/m^2 of incident UV radiation flux. © 2010 American Chemical Society. Originally published in Colina-Márquez et al. [7] under CC BY-NC-ND 4.0 license.

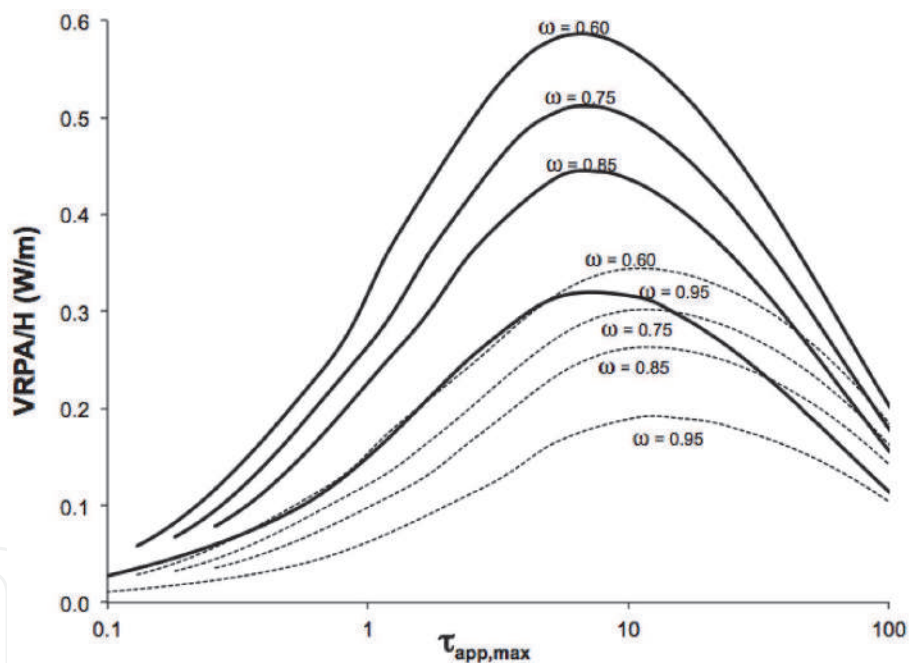


Figure 6. Volumetric rate of photon absorption per reactor length unit (VRPA/H) vs. apparent optical thickness; dashed line, tubular and solid line, CPC reactor, with 30 W/m^2 of incident UV radiation flux. © 2010 American Chemical Society. Originally published in Colina-Márquez et al. [7] under CC BY-NC-ND 4.0 license.

4. Design criteria

4.1 Preliminary considerations

The design of full-scale photocatalytic plants keeps several similarities with the design of conventional plants. It is essential to consider the following parameters before starting to make the engineering calculations for the photocatalytic plant:

- Type of reactor and reactor geometry.

- Type of process regime (batch or continuous).
- Photon source (artificial or solar).
- Catalyst (supported or slurry).
- Oxygen supply (artificial or natural).
- Total handled volume.

Considering the amount of data and information gathered during the pilot-scale tests, the most relevant aspects of the plant design must be detailed in this phase.

4.1.1 *Type of reactor*

The selection of the photoreactor is determinant for the photocatalytic performance. The rate of photon absorption is directly related to the type of photoreactor and construction materials. The selection depends on the type of photon source and the type of catalyst as well. A reactor with a fixed catalyst can have different geometry and specifications than a slurry reactor. The same considerations apply for solar photoreactors and artificial UV-based ones.

4.1.2 *Type of regime*

The type of regime defines, among other parameters, the size of the photocatalytic reactor. The plant size for a batch regime is usually larger than the size of a continuous regime; nonetheless, most of the literature about photocatalytic reactors [8–10] has been focused on the batch and the semi-batch regimes. This is generally associated with the small volumes (1–100 L) handled by the pilot-scale photocatalytic reactors.

4.1.3 *Photon source*

The UV photon sources can be from UV-lamps (artificial) or the sun (natural). The main advantage of the UV-lamps is that they supply a constant flux of radiation, but their energy consumption supposes an additional cost for the operation of a full-scale plant. whereas, the solar radiation is a cheap and abundant form of UV photon supply (depending on the location). However, the radiation flux is highly variable, and it is only available during the daytime hours.

4.1.4 *Catalyst*

The fixed catalyst does not need to be separated in a later stage of the process, but it has mass transfer and photon absorption limitations; whereas the slurry catalyst can be more effective (especially for photon absorption effect), but it needs an additional separation stage that increases the costs for a full-scale plant.

4.1.5 *Oxygen supply*

The concentration of dissolved oxygen in water must be kept near to the saturation in order to avoid slower oxidation rates in the photocatalytic process. This oxygen can be supplied by the free contact of the falling stream with the atmospheric air, or with an air compressor with a sparging device. The free contact can

be more suitable with small volumes, where the flow rate supplies enough turbulence to favor the vigorous contact between the water and the atmospheric air. Otherwise, the installation of an air compressor with the corresponding sparging system would be mandatory.

4.1.6 Total volume

One of the limitations of the heterogeneous photocatalysis, aimed for wastewater treatment, is the total volume handled by the reaction system. The larger volumes require larger installed areas for the photoreactors. Although the size of the plant depends on the kinetics of the photocatalytic reaction, the total volume determines the final dimensions of the full-scale plant.

4.2 Photoreactor selection

The criterion for selecting a reactor type considers two main aspects: performance and cost. The pilot-scale tests must provide the required information about these two features. Although we can find a wide variety of lab-scale and pilot-scale photocatalytic reactors in the scientific literature, we must ensure that the selected reactor is commercially available for full-scale applications or at least its assembling costs are affordable.

The photoreactors shown in **Figure 7** can use artificial or solar radiation as a UV photon source, except for the annular reactor that only can use artificial UV

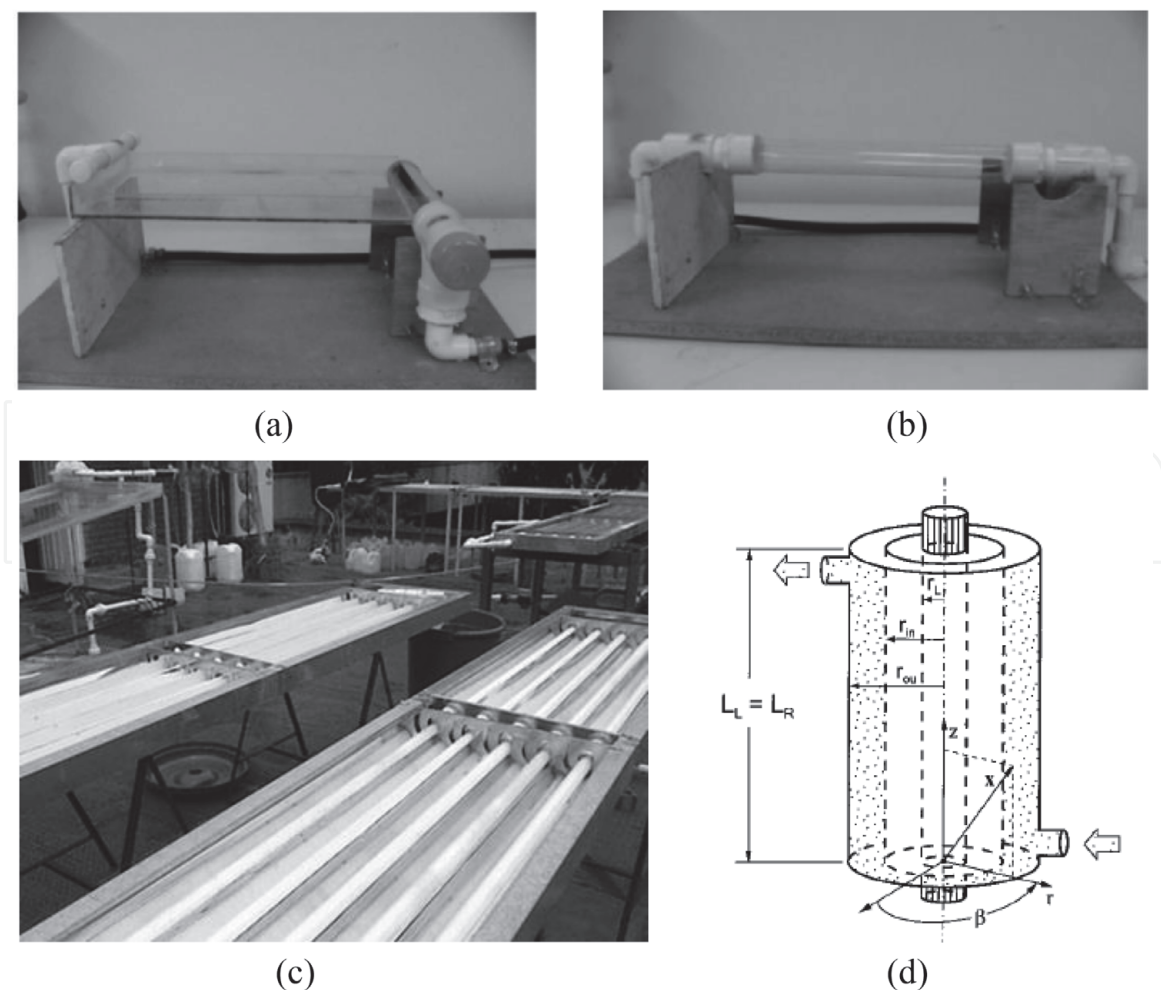


Figure 7. Photocatalytic reactors: (a) flat plate, (b) tubular, (c) CPC, and (d) annular. © 2010 American Chemical Society. Originally published in Romero et al. [11] under CC BY-NC-ND 4.0 license.

radiation. Besides, catalysts can be used as slurry or fixed plates in any of the depicted reactors. Regarding the selection of the UV-photon source, the suggested strategy consists of decreasing costs by using solar radiation whenever is possible. If the solar radiation is feasible as a UV photon source, the photoreactor should be selected based on its performance, considering the variability of the radiation intensity.

4.2.1 Tubular reactor

Figure 7b shows a bench-scale tubular reactor. This reactor geometry is quite simple because it only consists of a tube made of a material with good UV radiation transmittance. As the catalyst is usually used as slurry, this reactor must operate under the turbulent regime in order to avoid that the catalyst precipitates.

This technology can receive direct and diffuse solar radiation on the reactor part that is directly exposed. However, some disadvantages can appear due to the soiling or the reactor wall due to the catalyst, such as mass transfer limitations and a low photon penetration inside the reactor bulk [11].

4.2.2 Compound parabolic collector (CPC)

The compound parabolic collector (CPC) consists of two reflective screens located at the bottom of the tubular reactor [12]. These reflective screens are able to reflect the radiation to the bottom of the reactor, which improves the performance of this reactor over the tubular reactor (without collectors). The CPC configuration is one of the most used in reactors for solar applications [4, 5, 13, 14]. These collectors can redistribute the radiation and reflect it without concentrate, avoiding that the fluid temperature increases [15]. This reactor uses the diffuse and direct solar radiation as a UV photon source.

Figure 8 depicts the manner how solar radiation can be redistributed around the tubular receiver surface without concentrating the radiation. The equations that describe the curvature of the involute are as follows:

$$x_{CPC} = \pm R_R (\sin t - t \cos t) \quad (3)$$

$$y_{CPC} = -R_R (\cos t + t \sin t) \quad (4)$$

where x_{CPC} and y_{CPC} are the rectangular coordinates of an involute given point, R_R is the inside reactor radius, and t is a parameter that takes values from 0 to 2π radians.

4.2.3 Tilted flat plate

The tilted flat plate reactor is also known as the falling film reactor, and it does not have concentrators. Because of its simplicity and low-cost construction, it is one

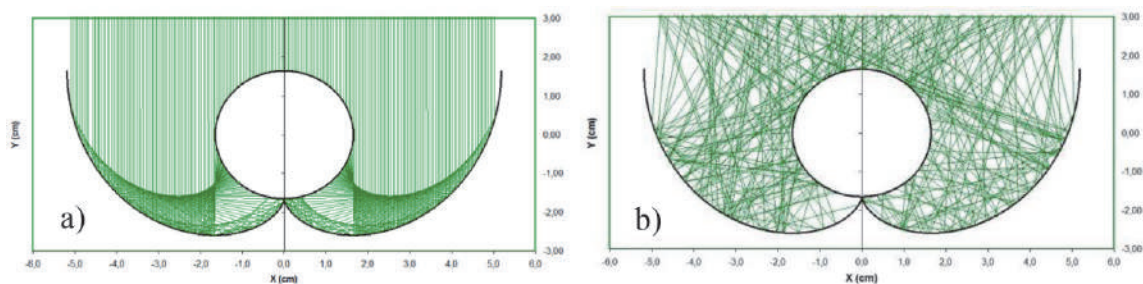


Figure 8. Solar radiation modeled with the ray-tracing technique: (a) direct radiation and (b) diffuse radiation.



Figure 9.
Pilot-scale solar flat plate reactor used for degradation of a model pollutant.

of the most used reactors for pilot-scale studies. **Figure 9** shows a solar flat plate with a supported catalyst. The main advantage of this configuration is that the entire falling film is exposed to solar radiation with no barriers. The optical thickness is smaller than the one observed in the tubular and the CPC reactors, which permits using higher catalyst loads and achieving better photon absorption rates. However, the most significant drawback of this type of reactor is the larger area occupied compared to that used in tubular reactors. In addition, there is no possibility of setting up this photoreactor like a modular unit because it would require a pump for each module.

4.2.4 Comparison of photoreactor configurations

The selection of the most suitable photoreactor depends not only on the reactor performance but also on its potential for being scaled-up. Moreover, the type and the concentration of the substrate are determinant for the photocatalytic reactor performance. A comparative assessment can provide useful information in order to make the right decision. This means that the pilot-scale tests must be carried out under the same operating conditions, or at least under very similar ones than the expected conditions of the full-scale plant.

Previous reports about photoreactor comparisons have been carried out with artificial UV-based and UV solar-based systems [16–19]. Bandala et al. [17] study focused on the comparison of several solar tubular reactors with different types of collectors and without collectors for oxalic acid degradation. Although there was no significant difference between the performances of the photoreactors with collectors, their performance was higher than that of the photoreactor without collectors.

Figure 10 shows a case where a robust experimental design was used for showing the performance of three different solar photoreactors in the degradation of a mixture of commercial pesticides. This criterion for choosing the more suitable reactor was based on the higher signal-to-noise ratio exhibited. The signal is the overall photocatalytic removal, and the noise is the noncontrolled parameter that affects the performance significantly. This noise parameter corresponds to the accumulated UV solar radiation within a fixed time lapse.

In short, the most robust photoreactor was the flat plate, followed very closely by the CPC. This means that the selected reactor would be the flat plate for this case; however, there is a critical drawback for this reactor: a large flat plate would be needed for treating higher volumes of polluted wastewater. Therefore, the scaling-up of the flat plate would be impractical, and the best option would be then the CPC

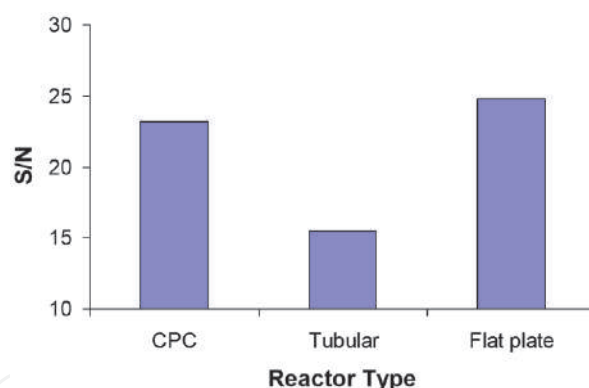


Figure 10. Signal-to-noise ratio (S/N) for pesticides degradation with three different solar photoreactors.

reactor. Additionally, this photoreactor can be used in modules, which can be mounted or dismounted easily.

4.2.5 Selection of construction materials

The construction materials can vary depending on the reactor geometry and type. Nonetheless, all the materials considered must fulfill a common condition: they must be resistant to the atmospheric corrosion or at least, they must have protection against this phenomenon. In the case of outdoor plants, such as the solar photocatalytic reactors, the materials must resist prolonged solar radiation exposition or not undergo photodegradation under these conditions.

For photoreactors with tubular geometry, the optical properties of the construction material of the reactor must ensure the maximal use of the available photons that reach the reaction space. Regarding this aspect, the material must permit the free pass of the UV photons through it. This means that must have a high transmittance within the UV absorption range of the catalyst (e.g., 275–390 nm for the commercial P25 TiO₂).

Figure 11 shows the transmittance of different materials used in photoreactors. According to Cassano et al. [20], the material with the best transmittance is the quartz, but commercial applications with this material would be expensive. The most feasible is then the borosilicate glass with low contents of iron (Pyrex® and Duran® commercial brands). However, polytetrafluoroethylene (PTFE) can be a cheaper option with comparable transmittance respect to the borosilicate glass.

4.3 Pilot-scale plant considerations

Figure 12 shows an example of a pilot-scale plant with a TiO₂-based LFFS photocatalytic reactor aimed to degrade salicylic acid [21]. The kinetic law and the mass balance can be estimated from the concentrations measured at the sample ports and the proposed model for this photocatalytic reactor. The feed tank must be kept continuously agitated in order to maintain a uniform distribution of the concentration. Furthermore, it is essential to ensure a constant oxygen supply for avoiding that the photochemical reaction rate decreases because of the oxygen consumption. The following features must be considered for full-scale plant design:

- Type, geometry, and construction materials of the photocatalytic reactor must remain the same for a full-scale plant.
- Fluid regime (Reynolds number must be kept as constant).

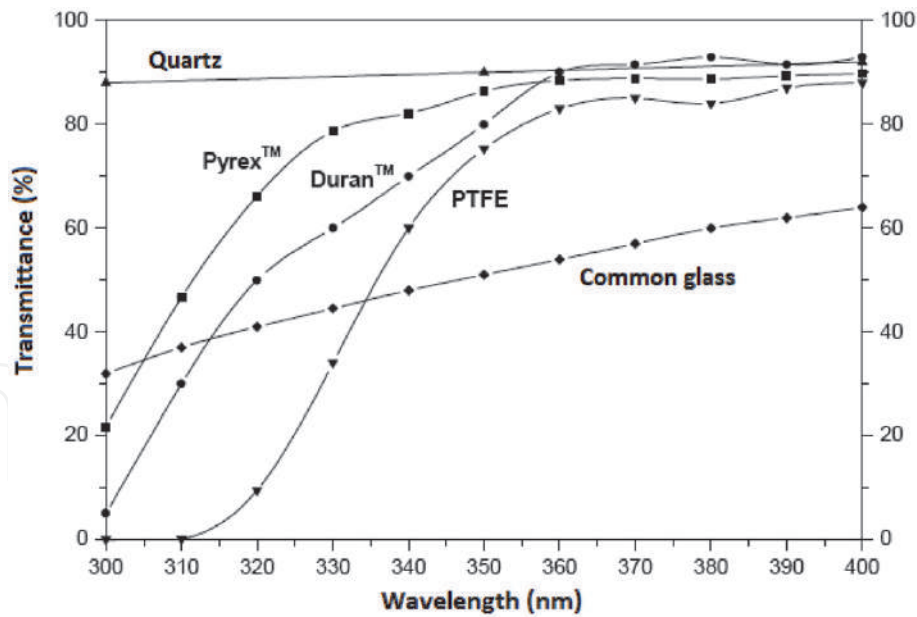


Figure 11.
Transmittance of different materials used in photoreactor design.

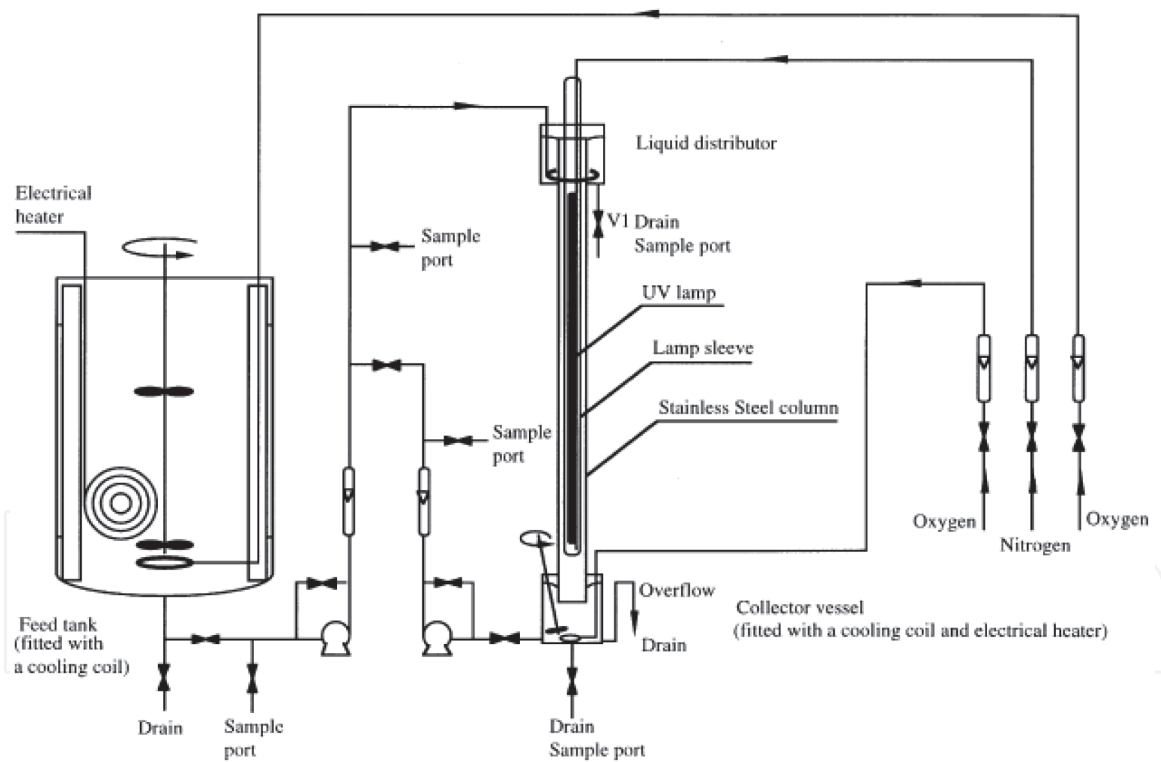


Figure 12.
Pilot plant for a laminar flow falling film slurry (LFFS) photocatalytic reactor. © 1998 Elsevier Science Ltd. Originally published in Li Puma and Yue [21] under CC BY-NC-ND 4.0 license.

- Sampling ports located at relevant streams for collecting information about substrate concentrations along the process.
- Instruments and process control for obtaining data of the operating variables such as temperature, UV radiation, pH, and dissolved oxygen.
- Easy operation.

Although the temperature may not vary significantly during the tests, it is recommendable to include cooling or heating systems for controlling the temperature, especially with systems that use UV artificial light as a photon source. Regarding the pH, it is not necessary to control it. Besides the tremendous difficulties for controlling the pH, the improvement in the photocatalytic reactor performance is not considered significant enough.

4.3.1 Plant layout

The full-scale plant can resemble the pilot-scale plant in many aspects; however, there are other stages of the process that need to be considered. Despite the process simplicity, details such as the auxiliary equipment, pumping, and storage tanks cannot be underestimated.

The photocatalytic plants are aimed usually for wastewater treatment. Thus, the final product plant (the treated water) can be reused or spilled on the surface water bodies. This aspect must be considered in the plant layout (e.g., temporal storage tanks or pipelines for conducting the treated water to its final destination). Another essential feature is the catalyst recovery. Since the catalyst is used as a slurry in most of the cases, a separation-recovery subprocess should be considered.

Figure 13 shows the isometric drawing of a demonstration plant where 2 m³ of wastewater polluted with NBCS were treated. It is recommended to simplify the subprocess for recovering the TiO₂ because of the installation and operation costs of a full-scale plant increase significantly. It is essential to specify the pump size correctly and consider the discharge pressure in order to avoid leaks or tubes breakage. As seen in the plant layout depicted in **Figure 13**, the modules were set up in two rows of 21 reactors each. This was done to reduce the pressure at the tube's joints, but the Reynolds number must remain constant to avoid mass transfer limitations [22].

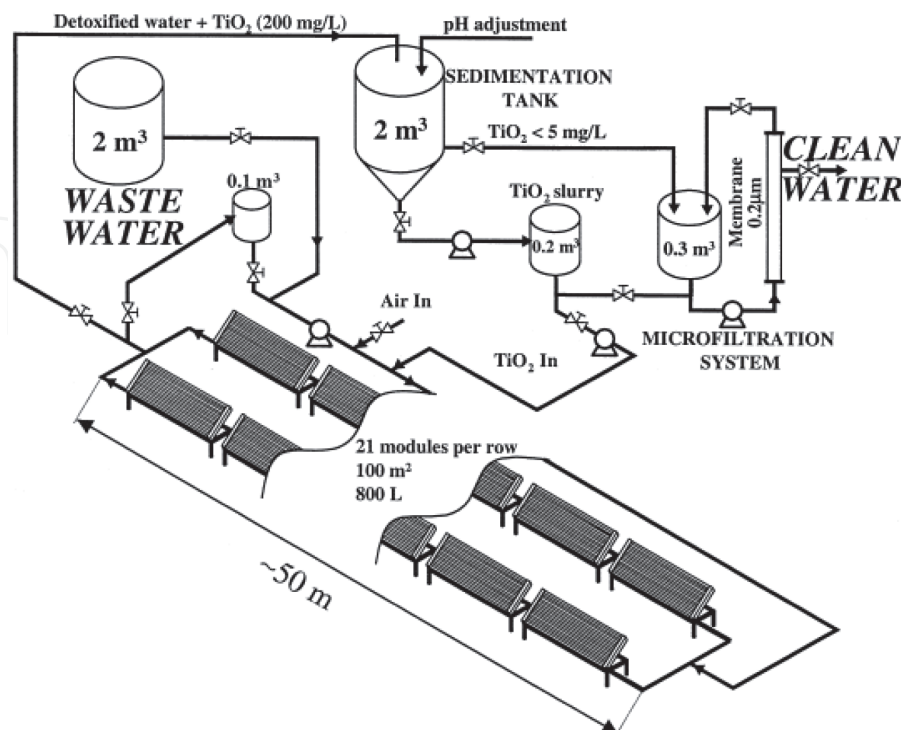


Figure 13. Isometric drawing of a demonstration solar photocatalytic plant for treatment of water contaminated with non-biodegradable chlorinated solvents (NBCS). © 1999 Elsevier Science Ltd. Originally published in Blanco et al. [22] under CC BY-NC-ND 4.0 license.

4.4 Design, assembly, and operation of a full-scale solar photocatalytic plant

This section presents the main aspects that were considered in the construction and the operation of a full-scale solar photocatalytic plant for treating industrial wastewater from a flexographic industry. This full-scale plant is the first commercial solar photocatalytic installation in America.

Previous studies on laboratory and pilot-scale photoreactors were conducted to determine the technical feasibility of using photocatalysis as a viable treatment of 2 m³/d of water contaminated with industrial dyes, and consequently, it served as the basis for a technology-transfer deal with the company and a patent application [23, 24].

4.4.1 Background and description of industrial process

A major company in Colombia that manufactures notebooks was facing issues with the treatment of the wastewater produced after washing the rolls used for printing the lines of the notebooks. This residual effluent was contaminated with the industrial dye, which has proven to be resistant to biological treatments. Therefore, it was necessary to apply a novel technology (such as heterogeneous photocatalysis) that could ensure the color removal.

The primary objective was the reuse of the treated water for washing the printing rolls. The most important innovation of this photocatalytic process was the simple way in which the solid catalyst is reused without using complex and expensive systems to recover after each treatment process. The use of solar radiation was another significant advantage since the location has good solar light availability.

The process flow diagram of the full-scale solar photocatalytic plant is shown in **Figure 14**. This scheme can be used for different kinds of wastewater and which can be treated by photocatalysts. This photocatalytic process was applied for treating industrial residual wastewaters contaminated with recalcitrant compounds, in this case, flexographic dye residues. The industrial wastewater is generated from washing the printing rolls soiled with dye residues after a typical work cycle. This wastewater is collected in the tank T-1 and then pumped to the recycling-feed tank

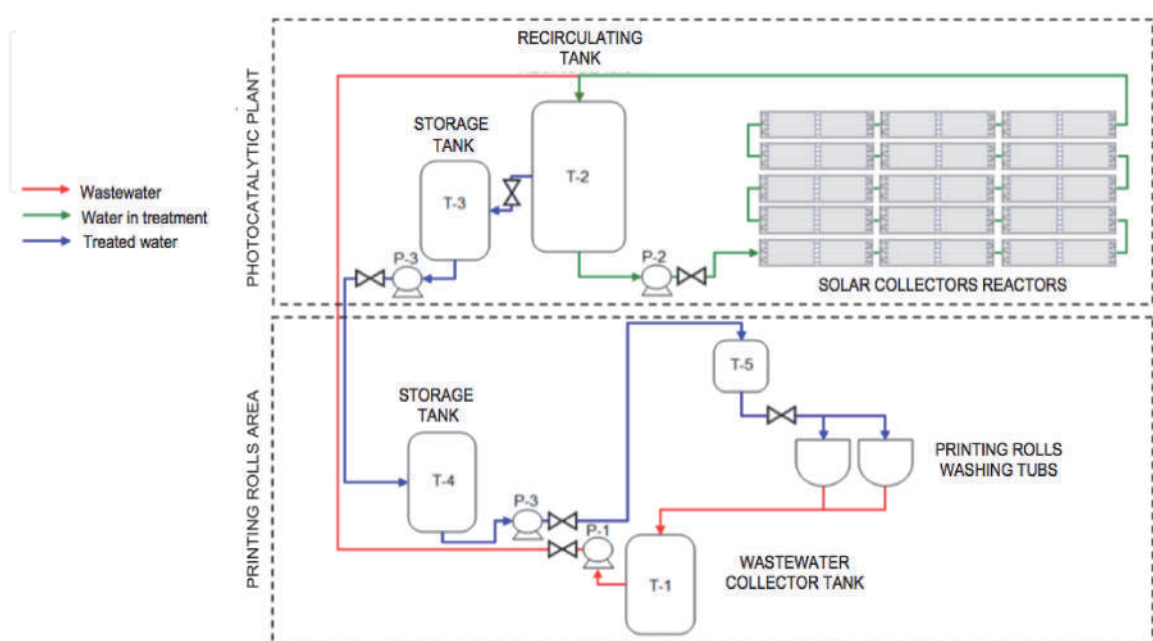


Figure 14. Process flow diagram of the full-scale wastewater treatment photocatalytic plant.

T-2 using the pump P-1. The wastewater stored in this tank is diluted with water in a ratio of 4:1. The first dilution of the process was made with fresh water; after that, treated water is used for this purpose. Once the tank was full, the catalyst was added for the first and the only time as far. The same catalyst has been reused in the subsequent treatments, since the plant started up in September 2009, and it will be removed when it has lost its activity.

The pump P-2 recirculates the slurry through the CPC photoreactors. As it was previously mentioned, the process has an average duration because it depends on the availability of solar radiation. The process is suspended under the following conditions: color removal from the contaminated effluent, adverse weather conditions (hard rain or strong winds), or if the sun has set. In case of the color removal, the next step is the catalyst settled down in order to separate the clear supernatant. This process lasts between 12 and 24 h, depending on the amount of treated water to be reused to wash the rollers.

Between 10 and 25% of the treated water from the recirculation tank T-2 are transferred by gravity to the intermediate storage tank T-3. When this tank has enough volume (1.5–2.5 m³), the treated water is pumped via P-3 to the secondary storage tank T-4. Finally, according to plant requirements, it is pumped via P-4 to the tank T-5, which is used to provide clean water for washing the soiled printing rolls, thus closing the treatment cycle [24].

4.4.2 Design of pilot solar photoreactor model

Each photoreactor module comprises 10 tubes placed in five rows over the CPCs (**Figure 15**). The glass tubes are 32 mm ID and 1.4 mm of thickness manufactured by Schott Duran®. The tubes were cut from their original length of 1.5 m to 1.2 m in order to correspond the length of the sheets used for constructing the collectors. The tubes diameter must be selected between 25 and 50 mm, since diameters smaller than 25 mm are not feasible because of pressure drop limitations; whereas, diameters larger than 50 mm present photon absorption issues due to a significant photon scattering.

The collectors were constructed in high-reflectivity aluminum (80–90% of reflectivity), which should be weather resistant as well. The involutes, characteristic of the CPCs, as seen in **Figure 15**, were molded using a folding machine based on

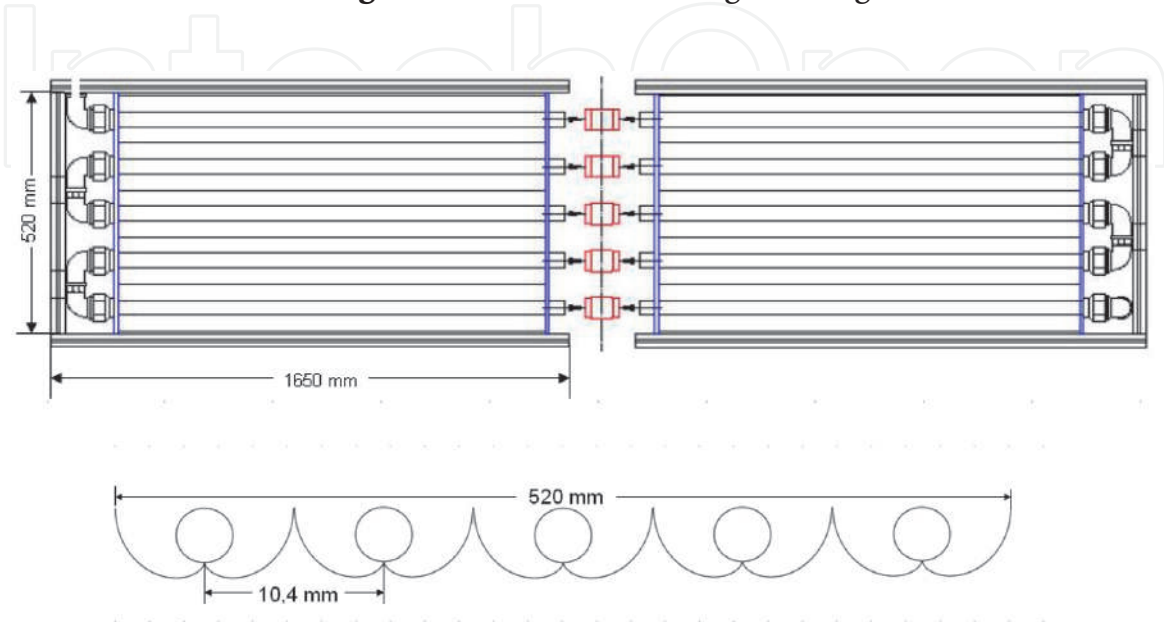


Figure 15.
Main structure of the CPC photoreactor type and cross section of tubes and manifolds for CPC.

numerical control. The supporting structure was constructed with galvanized zinc sheets, as well as the guides that supported the collectors and the glass tubes. Between the glass tubes, anti-slip PVC joints were located (red-colored joints shown in **Figure 15**), which could permit torsion without damaging the glass tube during maintenance processes.

As mentioned before, the flow regime is another crucial aspect to be considered in the pilot plant design and the scaling process. The recycling pump must be specified in order to ensure the turbulent regime of the flow through the photoreactor [23]. The Reynolds number must be larger than 15,000, and this means that the flow rate must be larger than 24 L/min (for a 32-mm tube diameter). **Table 1** shows the main accessories for hydraulic calculus.

From a simple mechanical energy balance (Bernoulli's equation), the pump theoretical power was estimated (0.241 HP or 179.5 W). The commercially available pump had a nominal power of 0.5 HP with a maximum flow rate of 35 L/min.

4.4.3 Evaluation of real wastewater at pilot solar CPC reactor

A set of pilot plant tests with a simulated mixture of effluent were performed to assess the technical feasibility of heterogeneous photocatalysis for the removal of color from industrial wastewater polluted with a printing dye. The aim was to find suitable conditions for the operation of a larger-scale plant that would allow total discoloration of the industrial effluent. For this purpose, it was considered a robust experimental design. Subsequently, a rate law was obtained, considering the UV accumulated radiation as the independent variable.

The procedure used for the experimental work consisted in treating a constant volume of the diluted mixture with different concentrations of catalyst and fixing the treatment time. The accumulated radiation was measured for sunny and cloudy days in order to observe the solar CPC photoreactor performance under these weather conditions.

The color removal was measured by UV-Vis spectrophotometry, whereby the concentration of the mixture of dyes was indirectly obtained. **Table 2** shows the conditions of the experimental pilot-scale tests.

The experimental results are shown in **Table 3**, and **Figure 16** shows samples collected before and after the photocatalytic treatment. The color was removed entirely, confirming the satisfactory performance of the solar photocatalytic reactor. This evidenced that the chromophore was eliminated. From these results, it was necessary to estimate the size of the full-scale plant for treating 2 m³/d of wastewater. The signal-to-noise ratios for the controllable factors (dilution and catalyst load) are shown in **Table 4**.

	Quantity per meter	K _{eq}
Elbows	15	0.69
Connections	5	0.50
Valve	1	340.00
Tank outlet	1	0.50
Straight pipe	17	—

Table 1.
Fittings and straight pipe of the pilot plant.

Item	Description
Photoreactor	CPC with ten tubes Schott Duran® (32 mm ID)
Area exposed	1.25 m ²
Pump	Centrifugal pump—½ HP of nominal power
Flow rate	32 L/min
Total volume	40 L
Dye composition	Black Flexo: 50% w/w; Basonyl Blue 636®: 50% w/w
Catalyst	Aeroxide® TiO ₂ P-25
Process water	Tap water
Initial pH	7.5
Temperature	25–35°C
Time of tests	10 am to 4 pm

Table 2.
 Experimental conditions.

Exp	Internal arrangement		External arrangement (Noise)	
	Design parameter		UV accumulated radiation (KJ/m ²)	
	[TiO ₂] (g/L)	Dilution	High (>700)	Low (<700)
1	0.4	1:8	89.3%	70.4%
2	0.8	1:8	90.0%	48.4%
3	0.4	1:4	47.4%	29.3%
4	0.8	1:4	91.5%	50.0%

Table 3.
 Color removal corresponding to the pilot-scale experiments. © 2009 Walter de Gruyter & Co. Originally published in Colina-Márquez et al. [23] under CC BY-NC-ND 4.0 license.

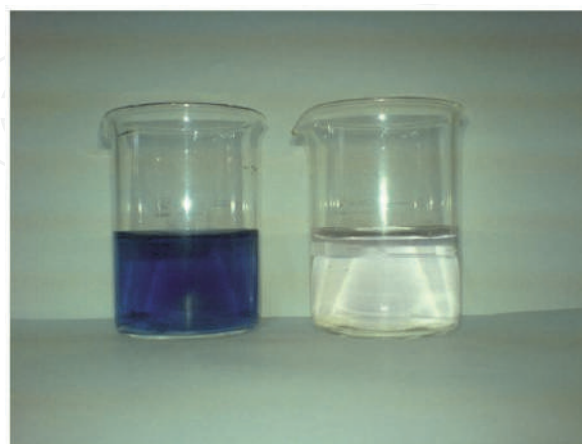


Figure 16.
 Samples collected during a typical experiment before (left) and after (right) photocatalytic treatment.

Table 5 showed the experimental data obtained for the color removal respect to the time and the accumulated UV solar radiation. This data was used for fitting parameters of a Langmuir-Hinshelwood modified model, as seen in **Table 6**.

Factor	Level	S/N ratio
Dilution	1:4	32.74
	1:8	36.59
[TiO ₂] g/L	0.4	33.15
	0.8	35.73

© 2009 Walter de Gruyter & Co. Originally published in Colina-Márquez et al. [23] under CC BY-NC-ND 4.0 license.

Table 4.
Signal-to-noise ratio (S/N) for the robust experimental design.

Time (min)	% Discoloration (sunny day)	Q _{uv} , KJ/m ³ (sunny day)	% Discoloration (cloudy day)	Q _{uv} , KJ/m ³ (cloudy day)
-30	0	—	—	—
0	58.1	0	0	0
20	64.5	5493.75	48.3	4481.25
40	71.0	12243.75	51.7	8953.13
60	74.2	18609.38	58.6	13312.50
80	80.7	25734.37	58.6	17690.63
100	83.9	32868.75	62.1	21881.25
120	83.9	40003.12	62.1	25218.75
180	90.4	59765.63	65.5	32681.25
240	90.4	73490.63	65.5	37762.50

Table 5.
Experimental data of the kinetic tests.

Type of day	Apparent rate constant (ppm·KJ/m ³)	Adsorption equilibrium constant (1/ppm)
Sunny	6.506×10^{-2}	3.213×10^{-4}
Cloudy	1.507×10^{-3}	9.419×10^{-3}

Table 6.
Kinetics parameters from Langmuir-Hinshelwood model.

The apparent rate constants seem to be dependent on the accumulated energy and the type of the day. This implies that the color removal will be faster on a sunny day with the same accumulated UV radiation.

Finally, for treating 2 m³/day of contaminated wastewater with a dilution ratio of ratio 1:4, a total of 31 modules of CPC photoreactors were estimated. Nonetheless, during the project development, there were modifications to the design considerations, and 15 modules were implemented at last. An initial isometric drawing is shown in **Figure 17**.

It is important to note that a conical-bottom tank and no secondary storage tank (for clear treated wastewater) were considered at first instance. Nonetheless, the tank was sized to handle 10 m³ per batch, and this was kept until the final design. The conical-bottom tank was selected as the first alternative in order to facilitate the catalyst precipitation and a future removal (when the catalyst was deactivated after several reuses).

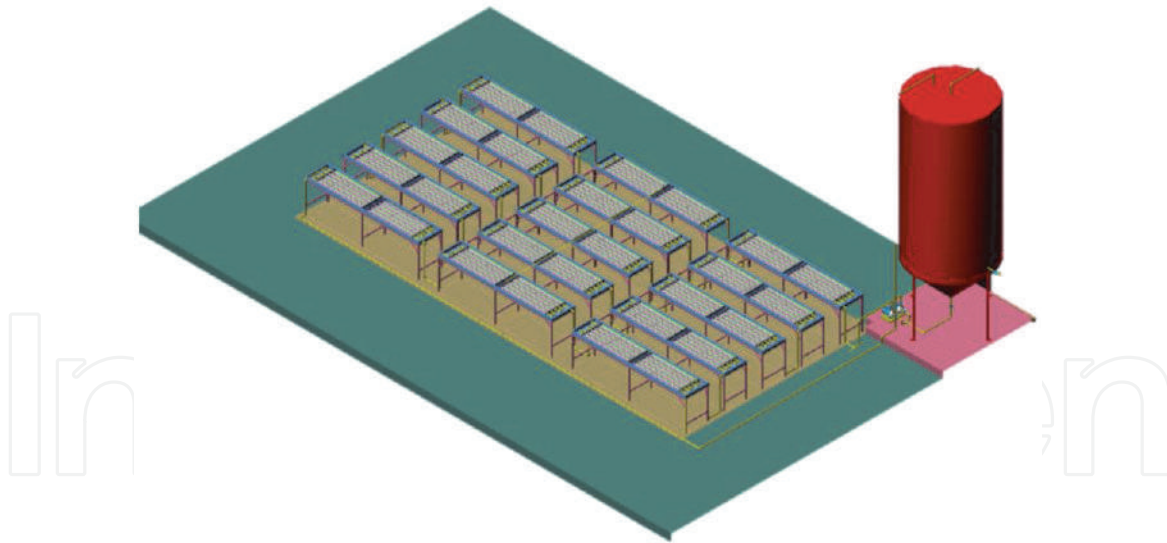


Figure 17.
Isometric draw of the solar photocatalytic plant with 15 CPC modules.

Two standard plastic tanks were selected for being installed in the solar photocatalytic plant: one of 10 m^3 , designed for handling the recirculating wastewater, and another one of 4 m^3 , for storing the treated wastewater. The air-sparging system in the bottom of the recirculation-feed tank was installed in order to maintain the wastewater saturated with oxygen and to avoid limitations in the photocatalytic rate due to the consumption of this chemical species. Moreover, the constant agitation of the water due to the air bubbling helped to maintain the catalyst in suspension and avoid mass transfer limitations because of the solid precipitation during the operation.

The catalyst was settled down after each operation day after turning off the air sparging system. The plant shut down at sunset and the catalyst precipitated overnight. The clear water was transferred to the secondary storage tank and later reused for washing the printing rolls. **Figure 18** shows an overview of the full-scale plant during its first day of steady operation in August 2009.

Currently, this plant is operating at full capacity (4 m^3 per day of wastewater). Some other contaminants are being fed to the photocatalytic system; therefore, it was necessary to include a pretreatment consisting of adsorption with activated carbon and a system for adding hydrogen peroxide.

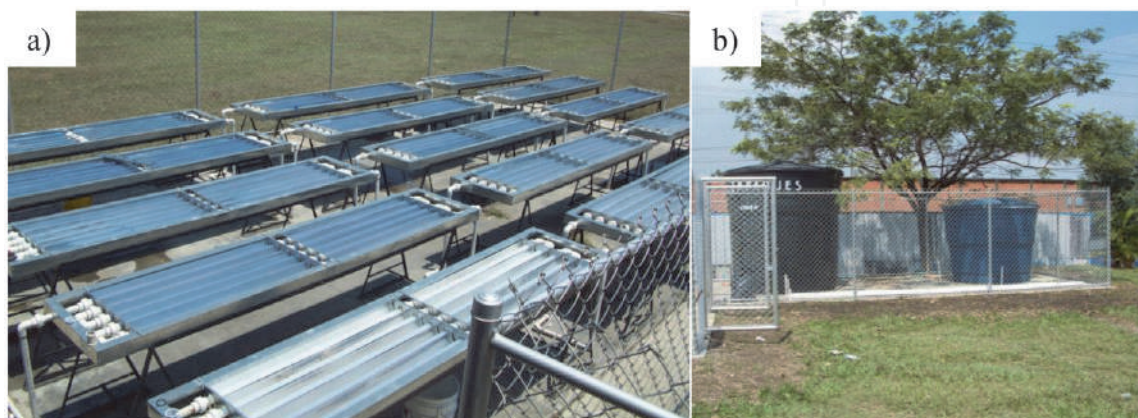


Figure 18.
Full-scale solar photocatalytic plant for dye-polluted wastewater treatment: (a) CPC photoreactors and (b) recirculation-feed and treated water storage tanks.

IntechOpen

Author details

Gianluca Li Puma¹, Fiderman Machuca-Martínez², Miguel Mueses³,
José Colina-Márquez³ and Ciro Bustillo-Lecompte^{4,5*}

1 Environmental Nanocatalysis and Photoreaction Engineering, Department of
Chemical Engineering, Loughborough University, Loughborough, UK

2 Chemical Engineering School, Universidad del Valle, Ciudadela Universitaria de
Meléndez, Cali, Colombia

3 Chemical Engineering Department, Universidad de Cartagena, Campus de Piedra
de Bolívar, Cartagena de Indias, Colombia

4 Graduate Programs in Environmental Applied Science and Management, Ryerson
University, Toronto, ON, Canada

5 School of Occupational and Public Health, Ryerson University, Toronto, ON,
Canada

*Address all correspondence to: ciro.lecompte@ryerson.ca

IntechOpen

© 2020 The Author(s). Licensee IntechOpen. Distributed under the terms of the Creative Commons Attribution - NonCommercial 4.0 License (<https://creativecommons.org/licenses/by-nc/4.0/>), which permits use, distribution and reproduction for non-commercial purposes, provided the original is properly cited. 

References

- [1] Li Puma G. Dimensionless analysis of photocatalytic reactors using suspended solid photocatalysts. *Chemical Engineering Research and Design*. 2005; **83**(7):820-826. DOI: 10.1205/cherd.04336
- [2] Castilla-Caballero D, Machuca-Martínez F, Bustillo-Lecompte C, Colina-Márquez J. Photocatalytic degradation of commercial acetaminophen: Evaluation, modeling, and scaling-up of photoreactors. *Catalysts*. 2018;**8**(5):179. DOI: 10.3390/catal8050179
- [3] Colina-Márquez J, Machuca-Martínez F, Li Puma G. Photocatalytic mineralization of commercial herbicides in a pilot-scale solar CPC reactor: Photoreactor modeling and reaction kinetics constants independent of radiation field. *Environmental Science & Technology*. 2009;**43**(23):8953-8960. DOI: 10.1021/es902004b
- [4] Braham RJ, Harris AT. Review of major design and scale-up considerations for solar photocatalytic reactors. *Industrial and Engineering Chemistry Research*. 2009;**48**(19): 8890-8905. DOI: 10.1021/ie900859z
- [5] Spasiano D, Marotta R, Malato S, Fernandez-Ibañez P, Di Somma I. Solar photocatalysis: Materials, reactors, some commercial, and pre-industrialized applications. A comprehensive approach. *Applied Catalysis B: Environmental*. 2015;**170-171**:90-123. DOI: 10.1016/j.apcatb.2014.12.050
- [6] Arias F, Ortiz E, López-Vásquez A, Colina-Márquez J, Machuca F. Photocatalytic decolorization of methylene blue with two photoreactors. *Journal of Advanced Oxidation Technologies*. 2008;**11**(1):33-48. DOI: 10.1515/jaots-2008-0104
- [7] Colina-Márquez J, Machuca F, Li Puma G. Radiation absorption and optimization of solar photocatalytic reactors for environmental applications. *Environmental Science & Technology*. 2010;**44**(13):5112-5120. DOI: 10.1021/es100130h
- [8] De Lasa H, Serrano B, Salaices M. Novel photocatalytic reactors for water and air treatment. In: *Photocatalytic Reaction Engineering*. Boston, MA: Springer; 2005. DOI: 10.1007/0-387-27591-6_2
- [9] Ola O, Maroto-Valer MM. Review of material design and reactor engineering on TiO₂ photocatalysis for CO₂ reduction. *Journal of Photochemistry and Photobiology C: Photochemistry Reviews*. 2015;**24**:16-42. DOI: 10.1016/j.jphotochemrev.2015.06.001
- [10] Porta R, Benaglia M, Puglisi A. Flow chemistry: Recent developments in the synthesis of pharmaceutical products. *Organic Process Research and Development*. 2016;**20**(1):12-25. DOI: 10.1021/acs.oprd.5b00325
- [11] Romero RL, Alfano OM, Cassano AE. Cylindrical photocatalytic reactors. Radiation absorption and scattering effects produced by suspended fine particles in an annular space. *Industrial and Engineering Chemistry Research*. 1997;**36**(8): 3094-3109. DOI: 10.1021/ie960664a
- [12] Saravia L. Diseño gráfico de concentradores tipo CPC. *Avances en Energías Renovables y Medio Ambiente*. 2004;**8**(1):25-30. Available from: <https://www.mendoza-conicet.gob.ar/asades/modulos/averma/trabajos/2004/2004-t003-a005.pdf>
- [13] Malato S, Blanco J, Fernández-Alba AR, Agüera A. Solar photocatalytic mineralization of commercial pesticides: Acrinathrin. *Chemosphere*. 2000;**40**(4): 403-409. DOI: 10.1016/S0045-6535(99)00267-2

- [14] Malato S, Blanco J, Vidal A, Richter C. Solar photocatalytic degradation of commercial textile azo dyes: Performance of pilot plant scale thin film fixed-bed reactor. *Applied Catalysis, B: Environmental*. 2002;**37**(1–3):344-352. DOI: 10.1016/j.desal.2008.03.059
- [15] Blanco J, Malato S, Peral J, Sánchez B, Cardona I. Diseño de reactores para fotocátalisis: Evaluación comparativa de las distintas opciones. Chapter 11. In: Blesa M, editor. *Eliminación de Contaminantes por Fotocátalisis Heterogénea*. CYTED: Buenos Aires (Argentina); 2001. pp. 243-266. Available from: <https://www.psa.es/en/projects/solwater/files/CYTED01/17cap11.pdf>
- [16] Dijkstra MFJ, Buwalda H, de Jong AWF, Michorius A, Winkelman JGM, Beenackers AACM. Experimental comparison of three reactor designs for photocatalytic water purification. *Chemical Engineering Science*. 2001;**56**(2):547-555. DOI: 10.1016/S0009-2509(00)00259-1
- [17] Bandala ER, Arancibia-Bulnes CA, Orozco SL, Estrada CA. Solar photoreactors comparison based on oxalic acid photocatalytic degradation. *Solar Energy*. 2004;**77**(5):503-512. DOI: 10.1016/j.solener.2004.03.021
- [18] van Grieken R, Marugán J, Sordo C, Pablos C. Comparison of the photocatalytic disinfection of *E. coli* suspensions in slurry, wall and fixed-bed reactors. *Catalysis Today*. 2009;**144**(1–2):48-54. DOI: 10.1016/j.cattod.2008.11.017
- [19] Romero V, González O, Bayarri B, Marco P, Giménez J, Esplugas S. Degradation of metoprolol by photo-Fenton: Comparison of different photoreactors performance. *Chemical Engineering Journal*. 2016;**283**:639-648. DOI: 10.1016/j.cej.2015.07.091
- [20] Cassano AE, Alfano OM, Brandi RJ, Martín CA. Diseño de reactores para fotocátalisis: conceptos fundamentales. Chapter 10. In: Blesa M, editor. *Eliminación de contaminantes por fotocátalisis heterogénea CYTED*: Madrid; 2001. pp. 201-241. Available from: <https://www.psa.es/en/projects/solwater/files/CYTED01/16cap10.pdf>
- [21] Li Puma G, Yue PL. A laminar falling film slurry photocatalytic reactor. Part II—Experimental validation of the model. *Chemical Engineering Science*. 1998;**53**(16):3007-3021. DOI: 10.1016/S0009-2509(98)00119-5
- [22] Blanco J, Malato S, Fernández P, Vidal A, Morales A, Trincado P, et al. Compound parabolic concentrator technology development to commercial solar detoxification applications. *Solar Energy*. 1999;**67**(4–6):317-330. DOI: 10.1016/S0038-092X(00)00078-5
- [23] Colina-Márquez J, López-Vásquez A, Díaz D, Rendón A, Machuca-Martínez F. Photocatalytic treatment of a dye polluted industrial effluent with a solar pilot-scale CPC reactor. *Journal of Advanced Oxidation Technologies*. 2009;**12**(1):93-99. DOI: 10.1515/jaots-2009-0111
- [24] Martinez FM, Colina-Márquez JA, Universidad del Valle. Photo-Catalysis Process Applied in Eliminating Recalcitrant Compounds in Industrial Residual Waters. U.S. Patent No. 9,394,186. Washington, DC: U.S. Patent and Trademark Office; 2016. Available from: <https://patents.google.com/patent/US9394186B2/en>